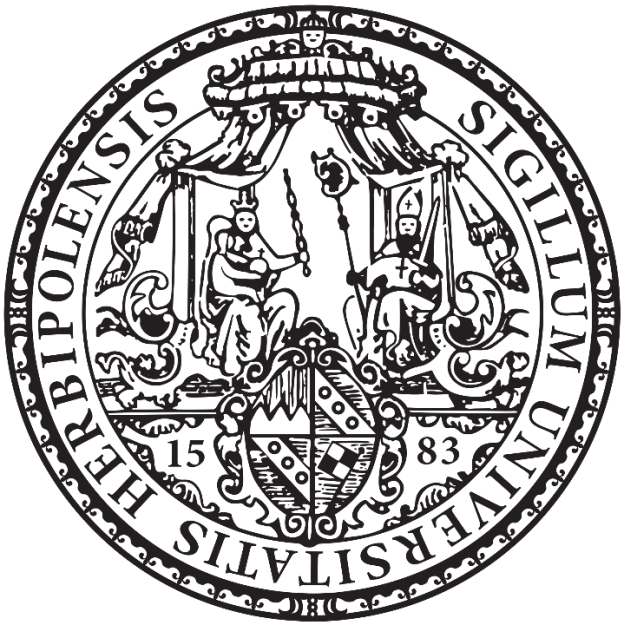

The Role of Acid Sphingomyelinase in *Staphylococcus aureus* Infection of Endothelial Cells

Dissertation for the academic degree

doctor rerum naturalium

(Dr.rer.nat)

at the Faculty of Biology

Julius-Maximilians-Universität Würzburg

Department of Microbiology

Author:

David Krones

from Frankfurt, Germany

Würzburg, 2022

Submitted on:

Members of graduation committee

Chairperson:

Primary supervisor: PD Dr. Martin Fraunholz, Group Leader *S. aureus*, Biocenter, Julius-Maximilians-Universität Würzburg, Germany

Secondary supervisor: Prof. Dr. Sibylle Schneider-Schaulies, Department of Virology, Julius-Maximilians-Universität Würzburg, Germany

Date of Public Defense:

Date of Receipt of Certificates:

Directory

Abstract

Staphylococcus aureus is a human bacterial pathogen responsible for a variety of diseases including bacterial pneumonia and sepsis. Recent studies provided an explanation, how *S. aureus* and its exotoxins contribute to the degradation of endothelial junction proteins and damage lung tissue [4]. Previous findings were indicating an involvement of acid sphingomyelinase (ASM) activity in cell barrier degradation [5]. In the presented study the impact of singular virulence factors, such as staphylococcal α-toxin, on *in vitro* cell barrier integrity as well as their ability to elicit an activation of ASM were investigated.

Experiments with bacterial supernatants performed on human endothelial cells demonstrated a rapid dissociation after treatment, whereas murine endothelial cells were rather resistant against cell barrier degradation. Furthermore, amongst all tested staphylococcal toxins it was found that only α-toxin had a significant impact on endothelial junction proteins and ASM activity. Ablation of this single toxin was sufficient to protect endothelial cells from cell barrier degradation and activation of ASM was absent.

In this process it was verified, that α-toxin induces a recruitment of intracellular ASM, which is accompanied by rapid and oscillating changes in cytoplasmic Ca^{2+} concentration and an increased exposure of Lysosomal associated membrane protein 1 (LAMP1) on the cell surface. Recruitment of lysosomal ASM is associated, among other aspects, to plasma membrane repair and was previously described to be involved with distinct pathogens as well as other pore forming toxins (PFT). However, with these findings a novel feature for α-toxin has been revealed, indicating that the staphylococcal PFT is able to elicit a similar process to previously described plasma membrane repair mechanisms.

Increased exposure and intake of surface membrane markers questioned the involvement of ASM activity in *S. aureus* internalization by non-professional phagocytes such as endothelial cells. By modifying ASM expression pattern as well as application of inhibitors it was possible to reduce the intracellular bacterial count. Thus, a direct connection between ASM activity and *S. aureus* infection mechanisms was observed, therefore this study exemplifies how *S. aureus* is able to exploit the host cell sphingolipid metabolism as well as benefit of it for invasion into non-professional phagocytic cells

Zusammenfassung

Staphylococcus aureus ist ein bakterieller Erreger, der für eine Vielzahl von Erkrankungen des Menschen verantwortlich ist, darunter bakterielle Lungenentzündung und Sepsis. Neuere Studien konnten einen Ansatz dafür liefern, wie *S. aureus* und seine Exotoxine zur Degradation von endothelialen Verbindungsproteinen beitragen und das Lungengewebe schädigen. Weitere Befunde weisen auf eine Beteiligung der sauren Sphingomyelinase (ASM) bei der Degradation der Zellbarriere hin.

In der vorliegenden Studie soll der Einfluss einzelner Virulenzfaktoren, wie z. B. Staphylokokkus α-Toxin, auf die Integrität der Zellbarriere *in vitro* sowie deren Fähigkeit, eine Aktivierung der ASM hervorzurufen, untersucht werden.Experimente mit bakteriellen Überständen die an humanen Endothelzellen durchgeführt wurden, zeigten eine rasche Dissoziation nach Behandlung, während murine Endothelzellen vorwiegend resistent gegen eine Degradation der Zellbarriere waren. Darüber hinaus wurde unter allen getesteten Staphylokokken-Toxinen festgestellt, dass nur α-Toxin einen signifikanten Einfluss auf endotheliale Verbindungssproteine und ASM-Aktivität hat. Die genetische Ablation des Toxins alleine reichte aus, um Endothelzellen vor einer Degradation der Zellbarriere zu schützen, und die Aktivierung von ASM blieb aus.

Dabei konnte nachgewiesen werden, dass α-Toxin eine Rekrutierung von intrazellulärem ASM induziert, die mit schnellen oszillierenden Veränderungen der zytoplasmatischen Ca2+-Konzentration und einer erhöhten Exposition von Lysosome associated membrane protein 1 (LAMP1) an der Zelloberfläche einhergeht. Die Rekrutierung lysosomaler ASM ist u.a. mit der Reparatur von Plasmamembran assoziiert und wurde bereits im Zusammenhang mit verschiedenen Pathogenen sowie anderer porenbildende Toxine (PFT) beschrieben. Mit diesen Befunden konnte jedoch eine neue Eigenschaft für α-Toxin beschrieben werden, die darauf hindeutet, dass das Staphylokokken-PFT einen ähnlichen Prozess auslösen kann wie zuvor beschriebene Plasmamembran-Reparaturmechanismen. Die vermehrte Exposition und Aufnahme von Oberflächenmembranmerkmalen stellte die Beteiligung der ASM-Aktivität an der Internalisierung von *S. aureus* durch nicht-professionelle Phagozyten wie Endothelzellen in Frage. Durch Modifikation des ASM-Expressionsmusters sowie Applikation von Inhibitoren war es möglich, die intrazelluläre Keimzahl zu reduzieren. Somit konnte ein direkter Zusammenhang zwischen ASM-Aktivität und den Infektionsmechanismen von *S. aureus* beobachtet werden. Diese Studie verdeutlicht somit, wie *S. aureus* den Sphingolipid-Stoffwechsel der Wirtszelle ausnutzen und für die Invasion in nicht-professionelle phagozytische Zellen nutzen kann

List of Figures

Diese Arbeit ist allen gewidmet, die mich auf diesem
unglaublichen und aufregenden Weg begleitet sowie unterstützt haben.
Ohne euch wäre Vieles nicht möglich gewesen.

Danke

Introduction

Endothelial Cells

Essential for homeostasis of body physiology and important regulator of immune signaling, endothelial cells (EC) line the inner walls of the vascular system. Commonly described with a cobblestone-like appearance, they are not rigid vessel building blocks, but rather responsible for controlled permeability of fluids, nutrition and even other cells. Whereas EC dysfunction is inevitably connected to disease development due to their strict mechanism of permeability control, they're an integral part to mediate directed immune response by actively changing transmissibility for e.g. immune cells [6]. Furthermore, their unique abilities are adapted to the surrounding tissue. Central nervous system EC form the distinct blood-brain barrier, EC of the endocardium are adapted to the constant heart function and arterial/venous EC exhibit specialized sprouting capacities [7-10].

Endothelial cell barrier

Essential for EC controlled permeability are flexible cell-cell connections. For this purpose, EC are decorated with multiple cell surface proteins expressed either on the apical or basolateral cell membrane. Alterations in their expression, distribution and structure allow a rapid reaction to intra- and extracellular stimuli, either permitting or prohibiting paracellular transport of water, ions, molecules or cells [11]. Cell-Cell connections may be compromised of tight junctions (TJ), adherence junctions (AJ) or gap junctions (GJ) [12,13]. Endothelial barrier function facilitated by TJ, AJ and GJ can be altered via interactions of EC with their microenvironment. Stimuli (e.g., neurotransmitter, cytokines) or conditions (hypoxia, proteolytic enzymes, reactive oxygen species) may either influence expression, relocation or phosphorylation of these proteins [14,15]. Again, as for EC in general, cell-cell connections are adapted to their specific surrounding tissue. The aforementioned EC compromising the blood-brain barrier form strong and highly restrictive barriers, whereas in other organs TJ on EC form specialized cavities, enabling rapid exchange of molecules [16].

Tight junctions

As for function, expression pattern of distinct TJ isoforms varies between different organs. The family of TJ is comprised of claudin, occludin, tricellulin, junction adhesion molecules (JAM), zonula occludens (ZO) and cingulin (Fig.1). These are usually

located on apical membrane surfaces and form the border between the apical and basolateral cell surface, although site of expression differs for TJ [17]. While claudin, occludin, JAM and tricellulin are transmembrane proteins, cingulin and ZO are cytosolic expressed scaffolding proteins associated to previous mentioned proteins [18-23]. By forming interconnected protein complexes, TJ operate as bidirectional signaling networks. Intracellular signals affect assembly and adhesion of transmembrane proteins, while transduction of extracellular stimuli have an impact on cell proliferation, migration and survival [24,25]. Additionally, TJ do not form exclusive connections with other TJ, in fact they are part of an interconnected network between AJ and focal adhesions, permitting cross communication and influence mutual assembly and function [26,27]. Noteworthy in this context are ZO proteins. They form transmembrane complexes with TJ, AJ and GJ and bind them to F-actin strains [28]. All three isoforms (ZO-1, ZO-2, ZO-3) convey important signal transduction pathways associated with gene expression and cell growth, hence their frequent nuclear localization after specific signaling events [29]. Furthermore, loss of function in ZO-1 and ZO-2 are directly linked to an increased permeability in epithelial cells [30]. A common alteration to influence TJ is the phosphorylation of these complexes, while higher phosphorylation is associated

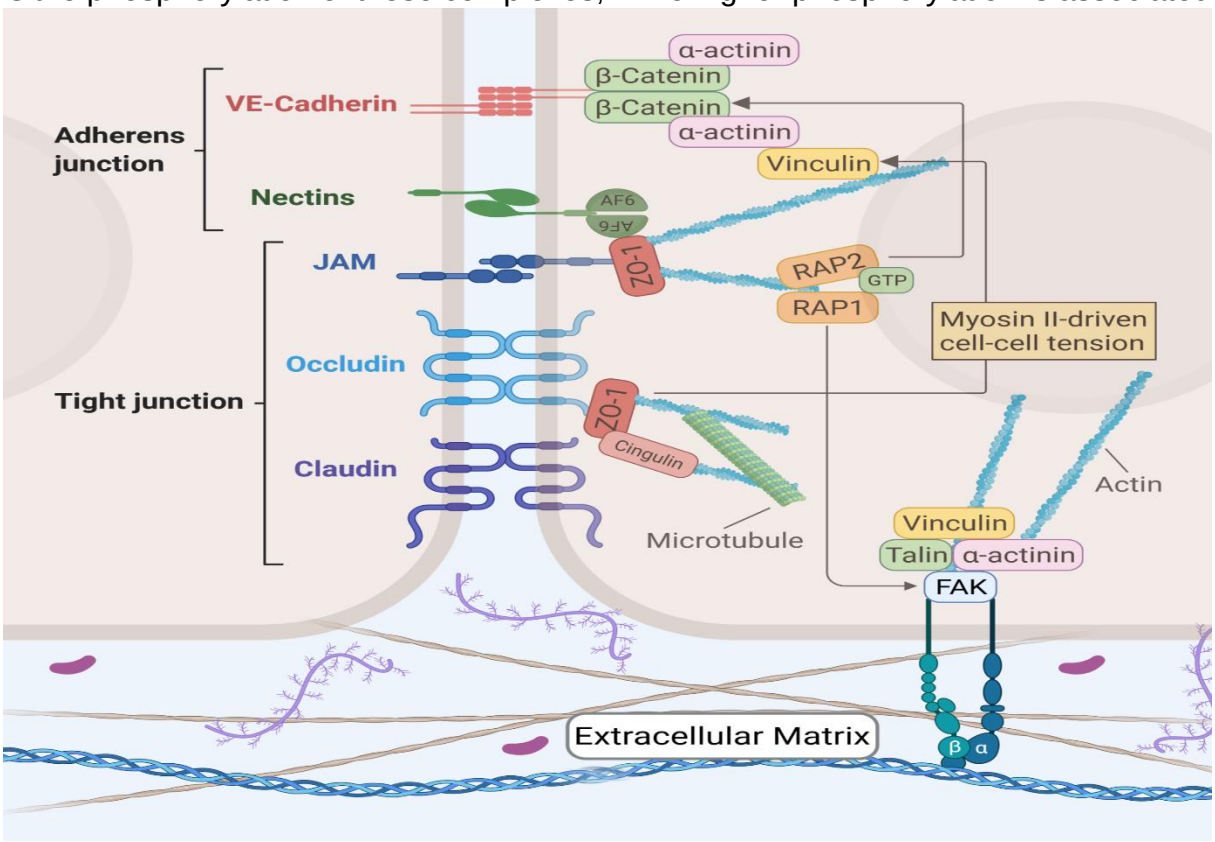

Fig. 1 ***Cell-Cell and Cell-ECM interaction points***
Intercellular connections via transmembrane proteins like adherence junctions or tight junctions form intricate networks, which are able to process extracellular signals and regulate intracellular as well as extracellular mechanisms like gene regulation or cell growth. Created with BioRender.com

to increased permeability and lower trans endothelial electrical resistance (TEER) [11,31]. The same applies to EC, where proinflammatory cytokines (IL-6, TNF-α) lead to a reduced expression and increased phosphorylation of ZO-1, increasing paracellular permeability [32,33].

Adherence junction

The basic structure of AJ in EC is supported by vascular endothelial cadherin (VE-Cadherin), which may interact with multiple cytosolic proteins [34]. The calcium-dependent adhesion glycoprotein consists of five extracellular repeats, a transmembrane domain and a highly conserved intracellular tail [35]. VE-Cadherin is one of the earliest EC-specific markers during development of vasculature and embryonic stem cell differentiation [36,37]. Thereby it participates in establishment of cell polarity and lumen formation in large vessels [38,39]. Although VE-Cadherin is not required for vessel formation, it is necessary for cell-to-cell contact. Ablation of VE-Cadherin results in uncontrolled sprouting and branching of EC, since they are not able to sense their neighboring cell. Therefore, it appears that VE-Cadherin plays a crucial role in regulating cell growth and mediating vascular stability [40,41]. In resting confluent cell monolayer, VE-Cadherin molecules form networks, allowing for signal transduction between each cell. Combined with a multitude of intracellular interaction partner, signaling via VE-Cadherin influences a myriad of cellular processes [34]. In a similar manner, EC are expressing N-Cadherin, which has been shown to be a substitute for VE-Cadherin. However, both proteins do not form heterodimeric interactions and expression of VE-Cadherin displaces N-Cadherin from AJ [34,42]. N-Cadherin is not exclusively expressed on EC and associated to cell adhesion and different cell signaling events [43]

The EC barrier – selective interaction partner and pathogen target

As highlighted previously, EC barrier integrity via its adherence and tight junction proteins is vital for selective transport or vascular stability. Further, proinflammatory cytokines may influence the permeability of the EC barrier, which is pivotal for a proper immune response. In case of localized tissue inflammation, a concerted response of EC results in the adhesion of circulating leukocytes and further invasion into the tissue. This multi-step process is facilitated by physical, chemical and biological factors which may lead to vasodilation [44,45]. In case of VE-Cadherin this would result in a reversible disengagement of homophylic interactions, thus increasing intercellular permeability

[46]. As leukocytes, pathogenic bacteria trigger similar effects resulting in major EC reorganization as well. For further establishment and invasion, pathogens need to cross the endothelial barrier to access tissue for dissemination. Therefore, pathogens evolved mechanisms to interact, manipulate or kill EC to disrupt cell barriers, preventing them from invading subjacent tissue. This reorganization of EC is caused via specific inhibitors or enzymes, which can degrade proteins crucial to maintain cell-cell contacts [47].

Staphylococcus aureus

Fig. 2 ***S. aureus* Electron Microscopy**
Picture G.Holand – Colouring by A.Schnartendorff – published by RKI [2]

One of those pathogenic bacteria is named after golden grape-cluster berries – a rough translation for *Staphylococcus aureus* [48,49]. Eponymous are its visual characteristics in form of golden-yellow pigmentation and clustered appearance under a microscope [50]. *S. aureus* is a commensal bacterium as part of the human flora. Such as other species of *Staphylococcus* (e.g., *S. epidermidis*) it colonizes the skin and mucous membranes (e.g., nasal area) of healthy individuals [51-53]. Despite its occurrence as a commensal bacterium, *S. aureus* is causative for a variety of diseases and labelled as the staphylococcal species with the highest pathopotency, further classifying it as a pathobiont [54-56]. It is a *Gram*-positive bacterial species, which can grow in temperatures between 18 – 40°C under aerobic as well as anaerobic conditions [57]. To distinguish *S. aureus* from other staphylococcal species, tests are applied for presence of catalase and coagulase activities, e.g. catalase activity (pathogenic *S. aureus* species), coagulase positive (differentiation from other species), novobiocin sensitivity (distinguish from *S. saprophyticus*) or mannitol fermentation (distinction from *S. epidermidis*) [54]. The main reservoir for *S. aureus* is humans, however it may colonize livestock and wildlife animals as well, leading to diverse transmission routes associated with *S. aureus* infection [58].

The development of antibiotic resistant *S. aureus* strains

Widespread introduction of penicillin in the early 1940s for treatment of bacterial infections caused the emergence of penicillin-resistant *S. aureus* strains a few years later [59,60]. Consequently, by 1960 these strains became pandemic and their prevalence remains high even to date [61]. Introduction of the antibiotic Methicillin in 1959 led to new treatment options, but also marked the beginning of a second wave of resistances with reports of Methicillin-Resistant *S. aureus* (MRSA) strains as early as 1961 [62,63]. Introduction of novel antibiotics was shortly after associated with the occurrence of intermediate or resistant *S. aureus* strains. Increasing cases of MRSA infections since the 1960s led to an increased usage of Vancomycin, which is considered a critical human drug and last resort antibiotic [64]. Under selective pressure of Vancomycin, new intermediate and resistant *S. aureus* strains (VISA / VRSA) have been isolated in clinical environments [65,66]. As already indicated, infection with MRSA are mostly associated with clinical environments and had their peak in Europe 2004 [67], but since 2012 a decline in case numbers is observed [68]. Independent of hospital acquired MRSA (HA-MRSA) infections, an increasing number of community acquired MRSA (CA-MRSA) infections is occurring since early 2000s. CA-MRSA are merely descendants of nosocomial MRSA strains, but rather differ in their genotype [69]. Moreover, these strains appear to be especially virulent, with the emergence of two distinctive cassette elements carrying *mecA* and genes encoding Panton-Valentine leukocidin (PVL), resulting in fulminant infections [70-72]. While circumstances in Germany were improved in the past decade, the ever emergence of new strains resistant to antibiotics and increased prevalence outside of hospitals might be a challenge in the near future. OECD (Organisation for Economic Co-operation and Development) predictions from 2019 are registering an increase in resistance to second- and third-wave antibiotics all across Europe, which in return will most probably lead to higher fatalities and high expenses for treatment of antimicrobial resistant (AMR) bacterial infections [73,74].

S. aureus virulence factors

As described beforehand, *S. aureus* can induce diverse diseases and is associated to difficult treatment. The pathogen may interact in different ways with its host and more specific with certain cell types due to an expression of a variety of virulence factors like exotoxins, surface receptors and enzymes. Each these factors are associated with

special events and simultaneously crucial for the establishment as well as dissemination of *S. aureus*.

α-toxin

One of the most prominent and well-studied toxins of *S. aureus* is the β-barrel pore-forming toxin (PFT) α-hemolysin (α-toxin, Hla). Secreted as soluble monomers, it binds to target membranes and oligomerizes into a heptameric structure (Fig.3) [75]. While new host cell interactions and effects on them are reported up to date, the lethal effects of *Hla* are known since the 19th century [76,77]. The initial event for an extensive investigation of staphylococcal α-toxin is reported to be the tragedy of Bundaberg in 1928. Burnet could show, that a staphylococcal contamination in diphtheria toxin immunization were responsible for the death of 12 children [78]. It wasn't until 1935 that the term α-toxin was formed by Glenny and Stevens [79]. Further proceedings in the isolation and purification of *Hla* in the 1960s allowed for distinct investigations and findings about structure and molecular events that helped expanding the understanding of this toxin [80,81]. These findings were responsible for the identification of binding targets on host cells. Main interaction partner is A Disintegrin and metalloproteinase domain-containing protein 10 (ADAM10) [82]. Beside the specific interaction with a proteinaceous receptor, staphylococcal α-toxin is reported to interact with cell membrane lipids [83]. Depletion of specific membrane contents or enzymatic digestion of lipids abrogates the binding of *Hla* [84,85]. In case of ADAM10, binding leads to a translocation into caveolin-1 enriched lipid rafts as well as activation of the sheddase, which initiates the disruption of cell-cell junctions [82,86]. Once the α-hemolysin pore is established, several events may occur, depending on toxin concentration or time of membrane disruption [87]. As a direct result of membrane disruption, a rapid ion in- and efflux will occur, enabling the uncontrolled exchange of K^+ and Ca^{2+} or molecules up to a size of 4 kDa [88]. Further it has been shown that

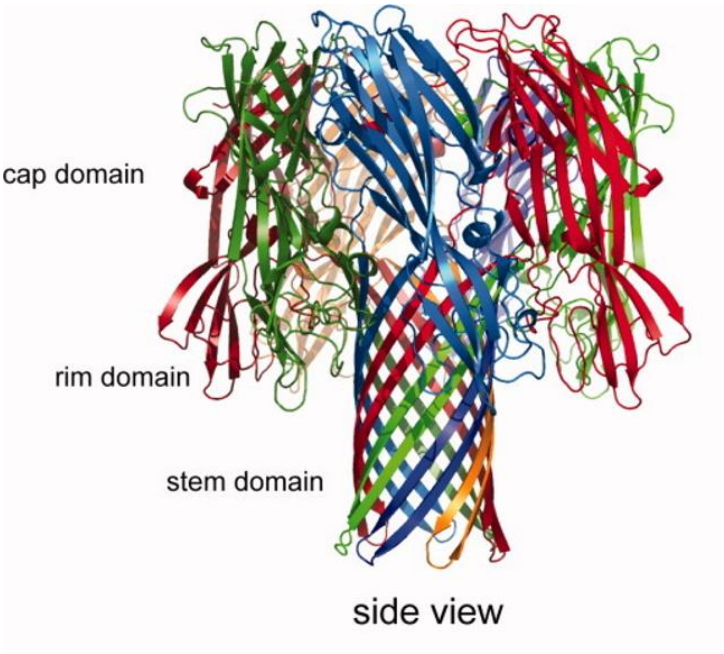

Fig. 3 ***S. aureus α-Toxin*** *Figure by Tanake et al.* [3]

varying toxin concentrations trigger host cell reactions, e.g., cytokine release, cell proliferation or cell death [89-91]. The effects reported for α-toxin are essential for *S. aureus* virulence and are considered the main contributor in development of diseases. During the second wave of antibiotic resistant *S. aureus* strains in 1950s and 1960s many patients suffered from skin/soft tissue infections, pneumonia, and sepsis [92,93]. Analysis of these strains revealed an increased expression of α-hemolysin, which is consistent with findings of current epidemic MRSA strains, e.g., USA300 [94,95]. Although its significant impact on disease establishment, Hla may impact host organs and tissues differentially. In animal models a reduced virulence of *S. aureus* Δ*hla* strains was registered for pneumonia, sepsis and skin infection, while increased expression were beneficial in some instances, e.g., endocarditis [81][96-98].

β-toxin

Described as a hot-cold toxin, *S. aureus* β-hemolysin (β-toxin, Hlb) may inflict lysis of various cell types [99-101]. First described by Glenny and Stevens in 1935 and sequenced in 1989, it was discovered that the observed hemolytic activity of β-toxin depends on cell membrane components, proposing sphingomyelin as a crucial factor for lytic activity [79,99,102,103]. In contrast to staphylococcal α-hemolysin, the hemolytic activity of β-toxin does not dependent on membrane pore formation. So far, the direct mechanism remains elusive but is proposed to be facilitated by the enzymatic duality of Hlb [102]. On the one hand staphylococcal β-toxin acts as a biofilm ligase, binding extracellular DNA into a nucleoprotein matrix, which is linked to establishment of biofilm *in vivo* [104]. On the other hand, it displays a phosphatidylcholine phospholipase C activity, promoting the cleavage of sphingomyelin on target cell membranes, thereby acting as a bacterial neutral sphingomyelinase (bSM) [105]. Common expression of β-hemolysin is associated with infection in animal, e.g. bovine mastitis, whereas expression in human is rather uncommon [106]. Low expression is caused by prophage lysogeny in human *S. aureus* strains, carrying the specific bacteriophage ΦSa3. However, recent publications were able to reveal a regulatory switch, which enables *S. aureus* to excise ΦSa3 from its genome and induce the expression of β-hemolysin [107,108]. Since β-toxin is involved in biofilm formation and production of vegetation in animal models, it is proposed that staphylococcal β-hemolysin acts as a crucial virulence factor in humans as well [108]. Cystic fibrosis patients, which were treated with ciprofloxacin and trimethoprim, exhibited chronic lung infections with β-toxin producing *S. aureus* strains [109,110].

Leukotoxins

Staphylococcal leukotoxins are PFT with a specific affinity for leukocytes. Leukotoxins consist of two distinct protein compounds and assemble into β-barrel octameric pores on target cell membranes [111,112]. Depending on composition, different leukocyte cell types are lysed [113]. Each leukotoxin is attributed to different events, involving *S. aureus* survival, lysis of neutrophils or colonization [114-117]. The most debated leukotoxin is PVL, since it is suggested to be involved in high virulence CA-MRSA strains. While PVL is only present in a small percentage of clinical *S. aureus* isolates (~5%), 85% of CA-MRSA infections, which cause severe cases of pneumonia and skin/soft tissue infection, exhibit expression of PVL [113]. Clinical studies revealed a higher fatality rate in patients, which were infected with PVL-positive *S. aureus* strains versus those infected with PVL-negative strains [118]. Additionally, PVL-positive strains were linked to higher capability for fatal infection in healthy people [119].

Phenol-soluble modulins

Described by Mehlin et al. in 1999, phenol-soluble modulins (PSMs) are three distinct peptides (PSMα, PSMβ, PSMγ) acting as a pro-inflammatory complex [120]. PSMs differ in their charge characteristics and attack cytoplasmic membranes in a non-specific way, resulting in membrane damage. Their ability to spread on cell surfaces is linked to biofilm formation [121]. Oligomerization of PSMs leads to pore formation, inducing inflammatory responses as well as lysis of human neutrophils, further promoting invasive infections [122,123].

S. aureus adhesive cell wall proteins

Survival of *S. aureus* heavily depends on its ability to adapt to environmental changes and the ability to interact with it. With a genomic size of ~2,8 mb, resulting in the expression of ~2700 proteins, only 24 proteins are expressed as cell wall-anchored proteins (CWA) [124-126]. While coagulase-negative staphylococci express fewer CWA, their general expression depends on environment, nutrition availability and growth stage [127-129]. CWA consist of proteins covalently attached to peptidoglycan and are classified after their structural motifs, e.g., microbial surface component recognizing adhesive matrix molecule (MSCRAMM) [125]. One of the most prominent CWA, staphylococcal immunoglobulin binding protein A (SpA), is essential for *S. aureus* immune evasion. SpA has been shown to be involved in establishment of persistent colonization, whereas attachment of SpA to host cell receptors induce specific signal

transduction events [130]. Interaction with tumor-necrosis factor receptor 1 (TNFR1) readily activates intrinsic cell death pathways triggering activation of cysteinyl-aspartate specific protease 8 (Caspase 8/Casp8) and successive release of tumor necrosis factor α (TNFα) of infected cells [131,132]. In B cells, SpA may act as a superantigen which leads to upregulation of CD95 and activation of caspases, inevitably triggering apoptotic signaling events [133]. Furthermore, adherence to platelets is facilitated via binding of SpA to von Willebrand factor (vWF), indicating an essential step for adherence of circulating *S. aureus* to immobilized collagen [134,135]. In addition, adherence to extracellular matrices (ECM) like collagen may be facilitated by collagen binding protein (Cna). Binding of collagen is facilitated through the collagen hug, a specific conformational change in Cna protein structure allowing for high-affinity adherence to collagen-rich tissue [136]. Binding of collagenous domains is not limited to cell surface targets since binding to collagenous domain of complement protein C1q has also been reported. This binding interferes with interaction of classical complement proteins, preventing formation of the C1 complex [137]. Despite indicated by its name, Cna acts as a multifunctional adhesive protein, promoting adherence to laminin, although with a lower affinity compared to collagen interactions [138]. Laminin specific interactions were already reported in 1985 and attributed to *S. aureus* ability for tissue invasion, hence laminin interaction could not be reported in non-invasive *S. epidermidis* strains [139]. Another major component of ECM are fibronectins, which are bound by fibronectin binding proteins (FnBPs). Fibronectin contains arginine-glycine-aspartate sequences that are readily recognized by e.g., highly expressed α5β1 integrin [125,140]. This specific interaction of *S. aureus* FnBPs and host cell α5β1 integrin via a fibronectin bridge was proposed as a key factor for invasion of *S. aureus* by Sinha in 1999 [141]. Efficient translocation of *S. aureus* through intact endothelial cell layers heavily dependents on FnBP expression, as indicated for numerous strains[142-144]. However, translocation negatively correlates with high expression of hemolytic factors as well as recruitment of intercellular adhesion molecule 1 (ICAM-1). Moreover, strains with minimal impact on transendothelial electrical resistance (TEER) and effective hemolytic activity on sheep blood agar were able to efficiently transmigrate. Early breakdown of barrier function could not be attributed to hemolytic activity of *S. aureus*, but rather intracellular interactions of *S. aureus* within endothelial cells [145].

S. aureus specifically targets EC barrier proteins

In case of *S. aureus,* the staphylococcal PFT α-toxin exhibits a major impact on EC. Binding of its specific receptor, ADAM10, leads primarily to disruption of VE-Cadherin and other cell-cell junctions, contributing to sepsis severity, secondary to induction of apoptosis in EC [146]. Furthermore, Hla has been shown to manipulate neutrophil adherence to endothelium. Increased adherence leads to vasoconstriction and evokes major endothelial dysfunction, hence intensifying paracellular permeability [147]. In aortic endothelial cells *S. aureus* β-toxin was able to inhibit IL-8 production, expression of vascular cell adhesion molecule 1 (VCAM-1) and impacts membrane morphology via its bSM activity [148]. Other toxins involved in EC interaction are *S. aureus* LukED and γ-hemolysin AB. Both toxins can bind to duffy antigen receptor for chemokines (DARC), resulting in pore formation damaging endothelial cells [149]. Effects which do not directly target EC but affect EC behavior have been observed for *S. aureus* toxins as well. PSMα4 provokes the release of heparin-binding protein (HBP) from neutrophils [150]. HBP in return is readily taken up by EC, increasing the expression of adherence proteins for neutrophils on the cell surface [151]. Finally, HBP induces a rearrangement of the endothelial cytoskeleton affecting cell-to-cell junctions and forming paracellular gaps promoting vascular leakage [152,153].

Plasma membrane repair counteracts effects of toxin on EC

Although not immune cells, EC possess several abilities to circumvent deleterious events exerted by pathogens. In case of *S. aureus* infection, EC may decrease the expression of α-toxin specific receptor ADAM10 on the cell surface by influencing post-transcriptional autophagy processes [154]. Autophagy, usually a natural process for cells to remove unnecessary or dysfunctional cell components, can be directed against invasive pathogens [155]. The process of foreign-eating, labelled as Xenophagy, is facilitated by engulfing the intracellular pathogen with isolation membranes, transforming them into autophagosomes, which then turn into pathogen-degrading autolysosomes [156,157].

Beside other intracellular immune receptors, e.g., melanoma differentiation-associated protein 5 (MDA5), retinoic acid inducible gene I (RIG-I) or toll like receptor (TLR), responsible for expression of cytokines, EC developed delicate strategies to repair membrane lesions caused by PFT [158,159]. Hereby plasma membrane (PM) repair can be divided into two distinct types, one revolving around exocytosis of membrane

patches, the other one utilizing endocytosis of membrane pores [160-163]. In both cases Ca^{2+} serves as a major trigger for induction of PM repair. Hence intracellular Ca^{2+} is actively maintained on low concentrations, the sudden change of localized and transient available Ca^{2+} via pore formation trigger cytosolic Ca^{2+} binding proteins to induce PM repair mechanisms [158,164].

As for endocytotic or exocytotic PM repair, ubiquitous proteins are required for proper sealing of membrane injury. The nonlysosomal cysteine proteinase Calpain has been shown to be involved in cytoskeletal clearance and employed for proper vesicle patch fusion [165,166]. Further, the family of Annexins, a phospholipid binding protein, is heavily involved in endocytosis and exocytosis of membrane patches or vesicles respectively. Depending on injury type, different isoforms of Annexins may be recruited, rendering them useful tools to investigate PM injury which has not been further identified [167-169].

Exocytosis as a bifunctional PM repair process

Exocytosis in PM repair enable eukaryotic cells to rapidly seal membrane injury sites and restore integrity. Therefore, two distinct models have been proposed and observed. One model involves the recruitment of peripheral vesicles, which fuse into a larger membrane patch, effectively sealing the wound site [170,171]. On the other hand, reduction of PM tension by extending PM surface size through vesicle fusion closes the gap left behind on injury sites (Fig. 4). Restoration of a disordered lipid phase to a continuous lipid bilayer facilitates rapid PM repair [172]. The vesicles utilized to expand membrane surface or for construction of large membrane patches are ubiquitously lysosomes. Although traditionally identified and regarded as organelles of terminal degradation, they were found to rapidly fuse with the plasma membrane in response to rapid changes in Ca^{2+} concentration [161,173]. Hereby lysosomal exocytosis acts bifunctional. Beside the repair mechanism, the degradative contents of lysosomes are released into the extracellular space. Although the extracellular space does not provide the optimal pH range of lysosomal enzymes, they are still able to act as defensive enzymes to digest pathogenic structures [174-176].

Endocytosis rapidly mends PM injury

The iterations crucial for PM repair are seemingly an increase of intracellular Ca^{2+} concentration and exocytosis of lysosomes. However, not in all cases of PM injury shedding of vesicles, recruitment of membrane patches or decrease of PM tension can be observed. In a different process, injured cells undergo a massive endocytosis event

after a Ca^{2+} triggered lysosome exocytosis occurs [162,163]. This unusual form of endocytosis acts independently of classical endocytosis markers (e.g., Clathrin) or ATP and depends on the presence of cholesterol in surface membranes [162]. Additionally, the lysosomal protein acid sphingomyelinase (ASM) initiates endocytosis and facilitates sealing of membrane pores. Externally added ASM has been shown to be beneficial for PM repair [177,178]. ASM activity at the outer cell surfaces initiates a degradation of sphingomyelin into ceramide, promoting formation of ceramide-rich platforms (CRP). This change of the outer PM leaflet results in a steric shift, inducing an invagination of CRP [179]. As a direct result membrane pores, such as bacterial PFT, are endocytosed and directed to degradation organelles [158,180].

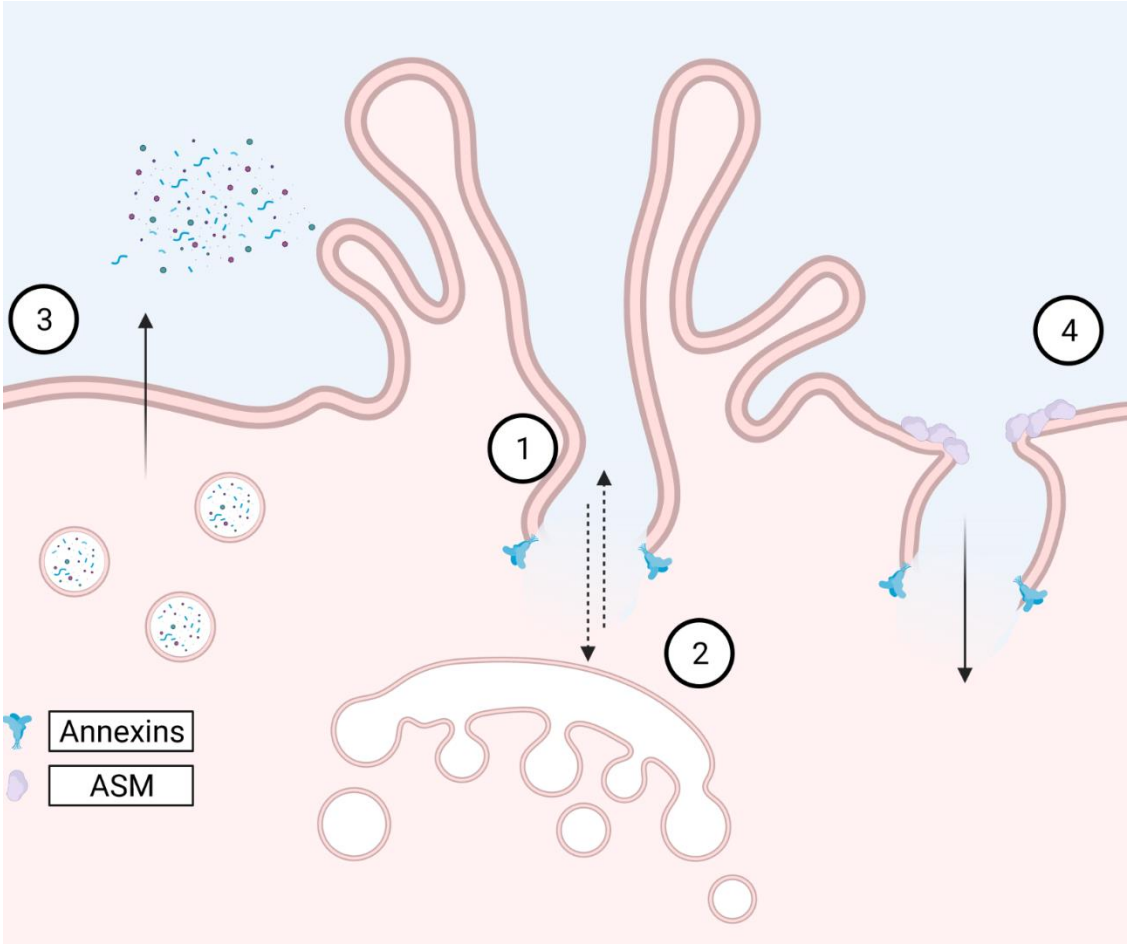

Fig. 4 ***PM repair counteracts effects of pathogen virulence factors***
*(**1**) Disruption of cell membrane integrity disables homeostatic ion concentrations. Rapid efflux as well as influx initiate manifold signaling pathways, leading to apoptosis, cell survival or plasma membrane repair mechanisms. (**2**) Sudden influx of Ca^{2+} may enable the fusion of peripheral vesicles into larger membrane patches, which act like a plug for the damaged membrane part. (**3**) Simultaneously exocytosis of peripheral lysosome caters to lessen the membrane tension as well as release lysosomal proteins, important for resealing of the membrane as well as degradation of extracellular pathogens. (**4**) Instead of sealing the plasma membrane with large patches, cells may endocytose membrane lesion entirely. Therefore, activity of lysozymes and the acid sphingomyelinase are important. In all described cases different types of Annexins are involved, facilitating the closure of membrane lesions, budding of intracellular vesicles to the plasma membrane or contribute to endocytosis. Created with BioRender.com*

S. aureus host cell invasion

Despite once classified as an obligate extracellular bacterium, *S. aureus* may invade and survive in host cells. First reports of this facultative intracellular phenotype were made by Hamill et al. in 1986, describing phagocytosis of *Staphylococci* connected to fibronectin availability[181]. Hereby adherence of *S. aureus* by interaction of FnBPs and α5β1 integrin was found to be major factor for invasion [141,182,183]. Since then the involvement of several other receptors were verified for uptake of extracellular *S. aureus*, some utilizing ECM contents, others independent of intermediate substrate [184]. Hence *S. aureus* was up until recently classified as an obligate extracellular bacterium, the intracellular life cycle raised question about the advantages it has to offer.

Persistence in immune and non-professional phagocytotic cells

In this context a differentiation between invasion/uptake of *S. aureus* by either professional or non-professional phagocytes must be made. Staphylococci infecting skin tissue may be phagocytosed by neutrophils but instead of being digested, *S. aureus* is able to reside in these immune cells. Further translocation of neutrophils contributes to metastatic dissemination, leading to infection of bone or heart tissue [185]. Neutropenic patients are less common to develop *S. aureus* bacteremia and if extinguished within first 48h, only 5% of these patients develop further complications. However, patients suffering from prolonged bacteremia persisting beyond 3 days, develop in 40% of cases additional complications, induced by resurfacing *S. aureus* hidden in tissue [186-188]. Prior to colonization of *Pseudomonas aeruginosa*, lungs of cystic fibrosis (CF) patients incur infection with *S. aureus*. Publications have shown that macrophages of CF mice readily internalize *S. aureus* present in the lung, but were incapable to lyse the bacteria. Hence this phenotype was proposed to be as result of insufficient fusion of phagosomes and lysosomes, contributing to chronic *S. aureus* infection. Healthy animals were able to clear *S. aureus*, directly linking this phenotype to CF [189].

Regarding infection of healthy donors, invasion into non-professional phagocytes offers protection from extracellular host defense mechanisms. Uptake by epithelial or endothelial cells have been reported on several occasions and is associated with small colony variants (SCVs) exhibiting increased antibiotic resistance as well as decreased metabolic activity [190-195]. First described in 1995, SCVs were attributed to persistent

and relapsing *S. aureus* infections as one of the first indicators for intracellular *S. aureus* causing chronic infection in patients [196]. In general SCVs are bacterial variants of *S. aureus* distinct in their metabolic genes, which develop through spontaneous mutations provoked through environmental stress factors (e.g. antibiotics) [197]. Especially this distinct auxotrophic bacterial subpopulation is linked to intracellular persistence. They are often found jointly growing with their wildtype counterpart but are rapidly outgrown, since their altered metabolism leads to longer generation time. This adaptation in metabolism and reduced expression of virulence factors (e.g. α-hemolysin) favor SCVs for intracellular life cycle [197]. Once *S. aureus* resides in intracellular compartments, they are associated with LAMP1 positive lysosomes or phagosomes [191,198]. Despite their reduced bactericidal properties compared to professional phagocytes, phagosomes of non-professional phagocytes exhibit antibacterial properties (e.g. acidification to pH 4.5) [199]. However, *S. aureus* inherits manifold strategies to counteract host cell antimicrobial activities, hence rendering them well equipped to survive inside intracellular compartments with abilities to modulate the intracellular microenvironment [200-202].

As reported for other pathogens, such as *Listeria monocytogenes*, *Shigella* and *Rickettsia* [203], *S. aureus* may escape its intracellular compartment as well. Phagosomal escape is directly associated with host cell death induction, since cells expressing cytoplasmic Lysostaphin were resistant against apoptosis [204]. Staphylococcal α-toxin has been labelled crucial for phagosomal escape; however Hla is expressed in an *accessory gene regulator* (*agr*)-dependent manner and all SCVs known are functionally deficient in *agr* system functions [205]. Yet transition to cytoplasm is facilitated by an *agr*-dependent factor, since translocation of *agr* deficient *S. aureus* strains does not occur [206]. Recent findings exhibited an increased expression of *agr*-system prior to phagosomal escape, which might be induced by phagosomal acidification [207,208]. Instead of proposed *S. aureus* α-hemolysin, PSMα found to be an essential mediator of phagosomal escape [208]. Hereby a concerted interplay between PSMα and additional factors appear to be necessary for phagosomal escape since non-escaping *S. aureus* strains overexpressing PSMα were still residing in intracellular compartments [206].

Consequences of escaping the phagosomal vesicles

Escape of *S. aureus* not only is connected to replication, but likewise to induction of cell death pathways in different cell types [209-211]. Hence *S. aureus* is expressing CWA and secreting proteins depending on its microenvironment or growth stage, various cell death pathways have been described so far. Likely dependent on cell lineage, *S. aureus* induces release of TNF-α and Interleukin-1 (IL-1) or production of TNF-related apoptosis-inducing ligand (TRAIL) while downregulating its decoy receptor osteoprotegerin (OPG) revealing *S. aureus* ability to induce extrinsic cell death pathways [212,213]. Simultaneously, intracellular *S. aureus* has been reported to induce shedding of biological active Fas ligand, whereby autocrine activation of surface expressed Fas is initiated, leading to the consecutive activation of Casp8 as part of the mitochondria-dependent intrinsic apoptosis pathway [214,215]. Beside classical apoptosis pathways, other cell death programs like pyroptosis, necrosis or autophagy were observed for cells infected with *S. aureus* [216-218]. Relevant parameter for *S. aureus* mediated cytotoxicity and invasion was revealed to be calcium-associated genes [219]. Stelzner et al. was able to provide insight into *S. aureus* influence on intracellular Ca^{2+} homeostasis and how it is affected during infection. Whereas secreted virulence factors induce a rapid oscillating Ca^{2+} influx, infection with *S. aureus* strains lacking virulence factors exhibited no significant change in cytoplasmic Ca^{2+} release. Furthermore, additional evidence for manipulation of intracellular Ca^{2+} storages was observed, indicating a process in which intracellular stores are depleted, thus leading to an influx of extracellular Ca^{2+} for replenishment of intracellular storages [219]. Accompanied with all Ca^{2+} dynamics is the activation of effector caspases 3/7, which are directly linked to apoptosis induction and cell lysis [220]

Sphingolipid metabolism

As an integral component, sphingolipids are crucial for plasma membrane function and beforehand mentioned repair mechanisms [158,221]. Albeit the concept of bioactive lipids remains not as a novel idea, only recent studies of the past decade were able to unravel the unprecedented and unanticipated complexity of these molecules. Early studies about inositol phospholipids and prostaglandins showed for the first time, that defined lipid species may elucidate specific stimuli [222]. Today an understanding of lipid metabolism has been established, exhibiting the highly regulated and complex changes in lipid molecules throughout the whole cell. Concomitant understanding of

lipid metabolism and their distinct cellular responses to changes in lipid composition or lipid-specific stimuli.

Dysfunctional sphingolipid metabolism contribution to disease

The before referred ASM is one of many enzymes involved in sphingolipid metabolism, influencing ceramide concentration and ceramide configuration as well. In 1914, the first patient with Niemann-Pick disease (NPD), a medical condition induced by sphingolipid accumulations as a result of reduced ASM activity, was described by German pediatrician Albert Niemann [223]. It was not until 1930 that the primary lipid accumulations were identified as sphingomyelin (SM) [224]. It took another 36 years, until Barnholz, Roitman and Gatt in 1966 were able to extract an enzyme, which readily hydrolyses sphingomyelin into ceramide and phosphoryl choline, labelling it as sphingomyelinase [225]. A Year later Schneider and Kennedy detected the absence of said enzyme in patients suffering from the lysosomal storage disorder Niemann-Pick disease [226]. Since then, more than 100 clinically relevant missense mutations of the ASM gene *SMPD1* were detected leading to enzyme variants with a decreased catalytic activity, causing autosomal recessive NPD type A and B [227]. Symptoms described for NPD depend on related organs affected by sphingomyelin accumulations. Sphingomyelin clustering in the central nervous system may cause coordination issues of muscles (Ataxia), speech impediments (Dysarthia) and swallowing difficulties (Dysphagia). Additionally abnormal posture of limbs, trunk, and face as well as rapid eye movements have been described. Disease involving the cerebral cortex may cause gradual loss of intellectual abilities with onset of dementia as well as seizures. Prognosis on pathophysiology and expected quality of live is highly variable. Infantile neurovisceral NPD type A usually is fatal before the age of 3. For NPD type B mortality before adulthood is common, however many patients live through adulthood and may expect a normal life span [224,228-231].

Hence NPD is a relative rare disease, with an incidence of 1 in 250.000, ASM deficient mouse models were created in 1995 for a deeper understanding of biological mechanisms involved in this disease [232]. This animal model enabled extensive research on enzyme replacement therapies and led to first clinical trials for NPD patients. More so did studies with these animals revealed the importance and unexpected role of ASM in distinct cellular events [227,233]. Beside genetical modified animal models, weak bases have been shown to inhibit ASM activity [234]. Hence some

of these inhibitors were already licensed via US Food and Drug Administration (FDA) as bioactive compounds and used as tricyclic antidepressants, they were posing a readily alternative to study ASM kinetics [235]. Functional inhibitors of ASM (FIASMA) are indirectly inhibiting SM conversion by accumulation in lysosomes, resulting in a protonation of vesicles. As a direct result ASM detaches from the lysosomal membrane, rendering it vulnerable against proteolytic degradation [236-238]. Direct inhibitors of ASM have been shown to be highly effective, however they suffer from accelerated resorption of bone tissue *in vivo* and low membrane penetration, cellular uptake respectively [239]. Nonetheless, with these opportunities observations about host/pathogen interactions were undertaken and revealed a prominent role of ASM for a variety of virus and bacteria [240,241].

Ceramides as a mediator of life and death

The aforementioned ASM acts as an example in the complex network of lipid metabolism. As one of the major eukaryotic lipid classes, sphingolipids are found to be involved in manifold cellular mechanisms. Starting point for the *de novo* biosynthesis of sphingolipids is the action of serine palmitoyltransferase in the endoplasmatic reticulum, utilizing serine and palmitoyl-CoA. Sequential enzymatic steps lead to the generation of ceramide, which may be further incorporated into complex sphingolipids such as sphingosine, glycosphingolipids (GSL) or sphingomyelin [242]. Ceramides are composed of a sphingosine molecule linked by an amide to a fatty acid residue. Modification of the 1-hydroxyl moiety by addition of a sugar residue will yield GSL. They are primarily expressed on the outer PM leaflet with sugar residues facing the extracellular space [243]. Feature of GSL seem to be rather basic, ranging from cell-cell interactions and modulating proteins on the same plasma membrane. For survival of singular cells GSL are not necessary, since they are still able to differentiate and proliferate [243]. However, for development of an entire organism GLS are indispensable, hence it is consensus that GSL mediate and modulate intercellular coordination in multicellular organism [243,244]. Modifications are not restricted to sugar residues, yet chain-length of fatty acid residues determine specific characteristics of ceramides. To generate ceramides with varying chain lengths, mammalian cells may express six different isotypes of ceramide synthases (CerS) [245-247]. Regarding their specific properties, ceramides are often described in a general manner, yet specific ceramides can be attributed to distinct effects. In case for autophagy, there is evidence that balance between long-chain (C14-C20) and very long-chain (C22-C26) ceramides

is crucial for induction of autophagy, which further has been described as an integral part of host cells act against pathogens [156,248]. Another example for chain-length specific effects of ceramide is the induction of apoptosis. Ceramides have long been implicated as a key factor for apoptotic pathways after responses to stimuli such as cytokines, radiation, or heat shock [249-251]. However, further investigations revealed a connection between higher expression of specific CerS or in ASM activation resulted in a shift in ceramide chain-length distribution, finally inducing apoptosis [252,253]. Although it has to be noted, that exogenous applied C2-C8 ceramides may redistribute in a non-physiological manner. Therefore, experiments conducted with short-chain ceramides must be interpreted carefully regarding their natural occurring counterparts [254,255]. As a breakdown product of ceramide, facilitated by ceramidases, sphingosine holds bioactive properties [251]. Further modification of sphingosine via phosphorylation yields sphingosine-1-phosphate (S1P), which labels the exit product of sphingolipid metabolism. Further enzymatic modification from S1P lyase dismantles S1P in single contents that finally yields fatty acyl-CoA [1]. As for other sphingolipid substitutes, S1P acts in various cellular mechanisms, e.g., inflammation [256] or autophagy [257].

ASM as an interaction factor for pathogens

In humans two distinct isoforms of ASM may arise from a single *SMPD1* gene as a result of different posttranslational modifications and trafficking processes [258]. One isoform resides in endolysosomal compartments (L-ASM), whereas the other form is released via the secretory pathway (S-ASM) [259]. Both forms differ in their molecular weight and glycosylation. Additionally does S-ASM possess an exceptional longer halftime and depends on the availability of Zn^{2+} [260,261]. Whether they act on different type of SM at membranes or exhibit different results via generation of differing ceramide products remains elusive [261]. Although ASM is ubiquitous expressed, specific cell types secrete significantly higher amounts of S-ASM or produce larger amounts of L-ASM. EC have been demonstrated to be a major source of ASM secretion. Compared to other cells types, e.g. macrophages or fibroblasts, EC express 20-fold higher levels of ASM at basal level, which can further increase upon stimulation via inflammatory cytokines [262]. As already depicted for plasma membrane repair, ASM is not only of importance for cell homeostasis, but it may also act as a disease marker and is considered important for therapeutic applications [239,263].

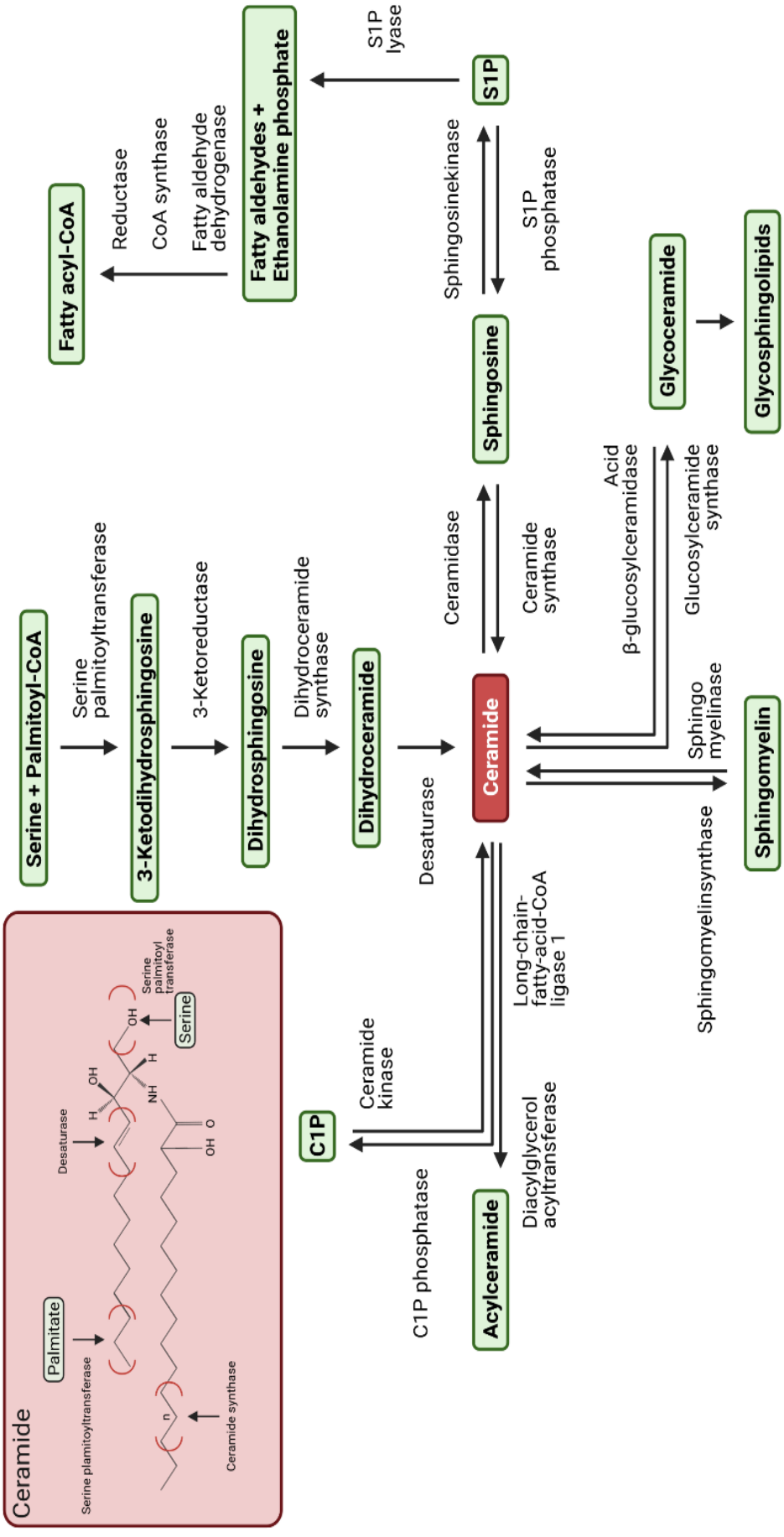

Fig. 5 ***Overview of sphingolipid metabolism***
De novo synthesis starts in the endoplasmatic reticulum by Serine palmitoyltransferase activity, followed by sequential reactions yielding ceramide. Ceramide is then included in various complex sphingolipids through modulation of the 1-hydroxyl position to generate C1P, sphingomyelin or glycoceramide. Catabolic reactions in lysosome deacylates ceramide to yield sphingosine, which may be further degraded into S1P. The sequential catabolism of S1P by S1P lyase marks the exit point of sphingolipid metabolism. [1]
Created with BioRender.com

The EC dependent release of S-ASM upon proinflammatory cytokine stimulation led to the assumption, that S-ASM may be involved in arteriosclerotic events [264]. Mice of advanced age have been shown to express higher concentrations of S-ASM, resulting in the elevation of certain ceramide species [265]. Further, ASM KO mice were shown to be protected against LPS induced sepsis, whereas WT mice were displaying an increased S-ASM activity [266,267]. However, ASM KO mice were affected by higher bacterial burden, increased phagocytotic events as well as enhanced cytokine storm [268]. Increased S-ASM activity have been implicated to be protective against invading microorganisms since hydrolysis of surface membrane SM have been shown to be crucial in primary immune reactions against pathogens [268-271]. Concomitant, sepsis inducing pathogen *S. aureus* has been found to interact with host cells, eliciting an increase in host cell ASM activity. Previously it has been described that *S. aureus* may express the bSM β-toxin itself, which has been proven to act on mammalian sphingomyelin [272,273]. Hereby it came apparent, that either bSM or host ASM is deployed to manipulate potential entry ways for these pathogens, simplifying the invasion of individual host cells or tissue. Hence expression of staphylococcal β-hemolysin depends on several factors, other elements have been implicated responsible for eliciting ASM activity in mammalian cells. Further observation revealed a link between release of inflammatory cytokines and *S. aureus* α-toxin induced ASM activity [274]. Additionally, as for LPS-induced sepsis, inhibition of ASM via genetic or chemical ablation was shown to protect mice from lethal *S. aureus* sepsis [275]. Main reason for sepsis protection was propagated to be disruption of TJ via ASM activity. The previously detected degradation of TJ and AJ proteins like ZO-1 or VE-Cadherin by ADAM10 activity seem to be interwoven with ASM activity, which in return were prevented by application of chemical inhibitors [5,275].

Aims of study

ASM has been implicated in the breakdown of TJ and AJ proteins in endothelial cells when exposed to either staphylococcal α-toxin or live bacteria.[5,275] Since *S. aureus* is capable of producing a variety of pore-forming toxins such as leukocidins, one goal of the present study was to elucidated, if other staphylococcal toxins instead of staphylococcal α-toxin are able to elicit similar effects to endothelial cell-cell adhesion proteins by stimulating ASM activity. For this purpose, mutants of *S. aureus* JE2 lacking individual virulence factors should be generated and tested for their impact on cell barrier integrity.

Additional experiments should clarify, how intoxication of endothelial cells with staphylococcal α-toxin induce ASM activity. Hence, activity assays should be developed in order to assay ASM activity in cell lysate as well as cell culture supernatant samples. Enzymatic activity then should be investigated after exposure of endothelial cells to various treatments including purified toxins as well as bacterial culture supernatants. Previously published data indicates an involvement of ASM mediated plasma membrane repair after PFT challenge [276]. Hallmark of this mechanism is the relocation of intracellular ASM to the extracellular space, which is accompanied by an increased exposure of LAMP1 to the outer cell membrane as well as rapid Ca^{2+} influx [221]. Hence it should be identified if a similar phenotype may apply to *S. aureus* α-hemolysin.

Recent studies revealed an interaction of obligate intracellular pathogens and ASM activity [270,277]. Since it was depicted, that PFT provoked repair mechanism may trigger an enhanced endocytosis of plasma membrane, it lastly should be elucidated if *S. aureus* may utilize this pathway to increase internalization into endothelial cells. Further, as described in Becker et al. [5], inhibition of ASM may influence the PFT triggered repair mechanism, therefore disrupt a potential way for endocytosis of *S. aureus*

Methods

Prokaryotic cell culture

Cell culture methods

All bacterial strains used in this study are listed in Table A. 1. *Escherichia coli* was grown in lysogeny broth (LB) or LB agar and *Staphylococcus aureus* was grown in brain heart infusion (BHI) medium or on tryptic soy agar (TSA), supplemented with appropriate antibiotics if required. Overnight cultures were grown aerobically at 37 °C in an orbital shaker at 180 rpm.

Bacteria grown for infection experiments were diluted 1:20 in equal growth medium and their optical density (OD) was measured at 600 nm. The overnight culture was diluted to exhibit an OD_{600nm} of 0.4 and grown for additional 45-60 min at 37 °C under constant shaking until an OD_{600nm} of 0.6 was achieved.

Cryo-preservation of bacteria

700 µl of bacteria culture was harvested from overnight cultures and washed thrice with sterile PBS. The pellet was resuspended in 300 µl cryo-preservation buffer and stored at -80 °C until further use.

Transformation of bacteria

E. Coli DH5α were thawed on ice and mixed by slight agitation. DNA or plasmid was added and incubated on ice for another 30 min. Bacteria were subsequent transferred to a heat block at 42 °C for 90 sec followed by an incubation on ice for 5 min. The transformation preparation was finally pipetted into a 15 ml tube containing 1 ml LB and incubated at 37 °C under constant shaking. Afterwards bacteria were centrifuged for 30 sec and supernatant was removed. The pellet was resuspended in 200 µl LB and streaked onto a TSA plate for further incubation overnight at 37 °C.

Phage transduction in *S. aureus*

Preparation of phage lysate

All bacteriophages used for this study are listed in Table A. 4. Propagation of phages for transduction experiments was performed in *S. aureus* strain RN4220. The day prior phage lysate production RN4220 was inoculated in BHI and grown overnight at 37 °C under constant shaking.

From RN4220 overnight culture 100 µl was pipetted into 10 ml LB supplemented with 5 mM $CaCl_2$ and further incubated for 2 h at 37 °C. After incubation, bacterial cultures were divided in 1 ml aliquots and heat shocked at 53 °C for 2 min. To each aliquot immediately 100 µl of phage stock was added and vortexed. The bacteria/phage preparation was then mixed with pre-warmed soft agar and poured on TSA plates. Plates were incubated at 30 °C overnight.

Following, plates with a near complete lysis of bacterial lawn were harvested, by scraping of the soft agar layer with a sterile inoculation loop. The agar was transferred to a 15 ml centrifuge tube containing 3 ml phage buffer. This preparation was incubated at room temperature (RT) for 2 h and then centrifuged at 4 °C for 15 min at 4.000 g. Finally, the supernatant containing the phage lysate was filtered with a 0.22 µm filter and stored at 4-8 °C

Preparation of transduction phage lysate

For the preparation of transducing phage lysate a strain of *S. aureus* JE2 was chosen from Nebraska Transposon Mutant Library[278]. The strain of choice was inoculated in 3 ml BHI broth and incubated overnight at 37 °C under constant shaking.

Overnight cultures were diluted 1:100 in 5 ml phage buffer and further incubated at 37 °C until an OD_{600nm} of 1 was achieved. For 1 ml of bacterial culture 100 µl phage lysate was added and vigorously vortexed. The preparation was then incubated at 30 °C until full clearance was detected. Following, the cleared lysate was centrifuged at 14.000 g for 1 min and the supernatant was finally sterile filtered. Phage lysates were stored at 4-8 °C.

Transduction of target gene

All gene transductions were performed in *S. aureus* strain JE2 (USA300), which was inoculated in 10 ml BHI broth and grown over night at 37 °C under constant shaking.

To overnight cultures 5 mM $CaCl_2$ was added and shortly vortexed. From cultures 300 µl was transferred to a sterile 1.5 ml tube and heated at 53 °C for 2 min. Then 100 µl of transduction phage lysate was added and incubated for 2 h 30 min at RT. The bacteria/phage preparation was finally mixed with pre-warmed citrate agar and poured on top of TSA plates supplemented with erythromycin (ERM). Plates were incubated for 48 – 72 h at 37 °C until *S. aureus* colonies were visible.

Mammalian cell culture

Cell culture methods

All cultured cell lines (see Table A.3) were kept in a CO_2 incubator at 37 °C and 5% CO_2. For seeding, cells were washed thrice with PBS and enzymatically detached by incubation with 1 ml TrypLE™ for 2-3 min at 37 °C. Cells were then mixed with complete growth medium and transferred to a new cell culture flask or multi-well plates.

EOMA were propagated in Dulbecco's modified Eagle's Medium (DMEM) supplemented with 10% (v/v) fetal bovine serum (FBS) and 1000 U/ml – 1 mg/ml Penicillin/Streptomycin. Cells were grown until a confluency of 80-90% was achieved and subsequently diluted 1:4 in the next passage.

The human lung microvascular endothelial cell line HuLEC-5a was kept in MCDB 131 medium supplemented with 5% (v/v) FBS, 2.76 µM Hydrocortisol, 0.01 ng/ml human Epidermal Growth Factor, 2 mM GlutaMAX, Penicillin/Streptomycin (1000 U/ml and 1 mg/ml, respectively) and 1x microvascular growth supplement (MVGS). Cells were grown until ≤ 95% confluency was achieved and subsequently diluted 1:3 into the next passage.

Cryopreservation and thawing of cells

For long-term preservation, confluent grown cells were detached and centrifuged at 800 g for 5 min. Cell growth medium was removed and replaced by 1 ml freezing medium (90% FBS and 10% DMSO). Cell pellet was then resuspended and transferred to a cryotube, which was kept for 24 h in a freezing box at -80 °C. For long-term preservation cells were stored in a liquid nitrogen cooled tank.

Thawing was undertaken by gradual heating to RT. Cells were then transferred to 6 ml growth medium and centrifuged at 800 g for 5 min. The supernatant was removed, and cells resuspended in warm complete growth medium for a transfer in a cell culture flask.

Site-specific gen editing using CRISPR-Cas9

Deletion of target genes was performed after protocols published by Ann Ran et al.[279]. Guide RNA (gRNA) sequences used in this process are documented in Table B. 1. Design of sgRNA was performed with web tool CHOPCHOP[280] and published in Labun et al.[281]. Prediction of efficiency, due to calculation of off-target binding or self-

complementarity, makes it a powerful tool to select the right sgRNA for the intended method (knock-out, knock-down, repression etc.). Since the final product differs in only 20-25 bases from the original vector used, the transformed plasmid was analyzed by microfluid sanger sequencing method performed by Microsynth Seqlab. Results were analyzed using ApE genome browser to determine the correct insertion of sgRNA into the vector.

Cell transfection methods

Cells were seeded into 6-well cell cultures plates and kept until a confluency of 70-80% was achieved. Transfection was performed according to manufacturer's protocol for 18-48 h. After detection of GFP-positive cells, samples were detached from culture vessels and prepared for single cell sorting by flow cytometry. Detached cells were pipetted through a cell strainer into a flow cytometer tube to prevent cell clumping. Single cells were sorted into a 96-well cell culture plate containing 200 µl/well complete growth medium. Transfected cells were cultured equally to normal cell cultures. As soon as confluency was reached, a small aliquot of cells was lysed. Cell disruption was either achieved by addition of radio immunoprecipitation assay buffer (RIPA) buffer for protein detection via western blot or DNA extraction buffer (Macherey-Nagel DNA extraction kit) for PCR-analysis.

S. aureus infection experiments

Harvested bacteria were centrifuged at 14.000 g for 1 min and washed with PBS thrice. After washing, bacteria were resuspended in infection medium and further diluted 1:20 for determination of bacterial count per ml. Infection of eukaryotic cells was adapted to the number of host cells to achieve a multiplicity of infection (MOI). After application of bacteria, cells were spun down at 800 g for 8 min to synchronize starting time of infection.

Protein quantification and detection

Sample preparation

For cell lysis RIPA buffer was added to cells and incubated for 5 min. Cell debris was scrapped then from the cell culture vessels and transferred into sample tubes. Samples were subsequently centrifuged at 14.000 g for 2 min to pellet left over cell debris. Samples were either used immediately or stored at -20°C.

Measurement of protein concentration

For determination of protein concentration, cell samples were analyzed with a Bicinchoninic acid (BCA) assay according to the manufactures protocol (Pierce). Samples were measured with a microplate reader (TECAN Mplex) at 562nm. Results were taken to analyze equal size of protein of different samples.

SDS-PAGE

Protein lysates were separated via dodecyl sulphate polyacrylamide gel electrophoresis (SDS-PAGE). Samples were loaded onto mini sized gels (8,5 cm x 10 cm) and concentration of running gel was adjusted according to the molecular mass of the protein to be detected ranging from 7,5% to 20%. SDS-PAGE was performed with buffers indicated as in Appendix C Buffers & Solution for 15 min at 80 V followed by a run for at least 60 min at 120 V.

Western Blot

After separation via SDS-PAGE, proteins were transferred to PVDF membrane by either semi-dry or wet transfer method. Transfer with a semi-dry approach was conducted at 1mA/cm^2 (60 mA per standard blot) and 10 V per blot for at least 1 hour. For proteins with high molecular weight (MW) or complex structure (e.g., high glycosylation, membrane protein etc.) transfer in a wet tank was performed at 400 mA and 100 V per blot for 2 h at 4 °C. Depending on protein of interest time of transfer and MeOH concentration was adapted. After blotting the membrane was washed in trycine buffered saline (TBS) followed by blocking of unspecific binding sides with an appropriate blocking solution (e.g., TBS-Tween supplemented with 5 % non-fat milk) for 1 h at RT or overnight at 4 °C. Dilution of primary/secondary antibody was taken from manufacture’s protocols. Visualization was performed by addition of enhanced chemiluminescence (ECL) solution.

Nucleic acid techniques

Polymerase Chain Reaction (PCR)

Eukaryotic genomic DNA was isolated with the Qiagen Blood Mini Kit. Confluent cell monolayer was harvested by scraping, centrifuged at 14,000 g for 2 min and washed twice with PBS. DNA was then extracted as indicated by the manufacturer’s protocol.

Extraction of *S. aureus* DNA was performed with the QIAmp DNA kit. Overnight cultures were harvested by centrifugation at 14.000 g for 2 min and washed twice with PBS. The bacterial pellet was resuspended in bacteria lysis buffer and incubated for 30 min at 37 °C under slight agitation. Remaining steps for DNA extraction were performed as indicated by the manufacturer's Gram-positive bacteria protocol.

PCR was performed with Phusion DNA polymerase after the manufacturer's protocol using 1 µl of genomic DNA as template. PCR products were analyzed by agarose gel electrophoresis using 1x TRIS-Acetate-EDTA (TAE) buffer system.

Isolation of plasmids from bacterial overnight cultures

For isolation of bacterial plasmids, the NucleoSpin Plasmid kit was used. Bacteria were grown overnight and harvested by centrifugation at 14.000 g for 2 min. The pellet was washed thrice with PBS followed by a lysis step, which was performed at 37 °C for 30 min under slight agitation. Remaining steps of plasmid isolation were executed as stated in the manufacturer's protocol.

Determination of nucleic acid quantity and quality

Eluted nucleic acid concentration from eukaryotic or prokaryotic origin was assessed using a NanoDrop^{TM} 1000 UV-Vis spectrophotometer. 260/280 nm absorbance ratios were calculated to determine purity of nucleic acids.

Cell cytotoxicity detection

Lactate Dehydrogenase assay

Detection of necrotic cell death was performed by measuring lactate dehydrogenase (LDH) activity in cell culture supernatants. Cell culture supernatant was removed from cells and centrifuged at 14.000 g for 2 min to remove cell debris. The supernatants were then pipetted in 96-well plates as triplicates for each sample taken. Detection of LDH activity was performed with Cytotoxicity Detection Kit^{PLUS} (Roche) according to the manufactures protocol. Analysis was performed with a microplate reader (TECAN infinite 200 PRO)

Hemolysis assay

The degree of hemolytic activity of *S. aureus* toxins was depicted by incubation of sheep whole blood with supernatants from *S. aureus* overnight cultures. For this purpose, 1 ml sheep whole blood was centrifuged at 150 g for 5 min. The supernatant

was carefully removed, and the cell pellet washed twice with 0.9% NaCl solution. The cell pellet was then diluted to yield a 1% cell dilution. *S. aureus* overnight culture was transferred to a 1,5 ml tube and spun down at 14.000 g for 1 min. The supernatant was collected and sterile filtered with a 0.22 µm filter. The 1% cell dilution was then incubated with 5% of overnight culture in a thermomixing apparatus for 1 h at 37 °C 550 rpm. After the treatment was performed, the cell pellets were once again spun down at 150 g for 5 min and supernatants were transferred as triplicates to a 96-well plate. Relative hemolysis was analyzed by an absorbance scan at 405 nm ± 9 using a microplate reader.

Acid sphingomyelinase activity assay

Sphingomyelinase activity was assayed with a modified protocol initially developed by Mühle et al [282]. Briefly, for determination of ASM activity, cells were grown in medium supplemented with FBS heat-inactivated at 70 °C to exclude background ASM activity from bovine serum. Polypropylene plastic was used in all following steps for its lower affinity to lipids. Cell culture supernatant was collected and transferred to a 1.5 ml tube, centrifuged at 14.000 for 2 min and put on ice until further use. Cell layers were washed thrice with PBS and incubated with ASM Lysis buffer for 5 min at 37 °C until full lysis of cells was observed. Cell lysate was transferred to a 1.5 ml tube and stored on ice until further use.

Subsequently, 1 µg of cell lysate sample or 100 µl of cell culture supernatant was incubated on a thermomixer (550 rpm) in the dark at 37 °C in either 100 µl ASM LYS buffer for 4 hours or ASM SNT buffer for 24 hours, respectively. Reactions were terminated by addition of 250 µl $ChCl_3$/MeOH (2:1 v/v) and vigorous vortexing. Then, samples were centrifuged at 13.000 g for 5 min and 100 µl of the organic phase was transferred to a new 1.5 ml tube. Samples were then evaporated in a SpeedVac vacuum concentrator for 20 min at 45 °C. Thereafter samples were dissolved in 20 µl $CHCl_3$/MeOH (2:1 v/v) and separated by thin layer chromatography (TLC). In a fume hood, a glass chamber was filled with $CHCl_3$/MeOH (80:20 V/V ; mobile phase) until the bottom was covered with 1 cm of mobile phase and a Whatman paper was inserted at the side of the chamber. The chamber was closed and incubated at room temperature for 5-10 min to establish a saturated atmosphere. Meanwhile 10 µl of each sample was spotted in 2.5 µl steps on a silica coated aluminum-backed TLC plate (ALU*GRAM*® Xtra SIL G aluminium sheets, ThermoScientific ; stationary phase). The plate was then placed into the glass chamber and developed until the solvent front had

advanced ¾ of the plate length. Since only one product was analyzed, Rf-values were insignificant for this approach and disregarded. The plate was then removed and placed for 5 min within the fume hood for evaporation of residual solvent. Finally, the plate was scanned with a Typhoon 9200 Laser imaging unit at 532nm excitation (Amersham, GE Healthcare). Oversaturation of signals was prevented by photomultiplier (PMT) settings. Acquired images were further analyzed as well as quantified with ImageJ.

Lysosome-associated membrane protein 1 (LAMP1) quantification

$0.5x10^5$ HuLEC-5a were seeded per well onto glass cover slips within 24-well plates and were grown for 48 hours. For the assay, cells were washed thrice with PBS. Then, 1 µg of anti-LAMP1 antibody (mAb H4A3, Santa Cruz) dissolved in regular cell growth medium was added per 10^6 HuLEC-5a. Following, cells were either left untreated or incubated with the indicated concentrations of α-toxin or bacterial supernatants for 30 min at 37 °C. Cell culture supernatant was subsequently removed, and cells were washed five times with PBS prior to fixation with 4% paraformaldehyde (PFA). After 15 min of fixing, cells were briefly rinsed with PBS, permeabilized and blocked with PBS containing 0.1% saponin and 5% FBS for 1 h at RT. Secondary antibody was diluted in PBS/0.1% saponin/5% FBS/ Hoechst 33258 and was left on cover slips for 1 h at 37 °C. The glass cover slips were finally removed, washed five times with PBS and mounted onto microscopy slides using Mowiol overnight at RT in the dark. Imaging was performed on a TCS SP5 confocal microscope (Leica Biosystems, Wetzlar, Germany) using a 63x oil-immersion objective (numerical aperture 1.4). Quantification of LAMP1 signals was performed with ImageJ software.

Calcium measurement

All in this experiment used medium or washing solution was pre-warmed to 37°C. HuLEC-5a were seeded one day prior Ca^{2+} measurement into 8-well µ-slide live-cell chamber (Ibidi) with a density of $3x10^4$ cells/well. Beforehand treatment, cells were washed with PBS and incubated with RPMI1640 supplemented with 4 µM Fluo-3AM (Invitrogen) for 30 min at 37 °C. Fluo-3AM containing medium was then removed and cells were again washed with PBS before applying RPMI1640. The cell culture dish was placed onto the microscopy table and the lid removed. Imaging was performed on a TCS SP5 confocal microscope (Leica Biosystems, Wetzlar, Germany) using a 63x oil-immersion UV objective (numerical aperture 1.4). Images were taken at 37 °C with

a resolution of 1024 x 1024 every 7.75 seconds for up to 15 minutes. Treatment with Ionomycin, toxin or supernatants was performed during image acquisition after 3-5 images of untreated cells were recorded.

Fluorescence microscopy

Cells were seeded at least two days prior to imaging on either untreated or coated glass cover slips. After treatment, cells were incubated with 4% PFA for 15 min at RT or 4 °C overnight. Briefly cells were rinsed with PBS, following a permeabilization step, which was performed by application of a PBS/5% FBS/0.1%Triton X-100 solution. Labelling of antigens was done in a humid chamber overnight at 4 °C with primary antibodies diluted in a solution indicated by the manufacturer's protocol. The next day cells were washed thrice with PBS and incubated with secondary antibodies for 1 h at RT. Lastly glass cover slips were rinsed three times with PBS and mounted on microscopy slides using Mowiol and let set overnight at RT. Imaging was performed with a Leica TCS SP5 confocal laser scanning microscope (Leica Biosystems, Wetzlar, Germany) using a 63x oil-immersion objective (Numerical Aperture 1.4). Excitation of fluorescence labelled secondary antibodies was performed as indicated from manufacturer's information (e.g., Cy3-conjugated antibodies Ex_{488nm}/Em_{532nm}). Processing of images was done with ImageJ software.

Results

Targeting acid sphingomyelinase gene expression

Knock-out of *Smpd1* in murine cell line EOMA

For a further understanding of how *Smpd1* might be involved in *S. aureus* infection mechanisms, EOMA were transfected with a corresponding CRISPRCas9 construct targeting the *Smpd1* gene. Success of transfection was investigated by flow cytometry sorting for cells expressing a high GFP signal. Transfected clones were propagated until cultivation in T25 flasks was achieved. These clones were tested via PCR, sequence analysis and western blot for a potential *Smpd1* knock-out. For one clone a deletion in the desired gene locus was identified by PCR (Fig. 6**A**), which was further confirmed though sequence analysis (S-Fig. 1). Western Blot analysis showed no expression of ASM (Fig. 6**B**), verifying the clone as a *Smpd1* knock-out strain. The strain exhibited no visual phenotypical changes besides a prolonged cell division time.

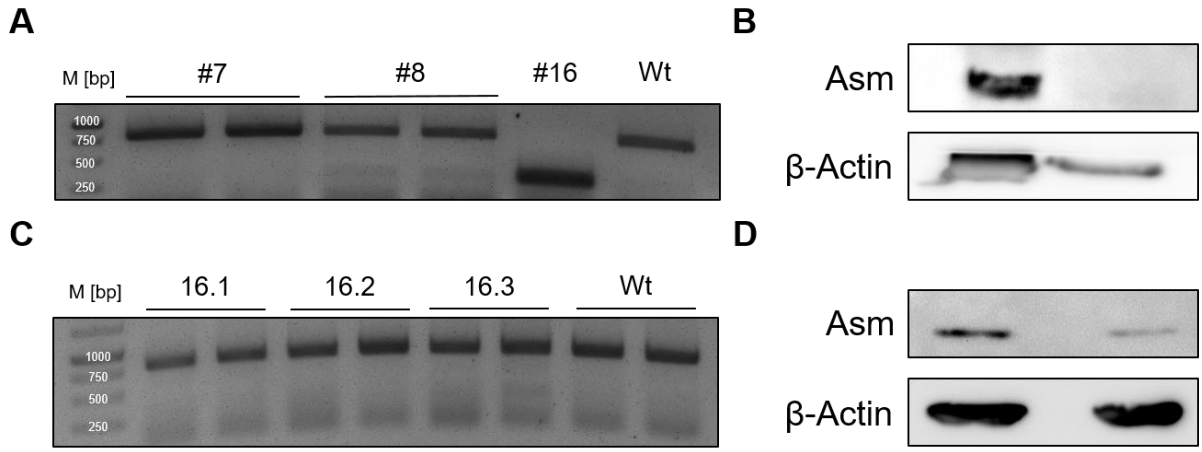

Fig. 6 ***KO of Smpd1 was achieved by CRISPRCas9 mediated genome editing***
*EOMA were transfected with Smpd1 targeting CRISPRCas9 constructs and propagated after single cell sorting. For a single clone (#16) a removal of several hundred base pairs could be detected (**A**), as well as a missing expression of target protein Asm (**B**). Genomic DNA of clone #16 was sequenced, which confirmed the previously detected deletion to be lost (**C**). Western Blot analysis of previous knock-out clones showed an expression of Asm again (**D**). M – 1 kb GeneRuler Ladder*

Knock-out cells were regularly tested for their ASM expression by western blot. After several passages it was discovered that cells were expressing ASM, and the deletion was lost (Fig. 6**C**+**D**). Cells were again growing at the same rate as wildtype (wt) EOMA, which might implicate a potential heterogenic culture of cells, consisting of K.O cells as well as wildtype cells. EOMA pose to be highly adhesive and prone to clumping, which potentially led to the sorting of several cells into a single well. Since wt cells grow at a faster rate, the K.O. cells were most probably outgrown and lost by

extended passaging. EOMA cells were ultimately surrendered, which is why not another deletion of *Smpd1* was performed.

SMPD1 Knock-out in human endothelial cell lines

Human lung microvascular endothelial cells (HuLEC-5a) were transfected and treated similar to EOMA with the corresponding CRISPRCas9 constructs respectively. A successful transfection was achieved, but single clones were not able to outgrow into larger colonies but rather succumbed rapidly after the sorting process. None of the adjustments undertaken for improved cell culture methods increased cell viability, hence the attempts for *SMPD1* knock-out in HuLEC-5a were dismissed.

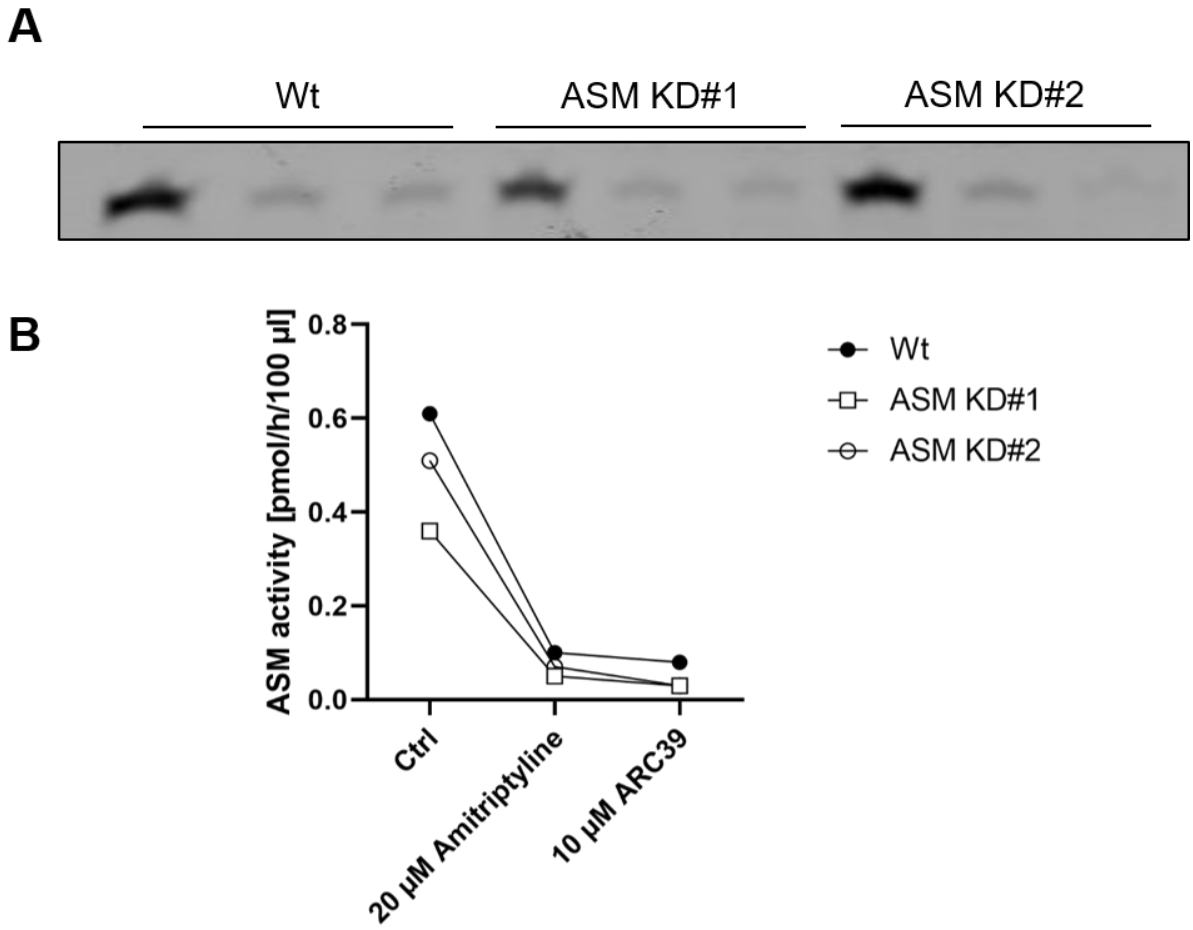

Fig. 7 ***HuLEC-5a SMPD1 knock-down clones demonstrate higher residual sphingomyelinase activity***
*HuLEC-5a were transfected with two K.D. constructs, which reduced ASM activity significantly. (**A**) TLC results from HuLEC-5a wt compared to SMPD1 Knock-Down constructs. First spot marks untreated cells, second spot inhibition with 20 µM Amitriptyline and third spot with 10 µM ARC39. Construct ASM KD#1 exhibits a slight decrease for ASM activity, nonetheless, compared to chemical inhibitors Amitriptyline and ARC39 the constructs posed to be inferior in their inhibitory qualities. This is further indicated by a quantification of TLC signals (**B**). Knock-down cells were generated by Kerstin Paprotka.*

SMPD1 Knock-down in HuLEC-5a

Already available *SMPD1* knock-down variants of the HuLEC-5a cell line were tested for their residual ASM activity and compared to chemically inhibition by application of Amitriptyline or ARC39. Both of the tested knock-down constructs showed a reduction in ASM activity, from which construct #1 revealed the greatest reduction (Fig. 7). Chemical inhibition of HuLEC-5a posed to be the far superior approach to reduce ASM activity, which is why application of ARC39 or Amitriptyline was chosen for further experiments.

ASM inhibitors Amitriptyline and ARC39 exhibit different dynamics

Chemical inhibition of ASM pose to be the most potent method for reduction of ASM activity. Therefore, both inhibitors were tested for their kinetic, concentration range and if they induce cytotoxic effects in HuLEC-5a. Cells were monitored for their intra- and extracellular ASM activity. For functional inhibitors of acid sphingomyelinase (FIASMA) their indirect mode of action is well known and described, therefore leading to a quick inhibition of intracellular ASM activity [236]. In HuLEC-5a Amitriptyline as well exhibits its highest inhibitory effect on intracellular ASM activity, whereas no significant reduction in extracellular ASM activity was measured (Fig. 8**A**). Further the effect on intracellular ASM activity could not be increased with an extended incubation time for up to 4 hours. In addition, extracellular ASM activity was not significantly affected by extended inhibition. Increasing concentrations of Amitriptyline showed a dose dependent effect on intracellular ASM activity, while extracellular ASM activity was only slightly reduced, if concentrations greater than 20 µM were used (Fig. 8**B**).

ARC39 is a direct inhibitor of ASM [239], however its use in cell culture has not been studied intensively. Contrasting Amitriptyline, ARC39 displays its highest inhibitory effects on extracellular ASM activity (Fig. 9). The optimal concentration for significant inhibition was reached with 10 µM ARC39. The intracellular ASM activity was only significantly reduced after extended incubation time. At the used concentrations, neither for Amitriptyline nor for ARC39 cytotoxic effects were detected by LDH-assays (Fig.10).

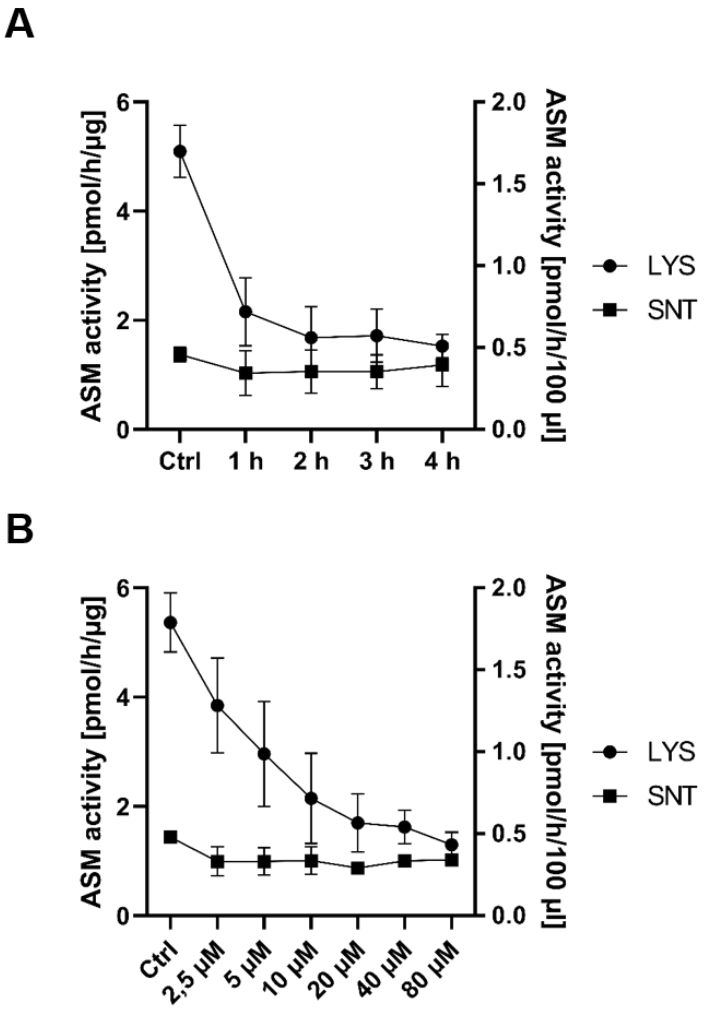

Fig. 8 ***Amitriptyline affects intracellular ASM activity***
The effective inhibitory range for the FIASMA Amitriptyline was assessed for HuLEC-5a for either 1 h and increasing concentrations or a fixed concentration (20 µM) for 1-4 h. Both intra- (LYS) and extracellular (SNT) ASM activity was measured.

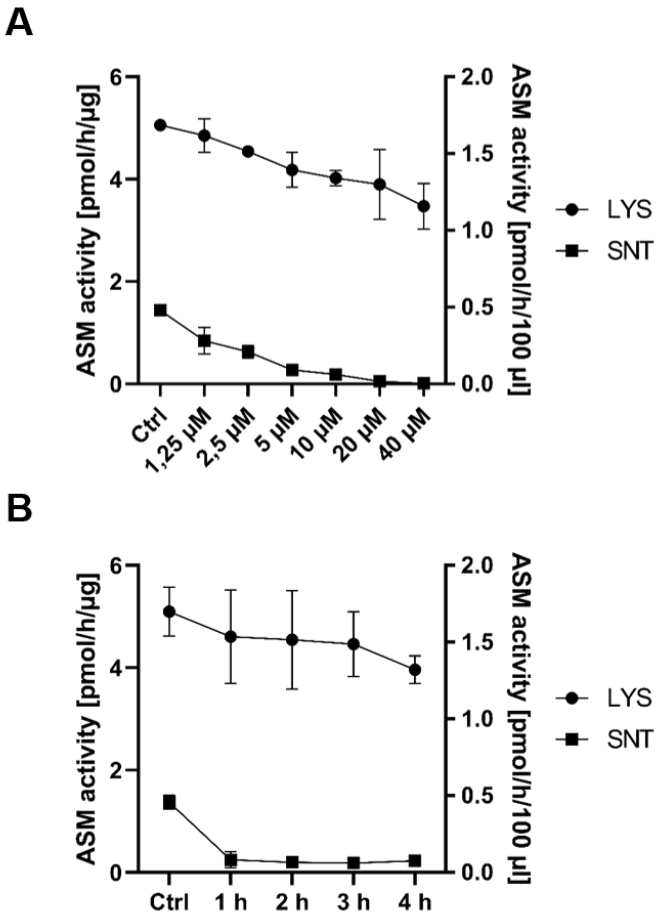

Fig. 9 ***ARC39 inhibition dynamics are different compared to Amitriptyline***
The effective inhibitory range for the direct ASM inhibitor ARC39 was assessed for HuLEC-5a in identical manner as for Amitriptyline. It was shown, that ARC39 leads to a rapid inhibition of extracellular ASM activity, but intracellular activity was not affected until high concentrations (40 µM) or prolonged incubation periods were used.

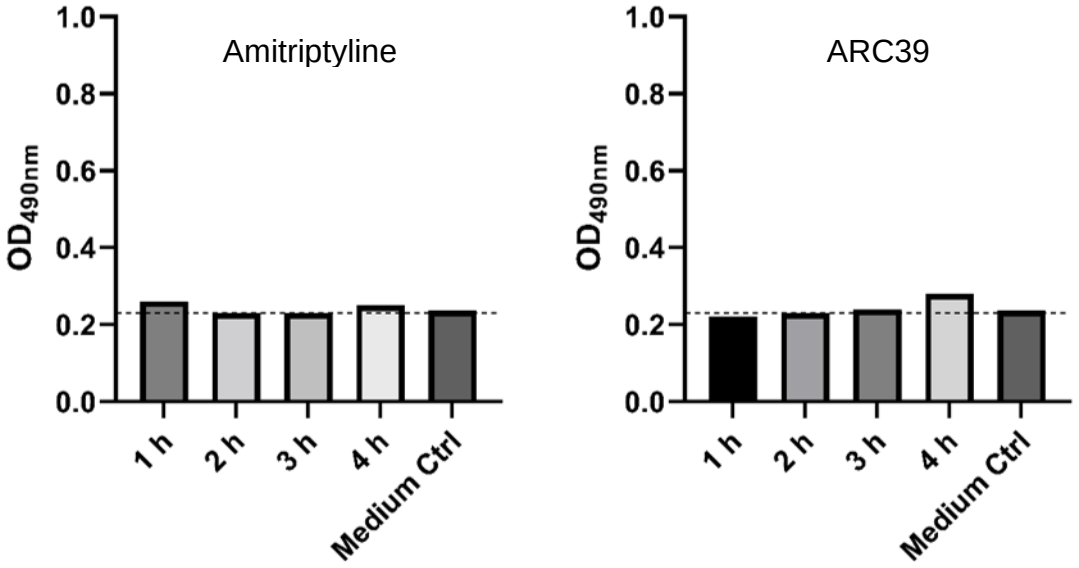

Fig. 10 ***ASM inhibitors do not induce LDH release from HuLEC-5a***
Cells were either treated with 10 µM ARC39 or 20 µM Amitriptyline for the indicated time period. Cell culture supernatant was removed from cells and LDH activity was assessed. Since no indication of LDH activity was measured, results are displayed in contrast to a medium control as OD_{490nm} values. Dashed line indicates OD-value of blank medium issued as zero-LDH controls.

Fluorescent tag on ASM is lost by post-translational cleavage

To investigate the involvement of ASM in *S. aureus* infection by inhibiting or extinguishing enzymatic activity, the mobility of this protein was of high interest as well. Cells expressing wildtype ASM::mCherry plasmid displayed a compartmentalization in vesicles, whereas cells transfected with the dysfunctional ASM variant exhibited a ubiquitous distribution over the whole cell (Fig. 11). Further it was shown, that the mCherry reporter was lost in ASM::mCherry wt constructs. While the tag was present in ASM::mCherry NPD constructs, the fluorescent protein gets cleaved from ASM and can be detected as a singular protein in ASM::mCherry wt cells.

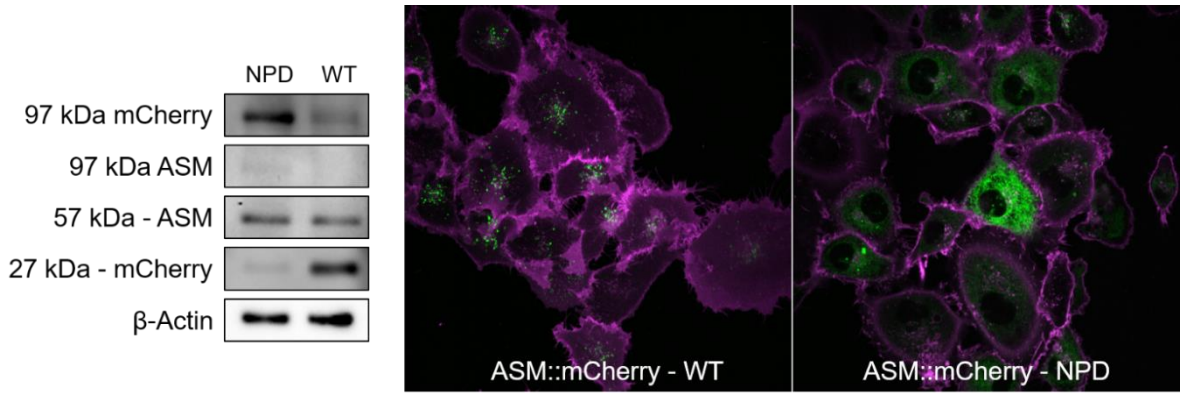

Fig. 11 ***Protein reporter attachments interfere with ASM localization****HuLEC-5a were either transfected with wildtype or NPD variant of ASM, which was tagged via mCherry fluorescent reporter. Western Blot of ASM::mCherry WT revealed cleavage of mCherry from ASM in vesicles. NPD variants were either caused by mutation or addition of mCherry held back in other compartments. Green – ASM mCherry ; Magenta – CellMask membrane staining. Image acquisition by Dr. Jan Schlegel.*

EOMA and HuLEC-5a require certain cultivation conditions for tight junction expression

Prior to experiments investigating the effects of *S. aureus* virulence factors on tight junction breakdown in endothelial cells and a potential involvement of ASM, a framework had to be established, in which cells expressed the desired proteins. Therefore, cells were seeded for varying time periods and onto surfaces with different coatings and were observed, how differing parameters influenced the expression of tight junction proteins like ZO-1, ZO-2 or VE-Cadherin.

Whereas a distinct expression of ZO-1 in EOMA may be observed after 2 days post seeding, cells were not able to express a tight and confluent monolayer (Fig. 12). ZO-1 expression seemed more frayed and disconnected. Coating of cell culture dishes with Collagen I, Fibronectin or a mixture of both increased the expression of ZO-1, nonetheless an extension of incubation time provided a superior expression of ZO-1 in

EOMA. After 7 days a coating with Collagen I, Fibronectin or mixture did not provide a significant benefit for ZO-1 expression, still cells displayed a more mature and distinct expression pattern for ZO-1.

A similar expression pattern was detected in HuLEC-5a, if treated like EOMA shown beforehand. Early development of VE-Cadherin was highly dependent on coating of glass cover slips, otherwise weak to no expression was detected (Fig. 13). Cells grown for 7 days did not show any benefit over cells grown for 2 days on coated glass cover slip, if observed for their expression pattern. The overall confluency although was highly increased and cells grown for 7 days did form a confluent monolayer compared to a semi-confluent cell monolayer after 2 days. This phenotype for HuLEC-5a was reported as well in Ades et al [283], indicating that tight cell to cell interaction will not appear until further scaffolding is provided.

EOMA exhibit high resistance against *S. aureus*-induced TJ/AJ degradation

Previous studies have shown a link between the degradation of TJ and AJ in murine endothelial cells and the activity of ASM. Inhibition of ASM by Amitriptyline depicted a cytoprotective effect in *in vitro* and *in vivo* models [275]. Therefore, it should be investigated, to which extent ASM activity was involved in this phenotype. EOMA were infected with *S. aureus* (MOI10) or treated with 10% of sterile bacterial culture supernatant that was harvested from overnight cultures of *S. aureus* JE2. Infection was terminated after 30 min by addition of Lysostaphin to cell culture media. By immunofluorescence microscopy, TJ as well as AJ were visualized, and potential degradation analyzed by western blot.

In this study, a degradation of TJ or AJ was not observed since infection of EOMA for 2 or 4 h had no impact on ZO-1 localization (Fig. 14). Replication of intracellular bacteria was further enabled for additional 2-24 hours (S-Fig. 2). Observation of these cells gave no evidence for TJ or AJ degradation; concurrent morphological changes were absent as well. Western Blot analysis of similar samples indicated a marginal decrease in ZO-2 protein after 4 h of infection whereas treatment with supernatants showed no decrease in signal.

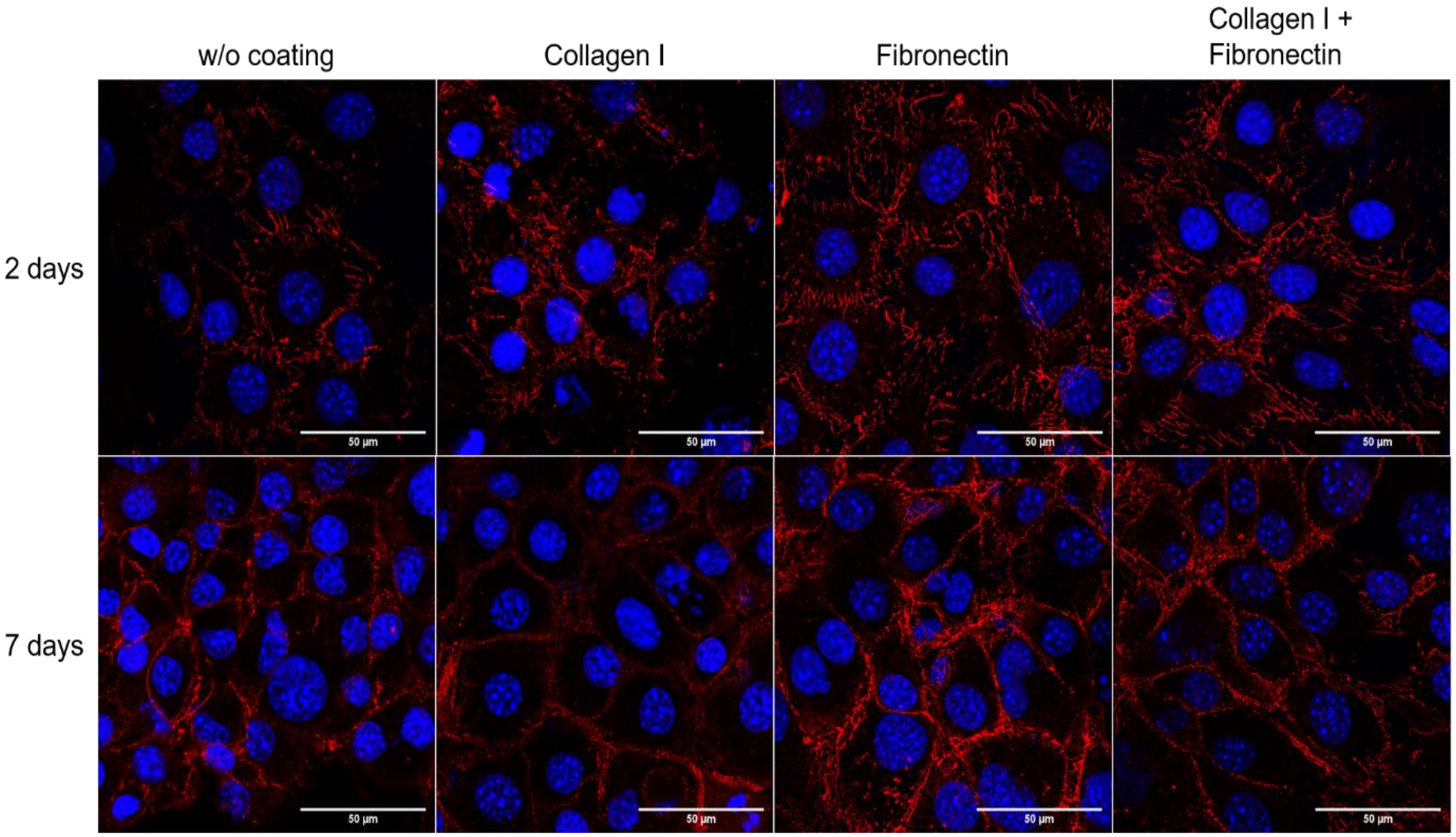

Fig. 12 ***Extension of incubation time provide mature ZO-1 expression pattern***
EOMA were seeded in 24- well plates with a density of 0,5x10^4 cells/well on pretreated glass coverslips. Cells were left to grow for 2 or 7 days and checked for expression of TJP. While coating provided a benefit for cells incubated for 2 days, cells grown for 7 days did not show significant differences if coverslips were coated. Overall cells grown for 7 days have shown a more distinct and mature ZO-1 expression pattern than cells grown for 2 days. Blue – Hoechst 34580 ; Red – ZO-1. Scale bar 50 µm

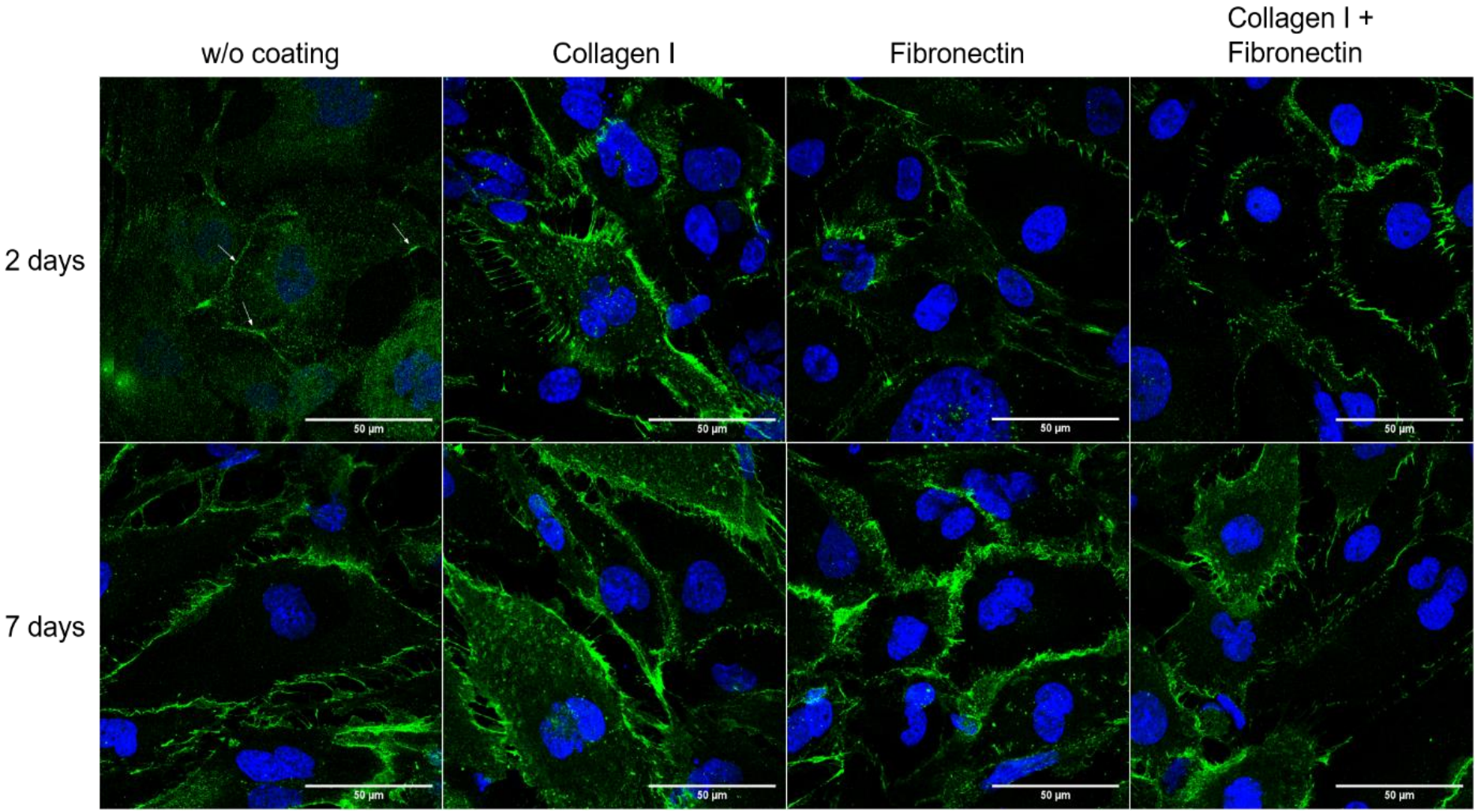

Fig. 13 ***Coating is essential for early development of AJ in HuLEC-5a***
Cells were seeded in 24-well cell culture dishes with a density of 0,5x10^4 cells/well on pretreated glass cover slips. HuLEC-5as were left to grow for 2 or 7 days and checked for expression of AJ. In comparison to EOMA, coating glass cover slips was essential for early development of VE-Cadherin. Cells did not show a tight connection even after 7 days, but indeed formed a confluent monolayer. Coating did not provide any significant benefit after 7 days, nonetheless expression pattern of VE-Cadherin was more mature and distinct. Blue – Hoechst 34580 ; Green – VE-Cadherin. Scale bar 50 µm.

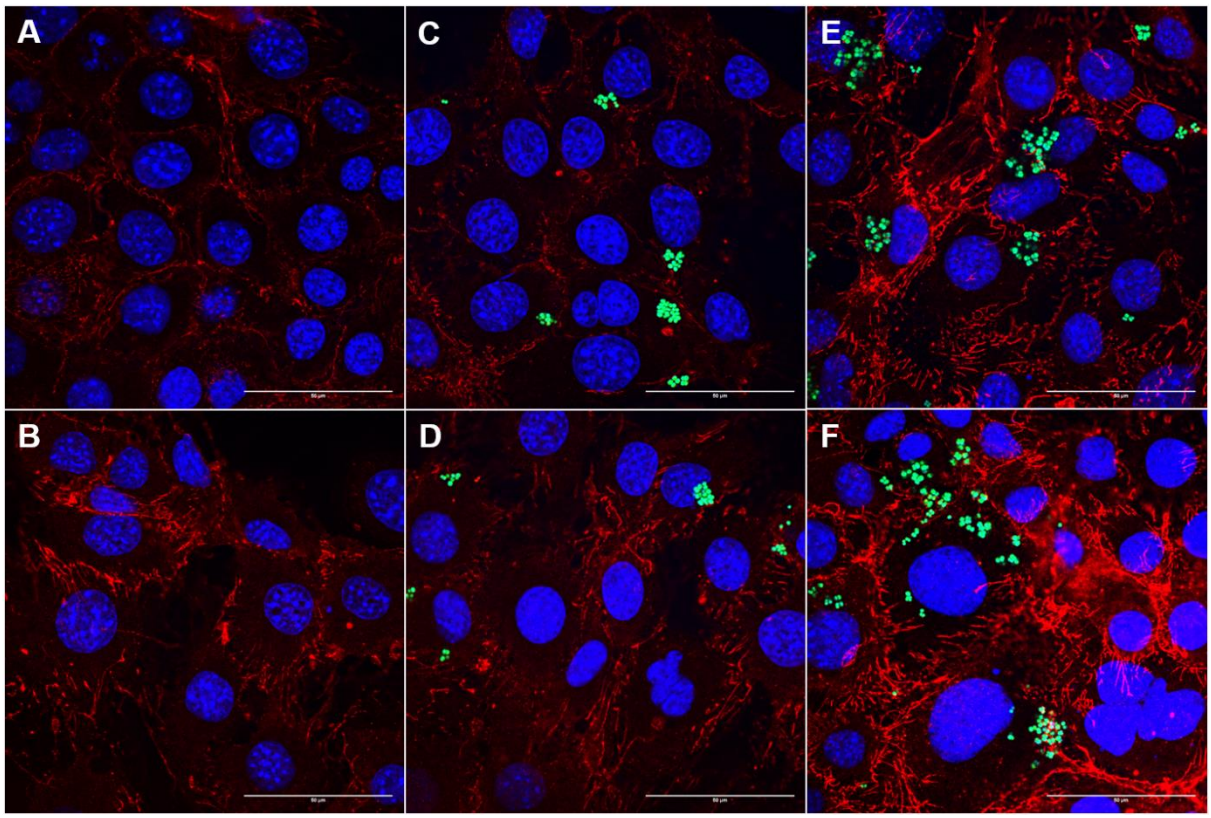

Fig. 14 ***Murine endothelial cells exhibit no ZO-1 degradation after infection***
*EOMA were seeded 2 days prior infection on untreated (**A**,**C**,**E**) or collagen coated (**B**,**D**,**F**) glass cover slips and then infected with S. aureus JE2 MOI10. After 30 min extracellular bacteria were lysed by application of Lysostaphin to cell culture medium. Infection was kept for additional 90 min (**C**,**D**) or 210 min (**E**,**F**). Afterwards cells were fixed and stained for indicated markers. Blue – Hoechst 34580 ; Green –S. aureus ; Red – ZO-1. Scale bar 50 µm.*

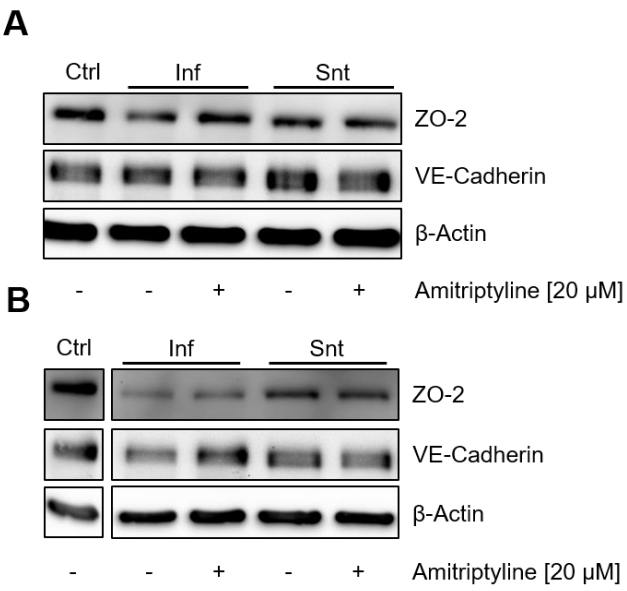

Fig. 15 ***Western Blot confirmed lack of TJ or AJ degradation in EOMA***
*Similar samples as shown above were subjugated to western blot analysis to investigate a potential degradation of ZO-2 or VE-Cadherin. After 2h of infection (**A**) no alteration in detected protein was observed. After 4h infection (**B**) a slight decrease in ZO-2 signal was detected, nonetheless the difference posed to be insignificant. 10 µg of protein were used per sample. Ctrl – untreated cells ; Inf – infected cells MOI10 ; Snt – cells treated with 10% S. aureus JE2 supernatant.*

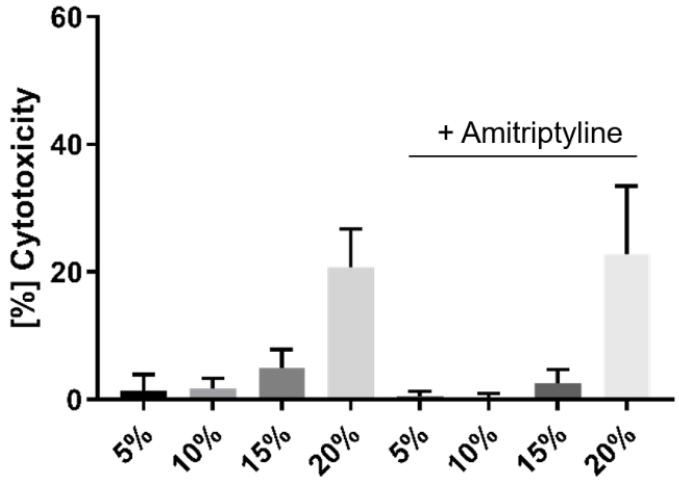

Fig. 16 ***High concentrations of supernatant induce LDH release from EOMA***
Prior to experiments, cells were either left in normal cell culture medium or incubated in cell culture medium containing 20 µM Amitriptyline. Cells were then treated with supernatants from overnight cultures of S. aureus JE2 strain for 2 h. Cytotoxicity was depicted via LDH-assay.

However, the reduced ZO-2 signal exhibited no significance (Fig. 15). Further, cells were releasing LDH only at supernatant concentrations, which were not tested in these experiments and therefore not relevant (Fig. 16). Hence it was not possible to induce a degradation of TJP or AJ under previously published conditions, the effect of ASM inhibition by application of Amitriptyline could not be assessed. Alterations in the experimental procedure were taken to induce the previously reported TJP or AJ degradation in EOMA. Therefore, cells were left growing for 7 days on collagen coated coverslips to achieve an increased expression of TJP and AJ as shown in Fig. 12+13. Additionally, extracellular bacteria were neither removed nor lysed after 30 min but left on cells for higher stress on extracellular matrix. Even these alterations were not able to induce a significant degradation of TJP as previously reported for EOMA. As depicted in Fig. 17**D** infecting EOMA for 6 h did not lead to a decrease in ZO-1 signal, although cells were overgrown with live bacteria and a significant increase in cytotoxicity was detected (Fig. 17**E**). Given the results from prior attempts and this data led to the assumption, that EOMA proof to be rather resilient against *S. aureus* JE2 infections and the previously reported breakdown of TJP could not be reproduced. Since the initial hypothesis was meant to deal with the involvement of ASM in TJP or AJ breakdown, which could not be tested in this cell culture model, a different cell line was issued for the following results shown.

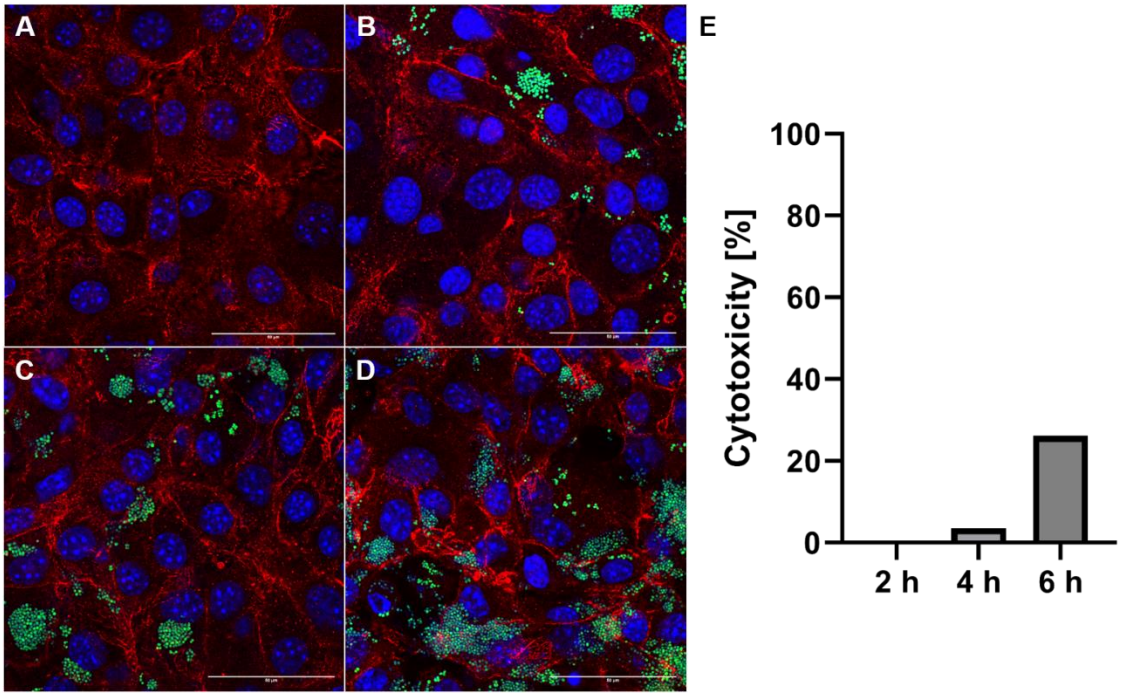

Fig. 17 ***Extended infection does not alter TJP pattern in EOMA***
*Cells were seeded 7 days prior infection on collagen coated coverslips and infected with S. aureus JE2 for either 2 h (**B**), 4h (**C**) or 6 h (**D**). Extracellular bacteria were not removed or lysed during the infection. After the indicated time points, cells were fixed and stained. Blue – Hoechst 34580 ; Green –S. aureus ; Red – ZO-1. Scale bar 50 µm.*

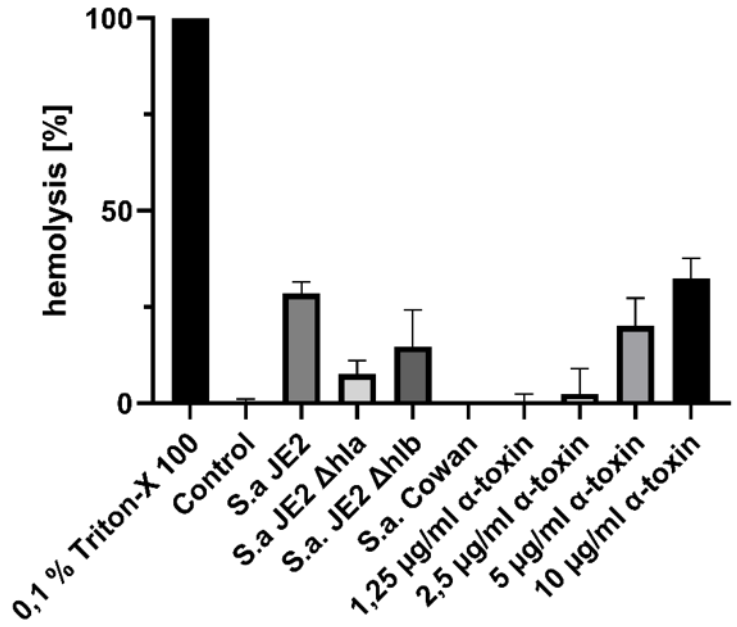

Fig. 18 ***S. aureus α-toxin and supernatants readily lyse red blood cells***
Whole sheep blood was carefully centrifuged and layer containing red blood cells was transferred. The solution was diluted to yield 1% red blood cells, which was then incubated with either 5% supernatant or purified α-toxin for 1 h at 37°C. Lysis of RBC was determined using a microplate reader.

Validation of purified α-toxin and *S. aureus* SNT hemolytic activity

Hence a TJP degradation could not be induced in EOMA, the general α-toxin activity of the purified preparation and bacterial supernatants should be validated. For this purpose, sheep red blood cells were incubated with a set concentration of 5% *S. aureus* SNT and increasing amount of purified α-toxin to further correlate the hemolytic activity of SNTs and preparation (Fig. 18).

Both bacterial SNT as well as the purified α-toxin proof to possess a hemolytic activity. As predicted, the hemolytic activity of JE2Δ*hla* SNT was significant lower compared to JE2 SNT, whereas the JE2Δ*hlb* SNT as slightly less hemolytic. In parallel, purified α-toxin was able to induce a dose dependent effect and stimulation with 5% JE2 SNT equaled ~ 7.5 µg/ml α-toxin in its hemolytic activity.

Generation of transposon-mediated mutagenesis in *S. aureus*

To investigate the impact of single virulence factors of *S. aureus* infection phenotype, a set of mutant strains (Table 1) were picked from the Nebraska Mutant Transposon Library (NTML) and screened for the correct insertion of mariner transposon element *bursa aurealis* as well as potential cross contaminations.

Table 1 Target virulence factors: *Impact of several S. aureus virulence factors should be investigated by genomic deletion in S. aureus strain JE2*

Strain	Gene name	Gene description
NE678	plc	1-phosphatidylinositol phosphodiesterase
NE1354	*hla*	alpha-hemolysin precursor
NE1848	lukS-PV	Panton-Valentine leukocidin, LukS-PV
NE558	lukE	leukotoxin LukE
NE1261	*hlb*	truncated beta-hemolysin (sphingomyelinase)
NE1386	lukA/lukG	Leukocidin G (A)
NE10		putative hemolysin III
NE1682	hlgB	gamma-hemolysin component B
NE286	spa	Immunoglobulin G binding protein A precursor
NE1532	agrA	accessory gene regulator protein A

To ensure a single transposon insertion, the mentioned strains were prepared as depicted in chapter Phage transduction in *S. aureus* and further introduced into *S. aureus* strain JE2. The correct insertion was verified via PCR and genome sequencing. For the strains NE558 and NE 10 the insertion transposon could not be verified, therefore relying on different methods to introduce site specific mutagenesis in these gene loci (Fig. 19).

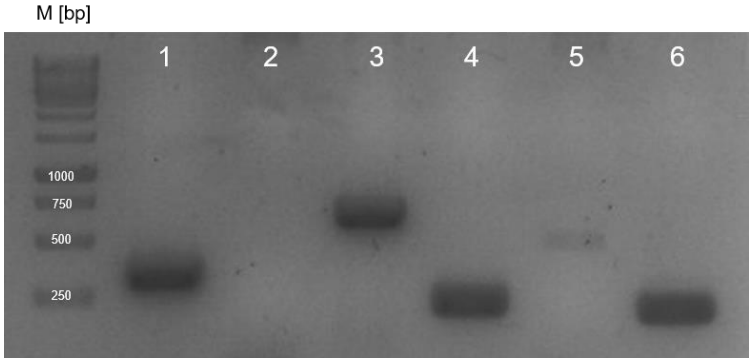

Fig. 19 ***Validation of transposon insertion in NTML strains***
Genomic DNA of S. aureus NTML strains was tested for the insertion of mariner transposon bursa aurealis by PCR. For each mutant a set of transposon specific and gene specific primer was used to determine the correct positioning. M – 1 kb GeneRuler Ladder ; 1 – NE678 ; 2 – NE558 ; 3 – NE1848 ; 4 – NE1682 ; 5 – NE10 ; 6 – NE1386.

Human endothelial cell line HuLEC-5a are sensitive to *S. aureus* supernatants

Prior to infection experiments, the initial susceptibility of HuLEC-5a was tested by application of *S. aureus* SNT. Therefore, cells were incubated with either 1% of JE2 or JE2 Δ*hla* SNT and observed for 2 h (Fig. 20). HuLEC-5a subjugated to JE2 supernatant underwent significant morphological changes (**B**), whereas cells challenged with JE2 Δ*hla* SNT did not alter their morphology (**C**). The changes in cell morphology were a result of ongoing cell necrosis, which was further undermined by examination of LDH release (Fig. 21**A**) and ZO-1 degradation (Fig. 21**C**). Both experiments provided a distinct time and dose dependent effect of JE2 SNT on HuLEC-5a, while SNT lacking α-toxin was unable to induce necrosis in endothelial cells (Fig. 21**B**). Since ZO-1 is associated to intracellular scaffolds, the degradation of extracellular AJ like VE-Cadherin was investigated as well. As for ZO-1, a clear degradation of VE-Cadherin was shown (Fig. 22). Cells challenged with identical concentrations as in Fig. 20+21 exhibit a significant degradation of VE-Cadherin, underlining the morphological changes shown in Fig. 20. Incubation with high concentrations of SNT (5%<) resulted in a fragmentation of VE-Cadherin or even loss of β-Actin signal.

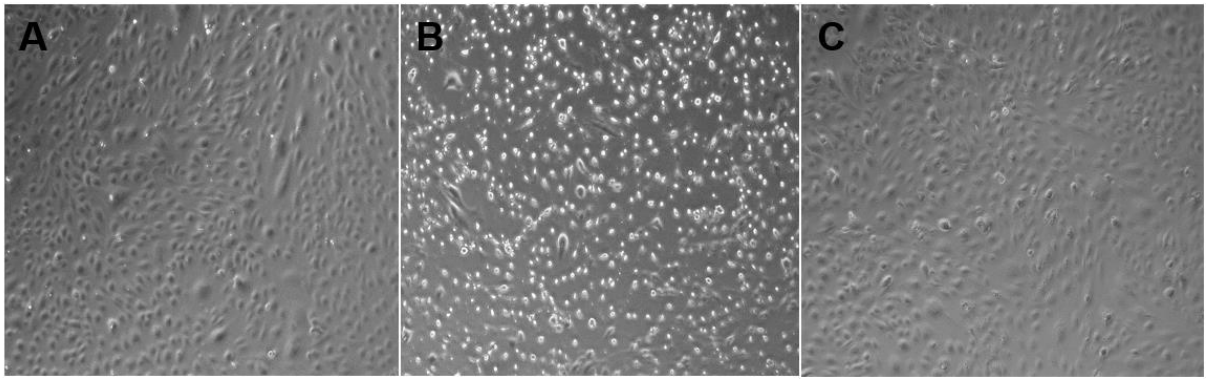

Fig. 20 ***Human endothelial cells are susceptible to toxin challenge***
*HuLEC-5a were grown for 14 days for sufficient monolayer establishment. Cells were then incubated with mock (**A**), 1% JE2 SNT (**B**) or 1% JE2 Δhla SNT (**C**) for 2 h. Images taken with 10x magnification on a bright field microscope.*

Amitriptyline does not provide protective mechanism against TJ/AJ degradation

Since HuLEC-5a proof to be susceptible against *S. aureus* supernatants, the impact on ASM inhibition and TJP or AJ degradation was observed. Hence cells were incubated with 20 µM Amitriptyline 1h prior to infection or supernatant challenge. Again, challenging cells with *S. aureus* JE2 supernatant led to detachment of cells, which was not prevented by the application of Amitriptyline (Fig. 23**B**). Cells incubated with JE2 Δ*hla* supernatants were comparable to untreated cells, indicating the extensive effect of α-toxin (Fig. 23**C**). IF microscopy and western blot analysis further undermined the observed changes. Cells challenged with JE2 supernatant exhibited only minute VE-Cadherin signals (Fig. 24**A**-**D**), which was apparent for cells incubated with Amitriptyline as well. Additionally, ZO-1 was relocated from its cell membrane location to cytosolic compartments. After 2 h no changes in ZO-1 abundance were observed, rather prolonged exposure to JE2 supernatant led to a decrease of ZO-1 protein in cells (Fig. 25**A**). Comparative western blot analysis of cells exposed to supernatants voided from α-toxin exhibited no significant reduction for ZO-1, ZO-2 or VE-Cadherin (Fig. 25**B**). Next, cells were infected for 2-4 hours and cell barrier integrity as well as cytotoxicity was assessed. Therefore, cells were either infected for 30 min, after which all extracellular bacteria were lysed by application of Lysostaphin to cell culture medium (Fig. 26**A**-**D**), or bacteria were let alive for the onset of the experiment (Fig. 26**E**-**H**). Killing of extracellular bacteria did not prevent infection of human endothelial cells, however removal of extracellular bacteria impeded cytotoxic effects in HuLEC-5a (**A**+**C**).

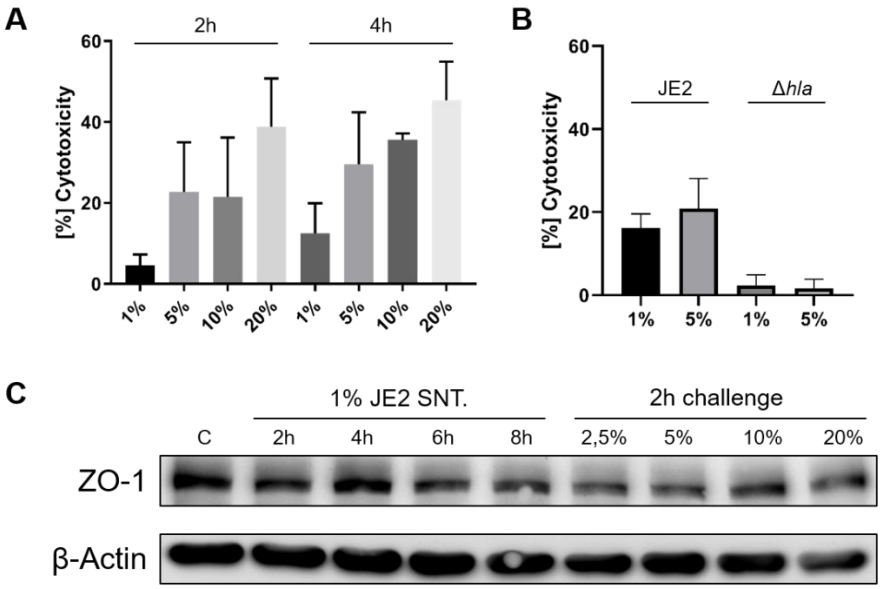

Fig. 21 ***High degree of cytotoxicity and ZO-1 degradation occur in HuLEC-5a***
*Cells were grown as indicated above and treated with JE2 or JE2Δhla SNT on different time points. JE2 SNT provoked a dose dependent cytotoxic effect in HuLEC-5a (**A**), which was abolished if α-toxin was absent in JE2 SNT (**B**). Incubation with JE2 SNT induced a degradation of ZO-1 in a dose and time dependent manner (**C**).*

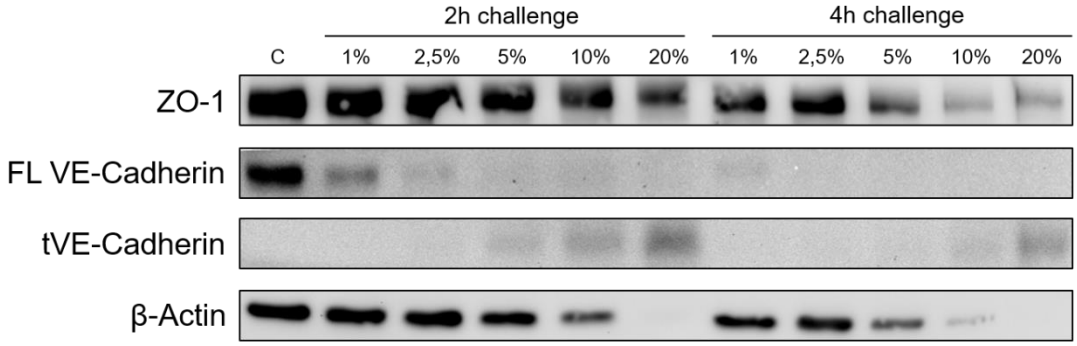

Fig. 22 ***VE-Cadherin is readily cleaved upon SNT treatment***
HuLEC-5a were prepared as indicated above. Treatement with JE2 SNT exhibit a time and concentration dependent degradation of VE-Cadherin, where even the smallest concentration induced a significant degradation. High concentrations of SNT were indicating a truncation of VE-Cadherin. ***FL VE-Cadherin*** *– full length VE-Cadherin ;* ***tVE-Cadherin*** *– truncated VE-Cadherin.*

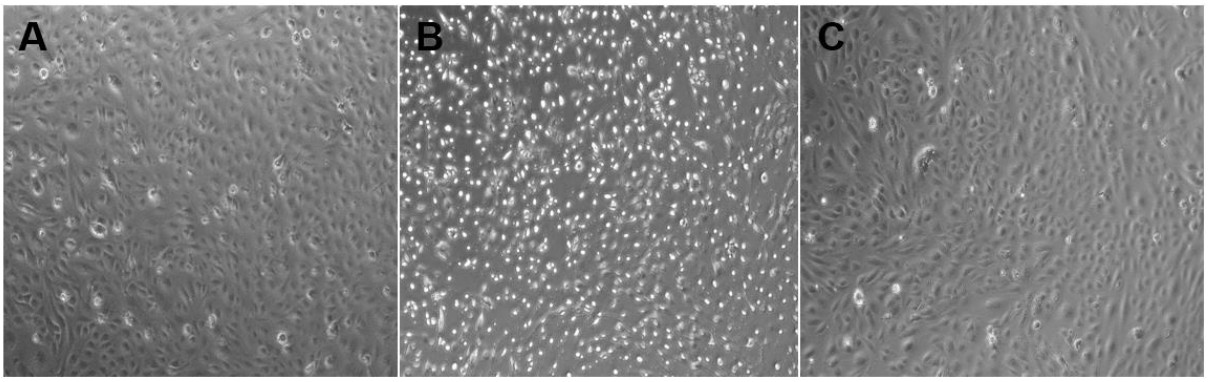

Fig. 23 ***Amitriptyline is not able to mititgate α-toxin induced cell rounding:***
*HuLEC-5a were grown for 14 days and pretreated with 20 µM Amitriptyline prior exposure to S. aureus SNT. Cells were either treated with mock (**A**), 1% JE2 SNT (**B**) or 1% JE2 Δhla SNT (**C**) for 2 h. Images taken with 10x magnification on a bright field microscope.*

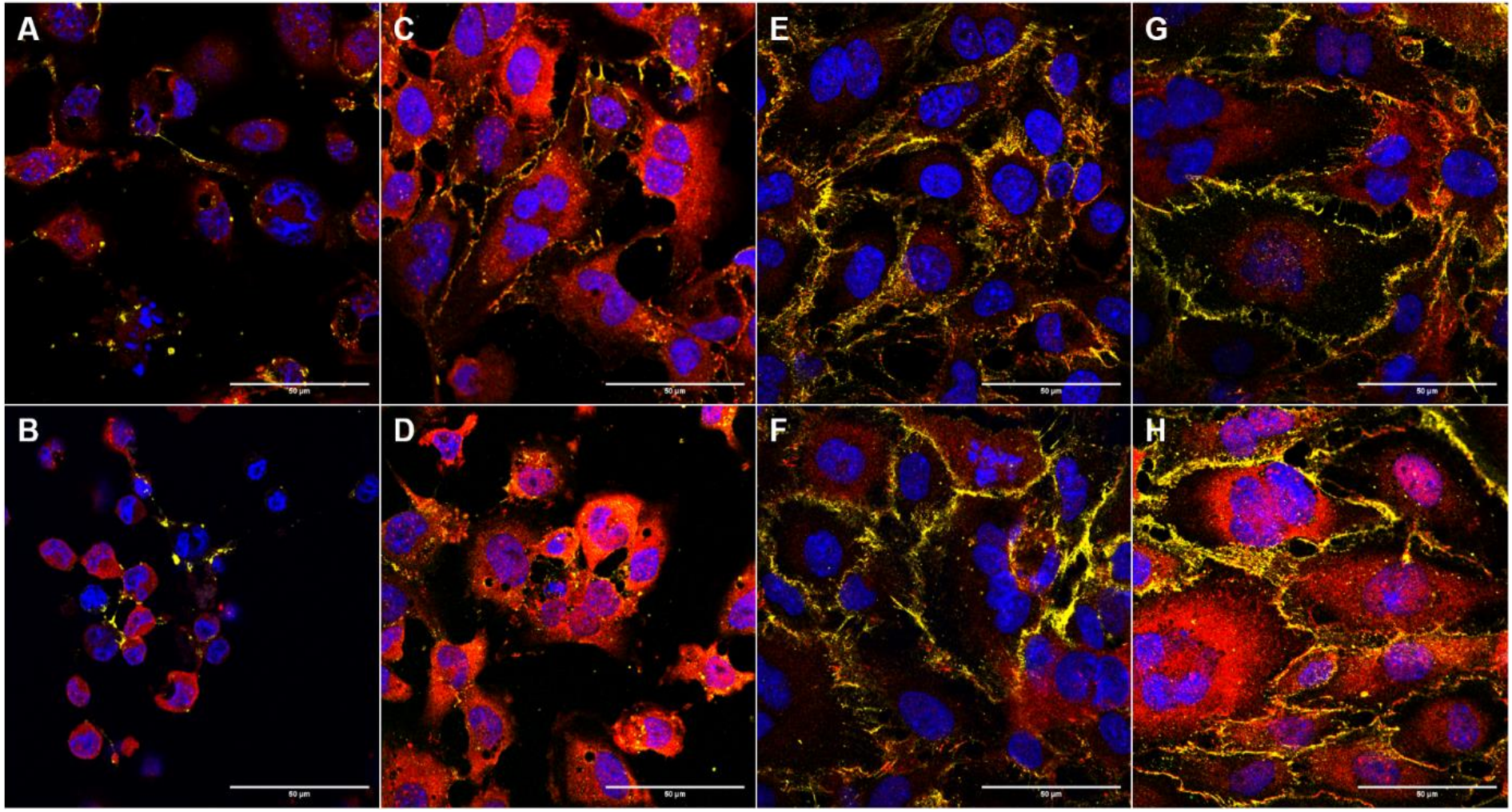

Fig. 24 ***ASM Inhibition does not prevent degradation of VE-Cadherin or ZO-1***
*HuLEC-5a were grown for atleast 7 days and checked for confluency by bright field microscopy as well as for ZO-1 and VE-Cadherin expression by IF microscopy. Challenging HuLEC-5a with 1% JE2 SNT for 2 h (**A**) or 4 h (**C**) shows a rapid detachment from substratum, which resulted in loss of signal for VE-cadherin and cytoplasmatic accumulation of ZO-1. If cells were pretreated with 20 µM Amitriptyline 30 min prior challenge, no difference was detected (**B**+**D**). Exposing cells to 1% SNT lacking α-toxin for 2h (**E**) or 4 h (**G**) does not alter expression of VE-Cadherin or ZO-1 in any way, which is also unchanged upon pretreatment with 20 µM Amitriptyline (**F**+**H**). Yellow – VE-Cadherin ; Red – ZO-1 ; Blue – Hoechst 34580. Scale bar 50 µm.*

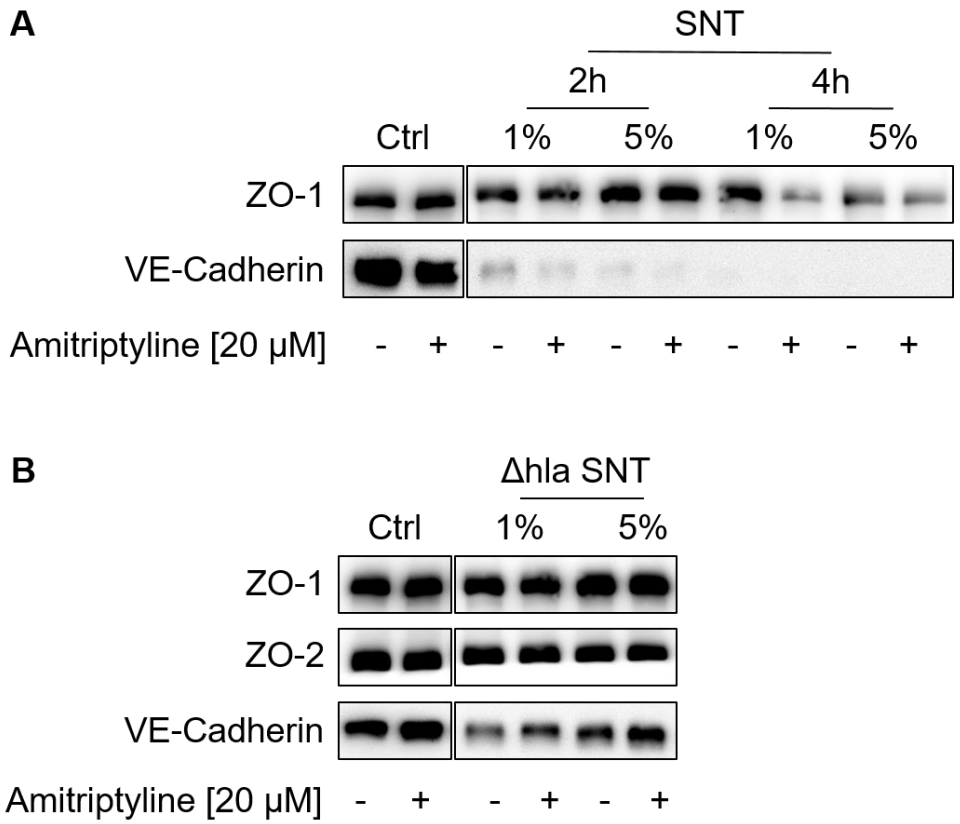

Fig. 25 ***Western Blot confirms effects of Amitriptyline on TJP/AJ degradation***
*HuLEC-5a were grown for at least 7 days a treated with S. aureus SNT for indicated time points and concentrations. Treatment with JE2 SNT led to full degradation of VE-Cadherin and ZO-1 independent of ASM inhibition via Amitriptyline pretreatment (**A**). Removal of α-toxin from JE2 SNT abolished TJP degradation (**B**).*

Hence TJP or AJ integrity was not hampered in this case, the effect of Amitriptyline on TJP or AJ degradation was not verifiable. However, visually fewer bacteria were detected in Amitriptyline pretreated cells (Fig. 27**D**). If bacteria were not removed from cell culture medium, unhampered bacterial growth was observed as well as loss of VE-Cadherin and ZO-1 signal. These effects were already prominent after 2 h of infection (Fig. 27**E**) and not altered by application of Amitriptyline (Fig. 27**F**). Prolonged infection time of 4 h further increased cell blebbing and loss of VE-Cadherin/ZO-1 signal, which was again not affected by Amitriptyline (Fig. 27**G**+**H**). Eventually, analysis of cytotoxic effects revealed, that cells infected for 4 h showed extensive necrotic cell death as well as degradation of ZO-1 and VE-Cadherin (Fig. 27**A**+**B**). Cytotoxic effects were independent of the strain, simultaneously application of Amitriptyline prior to infection had no effect on cytotoxicity. Concurrent to LDH-assay results, western blot analysis showed a degradation of all proteins (including β-actin) for both *S. aureus* strains. As cell viability experiments depicted beforehand, the application of Amitriptyline was not able to induce a rescue effect for TJP or AJ.

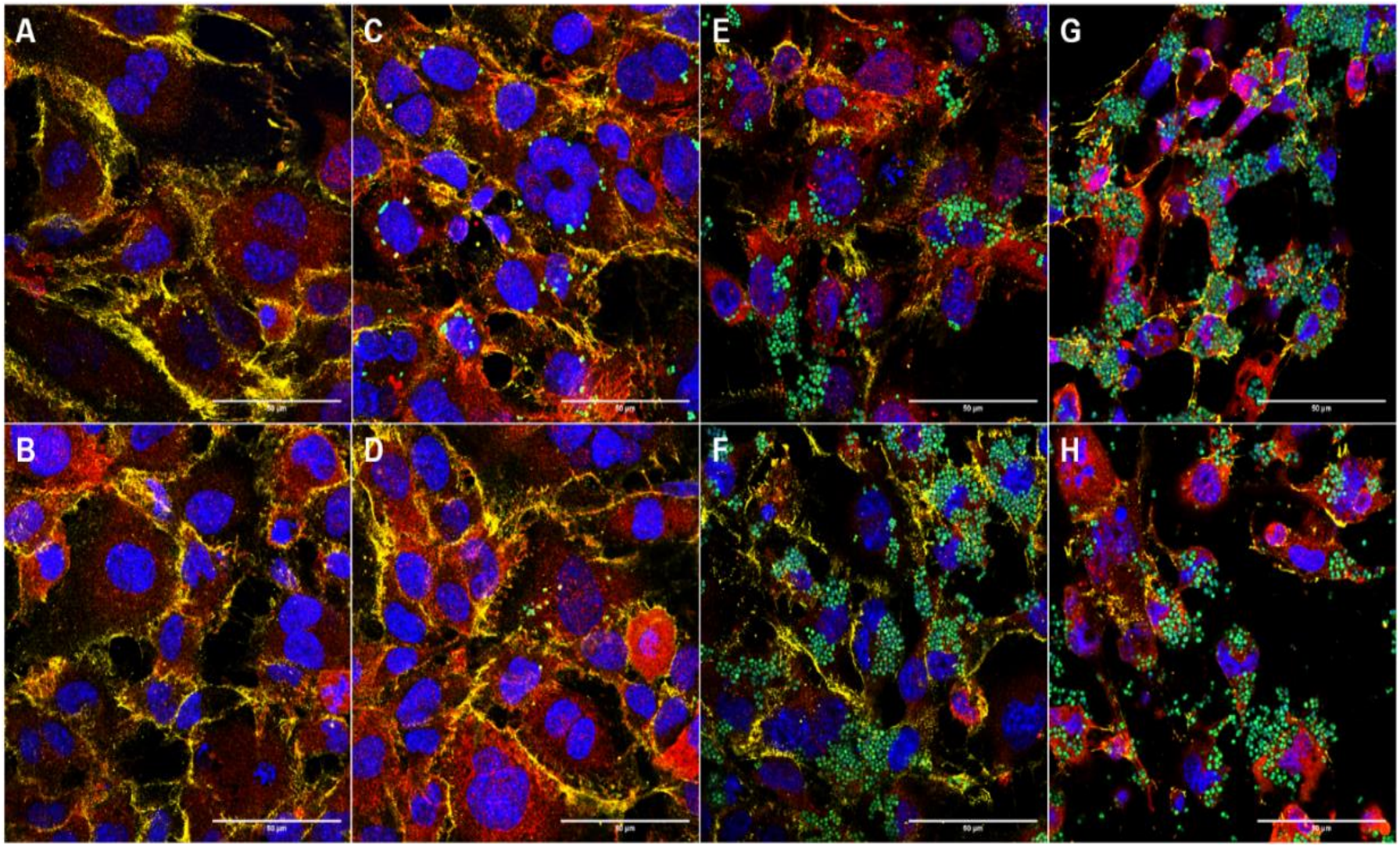

Fig. 26 ***S. aureus induces degradation of cell barrier proteins***
*HuLEC-5a were seeded 7 days prior infection and were either treated with 20 µM Amitriptyline (**B**-**H**) or left untreated (**A**-**G**). Cells were left uninfected (**A**+**B**), infected for 2 h (**C**-**F**) or 4 h (**G**+**H**). Extracellular bacteria were either removed by application of Lysostaphin 30 min after infection (**C**+**D**), or let live for onset of infection (**E**-**H**). Yellow – VE-Cadherin ; Red – ZO-1 ; Green – S. aureus ; Blue – Hoechst 34580. Scale bar 50 µm.*

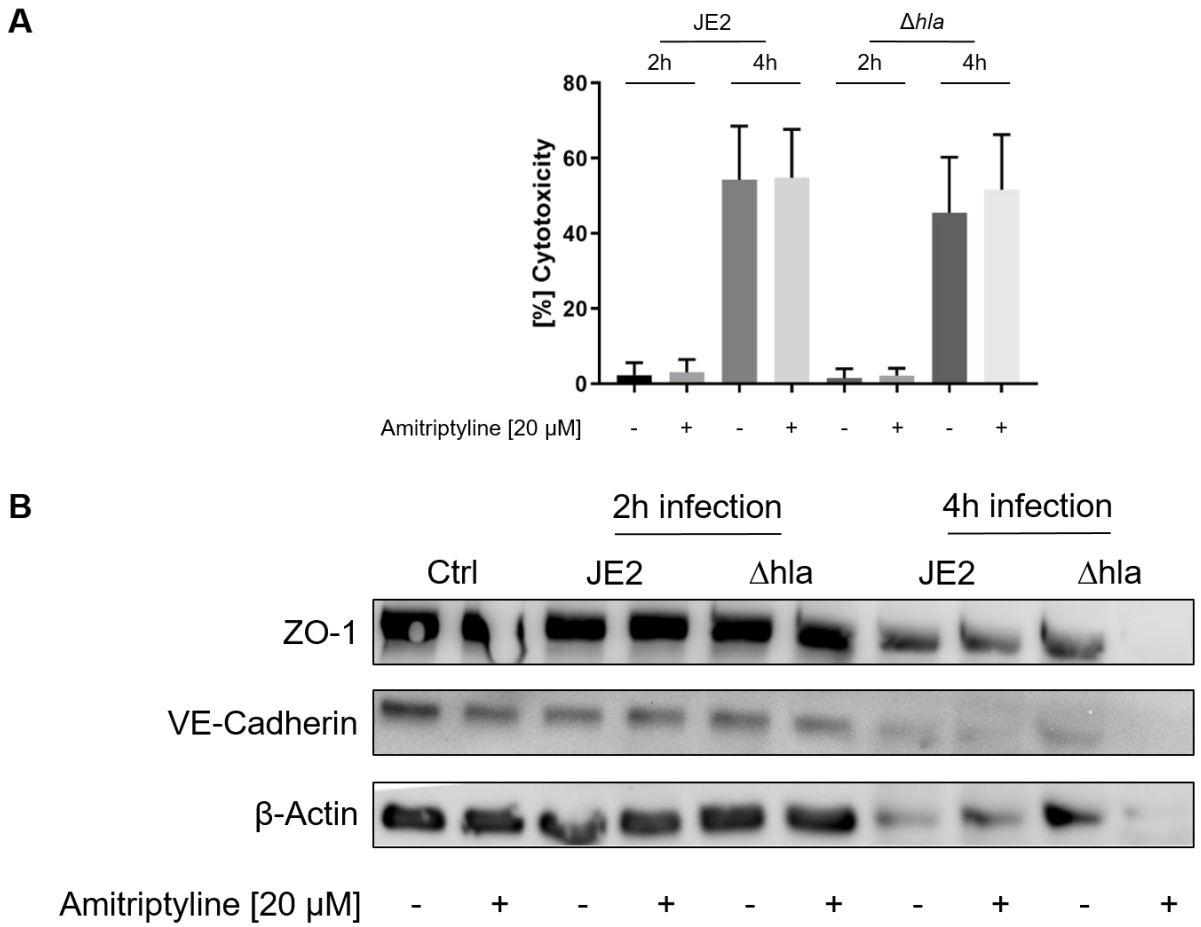

Fig. 27 ***S. aureus mediates detrimental effects indipendent of α-toxin***
*Cells were either infected with S. aureus JE2 or α-toxin lacking strain JE2Δhla for 2 to 4h, following an assesement of cytotoxic (**A**) or ZO-1 and VE-Cadherin degradation (**B**) effects under influence of ASM inhibtion.*

ASM assay conditions depend on sample origin

Since detection of ASM via western blot analysis or microscopy techniques posed to be either highly complicated or were delivering poor signal, the presence of ASM was further determined by measuring enzymatic activity. For this approach a protocol published by C.Mühle and J.Kornhuber [282] was adopted and adapted accordingly.

Endothelial cells are reported to be expressing ASM at higher concentrations, leading to a significant ASM activity in the extracellular space [262]. For better understanding of ASM kinetics, the enzymatic activity was depicted for cell culture medium (extracellular activity) and cell lysates (intracellular activity). The beforehand mentioned publication was suggesting a direct method for TLC which was compared to a conventional TLC approach. Whereas in a conventional approach for TLC samples are extracted and dissolved in an appropriate solvent, direct TLC involves application of samples directly after the enzymatic reaction is abolished by addition of solvent. This approach would omit several following steps, saving at least 60 min of additional sample preparation

before application to a TLC sheet. However, leftover substances (e.g. cell debris, DNA et.) is still present. Identical samples were treated in a conventional approach for a comparison, which led to multiple findings (Fig. 28):

- **Sample application:** Compared to application of samples prepared for conventional TLC, samples from direct TLC hardly dry on silica plates. This was resolved by constant heating of silica plates.
- **Sample spread:** Samples prepared for conventional TLC were dissolved in solvent, whereas direct TLC samples contain all contents from cell culture medium or cell lysate alongside to solvent. These residual contents lead to an increased spread radius of direct TLC samples on silica plates, resulting in diffuse signal bands (red arrow)
- **Signal quality:** the overall signal quality of samples prepared for conventional TLC exceeds those of direct TLC samples, which increases the precision of ASM activity calculation.

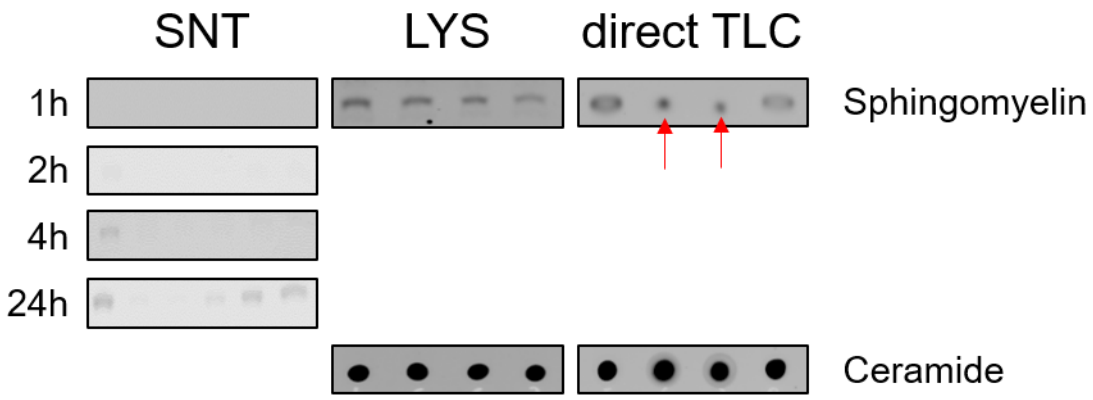

Fig. 28 ***Comparison of differing approaches to asses ASM activity***
Cell culture (SNT) or cell lysate samples (LYS) were either applied as in conventional TLC approaches or in a direct approach. Origin of enzyme (SNT or LYS) determines the time required to recieve an adequate signal. Direct TLC approach exhibited disadvantages compared to conventional TLC application.

Given the detrimental implications of a direct TLC approach compared to a conventional TLC approach, the time saving aspect does not compensate the loss of quality and precision for this assay. Aspects such as sample application or probe radius may be further improved by the application of different solvents. However, this aspect was not followed through since the conventional approach delivered sufficient results.

Comparing the development of samples from cell culture medium (SNT) to cell lysate (LYS) revealed the major disparity of ASM activity of intra- and extracellular space. Nonetheless of time investment, for both sample origins it was possible to detect

significant enzymatic activity. Thereby it was further possible to investigate potential recruitment of intracellular ASM to the extracellular space or vice versa.

Experiments essential for establishment of ASM activity assays

Initial experiments depicted the specific activity of ASM. However, replication of ASM activity assays showed high variances between individual experiments as exhibited in Fig. 29**A**. While a challenge with JE2 SNT led to a decrease of sphingomyelin conversion to ceramide over time, the opposite was investigated for JE2 Δ*hlb* SNT (red triangular shapes). Not only varied the product quantity (ceramide), the amount of primary substrate (sphingomyelin) was different for each sample as well (Fig. 29**B**). The reason for the depicted variances was further tracked down to the materials used in ASM activity assays. To further depict how the materials were interfering, a positive sample from cell culture medium was applied (Fig. 30**A** Sample 1). With the same pipet tip used for application of the positive sample, an equal amount blank sample consisting of fresh solvent only was applied right next to the positive sample. Thereby the amount of sample held back on the pipet tip was deducted. This was repeated twice more (Fig. 30**D Bleed-over effect**).

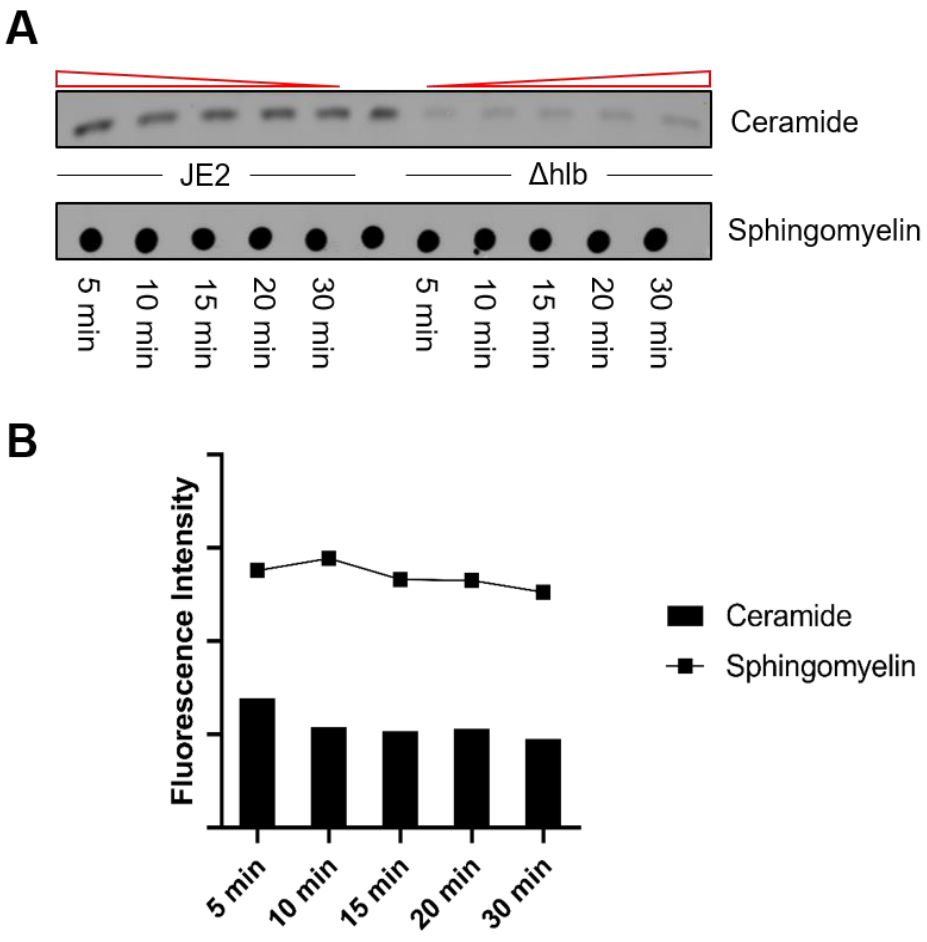

Fig. 29 ***Variancies in applied sample quantity impedes ASM activity detection***
Cells were treated with S. aureus SNT for indicated time points and cell culture medium was analyzed for ASM activity. Analysis of applied samples on TLC sheets revealed variable sample quantities, hindering the assesment of accurate ASM activity in samples.

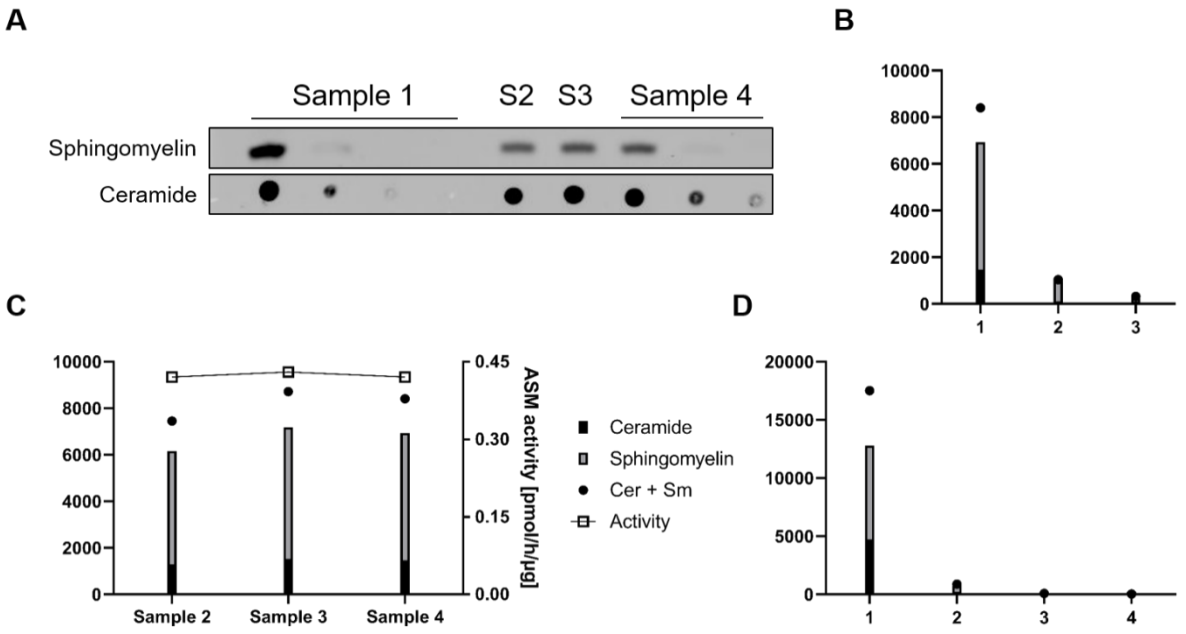

Fig. 30 ***Factors influencing Sample application in ASM activity assays***
*Identical positive samples were applied in different ways to depict retention of sample on pipet tips (Sample 1), centrifuge tubes (Sample 4) or to identify consistency of sample application (Sample 2-4) (**A**). After sample 1 was applied, with the identical pipet tip fresh solvent was added onto twice more. Residual sample was detected, which carried over when using same pipets tips (**B**). Analysis of three identical samples (**C**) revealed different amounts of ceramide (Cer) and sphingomyelin (SM) applied. However, calculating ASM activity from Cer and SM combined led to comparable results for all three samples. Depicting retention of sample in centrifuge tubes (**D**) exhibited similar left-over sample as for pipet tips.*

Consistency of the assay was tested by application of an identical sample in equal volume thrice (Fig. 30**A** Sample 2-4). Furthermore, after Sample 4 was applied, the empty sample centrifuge tube was filled again with an equal amount of blank sample consisting only of fresh solvent and was reapplied twice (**Retention effect**) (Fig. 30**A** Sample 4). For analysis of each sample the total quantity of ceramide, sphingomyelin, ceramide + sphingomyelin and enzymatic activity was depicted. The refilling of the centrifuge tube which contained sample 4 showed a significant **retention effect** of sample in the tube even after repeated refills (Fig. 30**B**). Analysis of **consistency** with sample 2-4 showed an equal quantity of ceramide (black bar), yet sphingomyelin (grey bar) yield differed between the samples. Although these samples should depict the identical enzymatic activity, a variance was illustrated for the combined amount of ceramide and sphingomyelin (black circle). However, if enzymatic activity was calculated (grey square), the variances were equalized (Fig. 30**C**). Results for a **bleed-over effect** from sample on pipet tips showed comparable result to sample retention in centrifuge tubes. While a significant quantity of sample 1 was withhold on pipet tips (Fig. 30**D**), this effect could not be improved by utilizing other materials (e.g., glass capillary tubes – Data not shown).

Since cell lysate should yield a significant higher ASM activity, a similar experiment was performed depicting the **consistency** (sample 1) and **retention effect** (sample 2) in cell lysate samples (Fig. 31**A**). Although enzymatic activity in lysate samples was several folds higher than in cell culture medium, the variances for identical samples was higher (Fig. 31**B**). However, these variances did not affect the calculated enzymatic activity significantly. The retention effect was comparable to the results of cell culture medium samples (Fig. 31**C**).

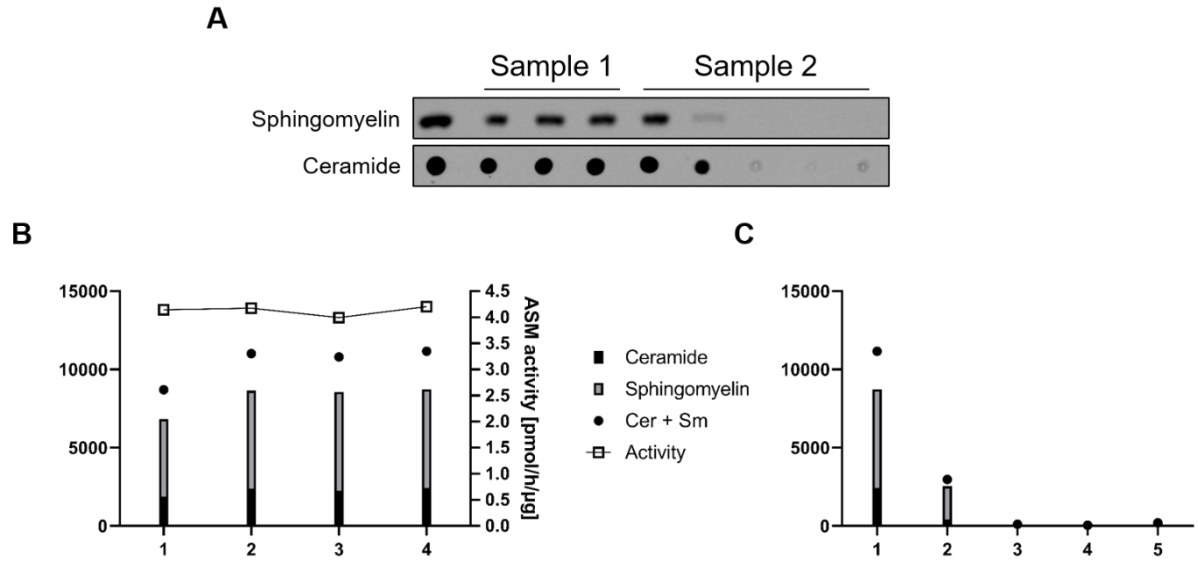

Fig. 31 ***Sphingolipid and polypropylene interactions induce variances in TLC spotting***
As for SNT samples, two positive samples with identical ASM activity were applied and checked for their consistency (Sample1) and retention in centrifuge tubes (sample 2). Both approaches exhibited similar results as for SNT samples.

These results showed that the variances could be disregarded if calculation of ASM activity was based both on sphingomyelin as well as ceramide signal. Hence the retention of sample on pipet tips and centrifuge tubes could not be reduced, further sample preparation was adapted by dissolving all samples in 20 µl of solvent. Of these 20 µl sample only 10 µl were finally applied onto silica plates, hence guaranteeing that for each assay an equal volume was applied. Due to the solvent high volatility and quick evaporation, this cannot be ensured, if samples were dissolved only in 10 µl.

Fetal bovine serum exhibits high ASM activity

Early experiments investigating ASM activity uncovered, that cell culture medium exhibits an ASM activity by itself. Further investigation performed by M.Sc. Marcel Rühling revealed a difference of untreated and heat-inactivated FBS in their ASM activity (Fig. 32**A**). While miniscule amounts of untreated FBS exhibited a high ASM activity, which left samples undiscernible, heat-inactivation of FBS for 30 min at 55°C

led to a drastic reduction in background ASM activity. However, FBS cannot be omitted from cell culture medium, which posed to be a detrimental factor for ASM activity assays. Therefore, FBS was treated for 30 min at 70°C, which abolishes ASM activity in total (Fig. 32**B**).

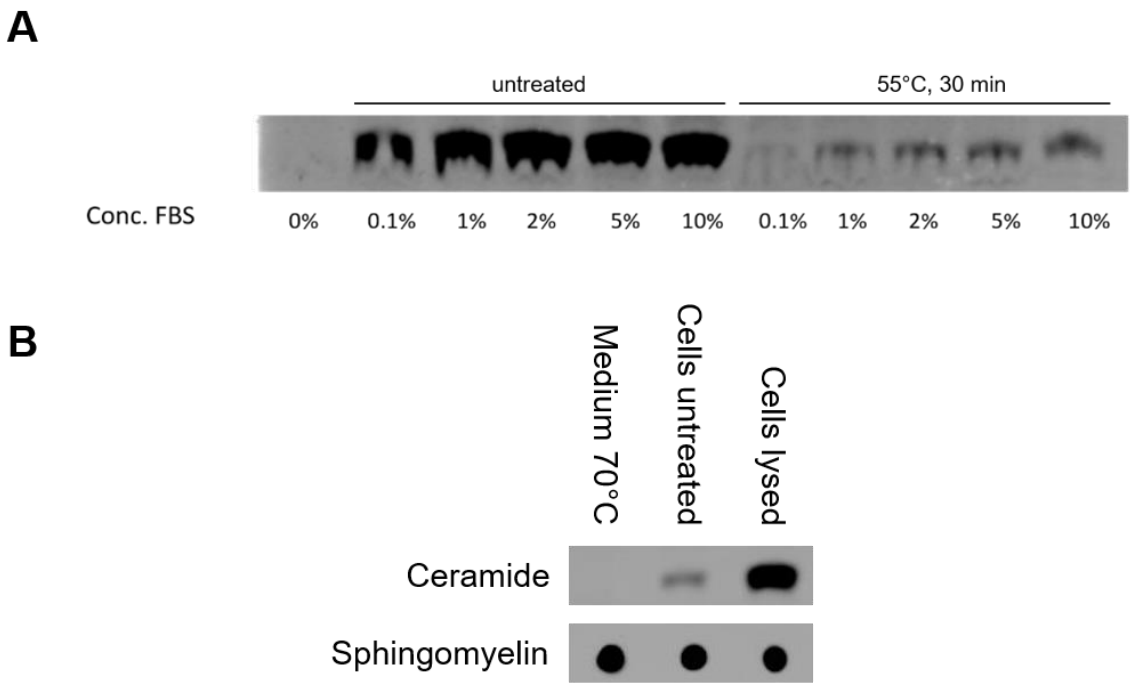

Fig. 32 ***Fetal bovine serum exhibits strong ASM activity***
*Cell culture medium with indicated FBS concentrations was tested for ASM activity. FBS was either left untreated or was heat-inactivated for 30 min at 55°C (**A**). While heat treated FBS holds significant lesser ASM activity, it is still detectable and may interfere with ASM activity assays. Treating FBS for 2 h at 70°C abolished ASM activity in cell culture medium entirely. ASM activity measurements for untreated or 55°C heat inactivated FBS was performed by Marcel Rühling.*

SNT of *S. aureus* cultures elicit sphingomyelinase activity

Prior to exposure of cells to supernatants from different *S. aureus* strains, JE2 genotypic variations or *S. carnosus* TM300, supernatants of overnight cultures were tested for their ability to convert sphingomyelin (Fig. 33). *S. aureus* strains RN4220 and 6850 exhibited a high conversion of SM to Cer, whereas *S. aureus* Cowan and *S. carnosus* TM300 were not able to convert SM to Cer. Interestingly *S. aureus* JE2 was able to induce a conversion as well, although the JE2 strain harbors the lysogenic prophage φSa3 within the β-toxin (*hlb*) gene locus. Bacteria yielding this prophage are rendered unable to express the bacterial sphingomyelinase (bSM) β-toxin. Only an introduction of an additional transposon insertion in the *hlb* gene was able to eliminate SM activity of *S. aureus* JE2 strain. In comparison to strain RN4220 and 6850 bSM activity of JE2 seems miniscule, even ASM activity of unchallenged HuLEC-5a was higher.

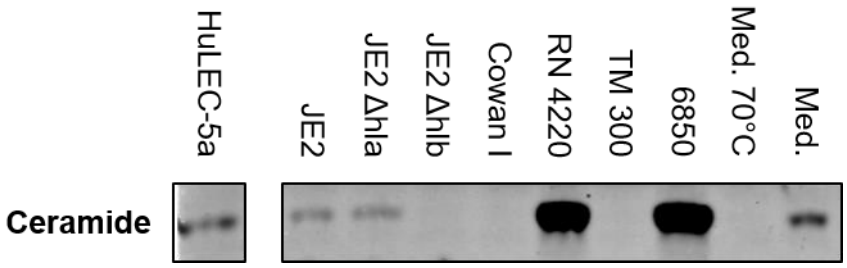

Fig. 33 ***S. aureus exhibits toxin specific sphingomyelinase activity***
Supernatant of S. aureus overnight cultures were tested for sphingomyelinase activity under same conditions cell ASM activity was measured. S. aureus proofs to exhibit a strain and toxin specific conversion of sphingomyelin to ceramide under tested conditions [284].

Given that the SM activity of medium was attenuated to further narrow down variances in the ASM assay, experiments were additionally performed with the insertional transposon mutant JE2 Δ*hlb*. Thereby effects of strain JE2 and JE2Δ*hla* should be controlled and investigated without a bSM background effect.

S. aureus α-toxin induces ASM release from endothelial cells

Cells were challenged with either 10% bacterial supernatant or 10 µg/ml purified α-toxin for 2-30 min and ASM activity for cell culture medium or cell lysate was assessed (Fig. 34). HuLEC-5a incubated with JE2, JE2Δ*hlb* or purified α-toxin exhibited an increased ASM activity in cell culture medium, whereas simultaneously enzymatic activity of cell lysates was reduced significantly. Comparing results for cells treated with JE2 SNT (**A**) or JE2Δ*hlb* SNT (**C**), the beforehand mentioned bSM activity contributed to an increased SM activity in cell culture medium of samples treated with JE2 SNT. Nonetheless, this had no impact on the observed phenotype. Solely cells treated with JE2Δ*hla* supernatant did not exhibit this phenotype (**B**). Treatment with purified α-toxin (**D**) resulted in nearly mirrored results, as described for JE2 and JEΔ*hlb* SNT, further undermining the potential importance of *S. aureus* α-toxin contribution to an indicated release of ASM to the extracellular space.

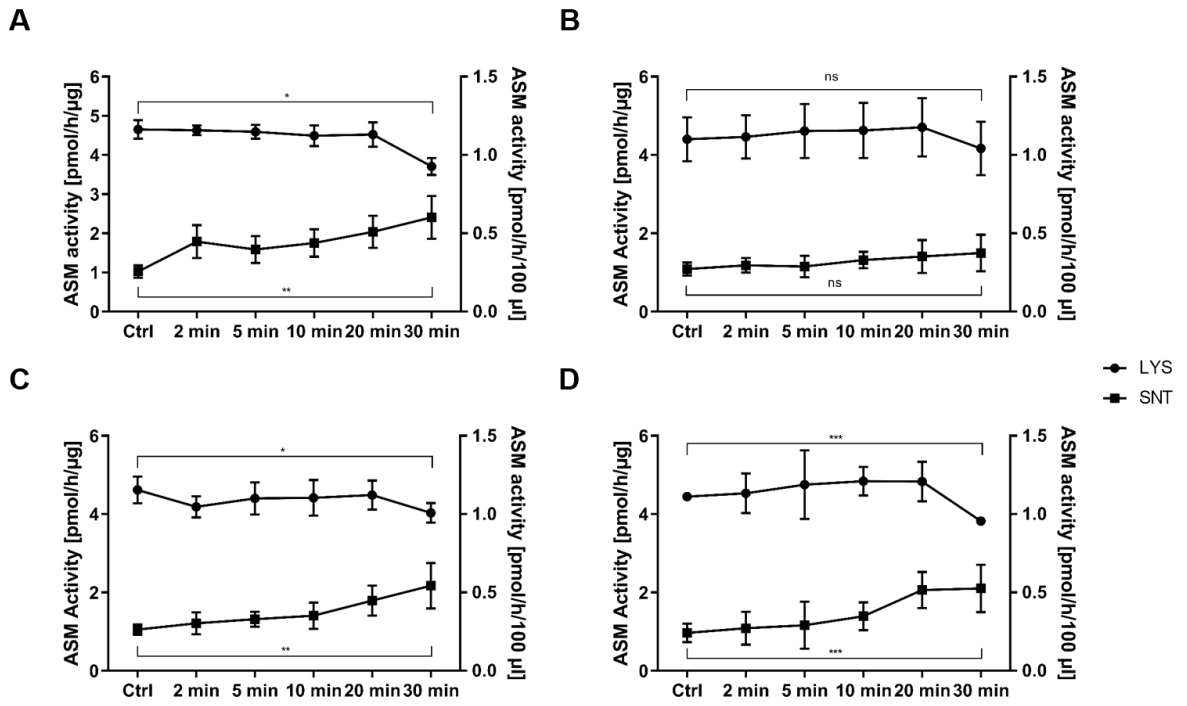

Fig. 34 ***Staphylococcal α-toxin induces ASM release from endothelial cells***
*HuLEC-5a were either challenged with 10% bacterial culture supernatant of (**A**) S. aureus JE2 WT (SNT WT), (**B**) JE2 lacking α-toxin (Δhla SNT) or (**C**) JE2 lacking ϐ-toxin (Δhlb SNT), were treated with 10 µg/ml of purified α-toxin (**D**) or were left untreated (Ctrl). ASM activity was measured at the indicated time points in cell culture medium ("SNT", square points) as well as in endothelial cell lysate ("LYS", circle points). ASM activity of lysates are given in pmol/h/µg (left y-axis) and were normalized to the total protein amount in cell lysates. ASM activities in culture media are given as pmol/h/100 µl (right y-axis).*

Staphylococcal α-toxin provokes oscillating cytosolic Ca^{2+} signals

Staphylococcal α-toxin is reported to induce an influx of calcium ions shortly after its assembly on the plasma membrane [285]. Therefore, cells were treated with the fluorescent reporter Fluo-3am to further observe cytosolic changes in calcium concentrations. Endothelial cells were either treated with *S. aureus* JE2 supernatant, supernatant without α-toxin, purified α-toxin or the ionophore Ionomycin (Fig. 35). All treatments were introduced in a live-cell microscopy setup, which enabled recording the moment treatment was applied. While Ionomycin induced an imminent and high increase in Ca^{2+} concentration, a treatment with JE2 SNT or purified α-toxin led to a delayed increase of cytosolic Ca^{2+}. For cells treated with JE2Δ*hla* SNT no discernible changes in Ca^{2+} were detected. Compared to the constant increase of cytosolic Ca^{2+} induced by Ionomycin, a stimulation with JE2 SNT or α-toxin showed an oscillating fluorescence pattern, indicating a rapid ion exchange in these cells (Vid. 1).

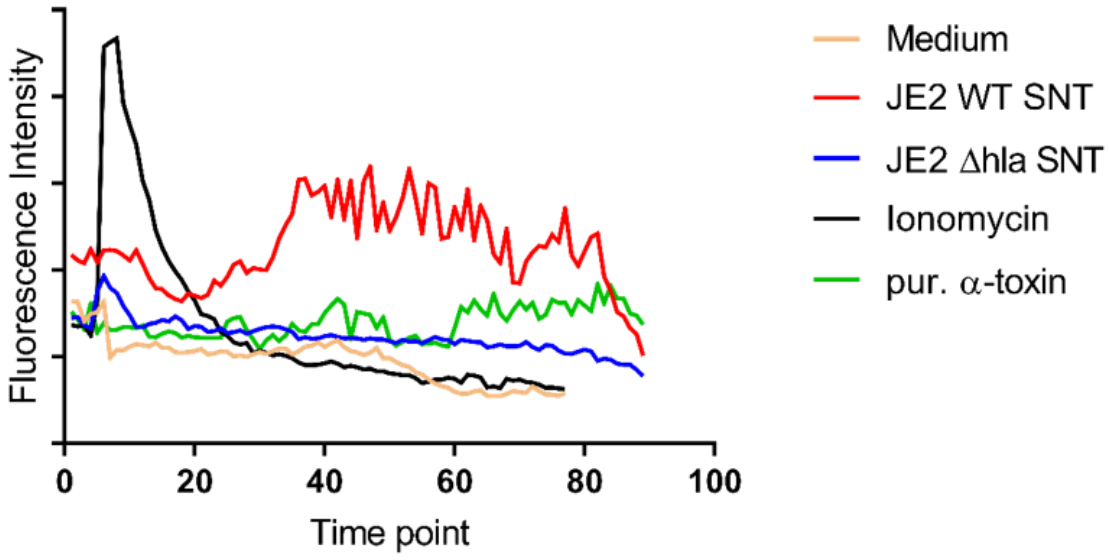

Fig. 35 ***Staphylococcal α-toxin induces influx of Ca^{2+} into endothelial cells***
HuLEC-5a were incubated with 4 µM Fluo 3-AM for 30 min at 37°C/5% CO_2 and subsequently analyzed for calcium-specific increase of fluorescence. Cells were treated with 500 nM Ionomycin, 5 µg α-toxin or 2.5% supernatant of JE2 WT (JE2 SNT) or mutant JE2 lacking α-toxin (JE2 Δhla SNT). Each time point represents a time frame of 7.75 seconds. Image depicts representative results of three independent experiments

α-toxin elicits increased LAMP1 cell membrane exposure in HuLEC-5a

Elevated Ca^{2+} concentration from extracellular origins or intracellular storages activate manifold signaling pathways including a fusion of peripheral vesicles with the plasma membrane [221,286]. A prominent protein associated with these vesicles is the Lysosome membrane associated protein 1 (LAMP1), which may be exposed to the cell surface once the vesicle fuses with the cell membrane and releases its contents. One of the contents, may be ASM, as it was shown for other cell types [287]. To further validate the potential source of ASM, which was observed to be released from endothelial cells after intoxication with *S. aureus* α-toxin, the quantity of exposed LAMP1 for endothelial cells was validated. For this assay, a modified approach for immunofluorescence labelling was introduced (Fig. 36). Following this approach, only a miniscule number of LAMP1 events were detected on HuLEC-5a if left untreated (Fig. 37**A**). However, challenging endothelial cells with staphylococcal α-toxin or toxin containing SNT, an accumulation of LAMP1 signals was detected. Once again, this phenotype was abolished, if cells were treated with bacterial SNT lacking α-toxin (Fig. 37**B**). The highest increase of LAMP1 events per cells was demonstrated after treatment with Ionomycin (Fig. 37**C**), which also elicited the highest fluorescence spike for Ca^{2+} concentration detection.

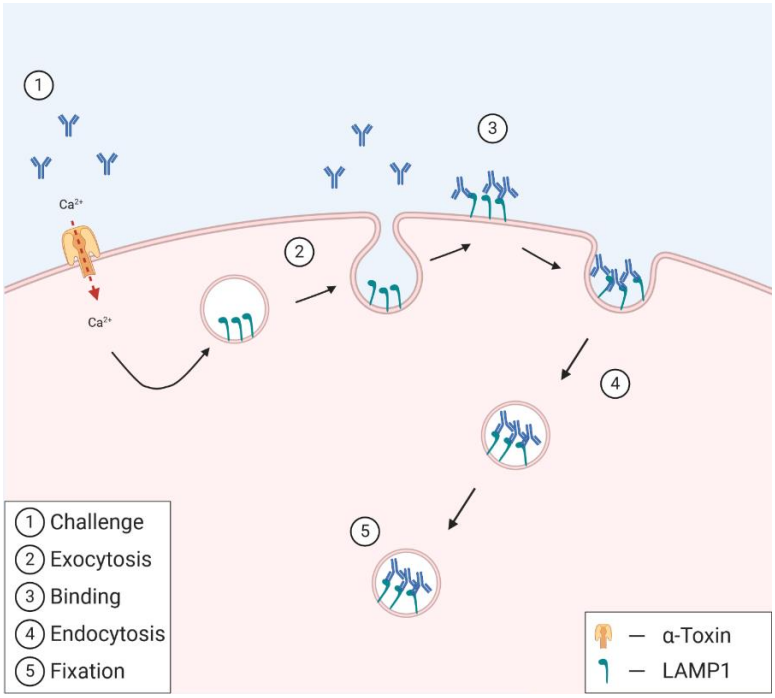

Fig. 36 ***Schematic depiction of LAMP1 cell surface detection experiment***
*(**1**) HuLEC-5a were incubated with solution containing α-toxin and LAMP1 antibodies. Effects of Hla are proposed to recruit peripheral vesicles, decorated with LAMP1 protein, which upon recruitment to the cell membrane are exposed to the extracellular space (**2**). Presented LAMP1 is detected accordingly by antibodies (**3**) and endocytosed by follow up processes (**4**). After an arbitrary time point the experiment was terminated by washing cells and addition of 4% PFA (**5**).*

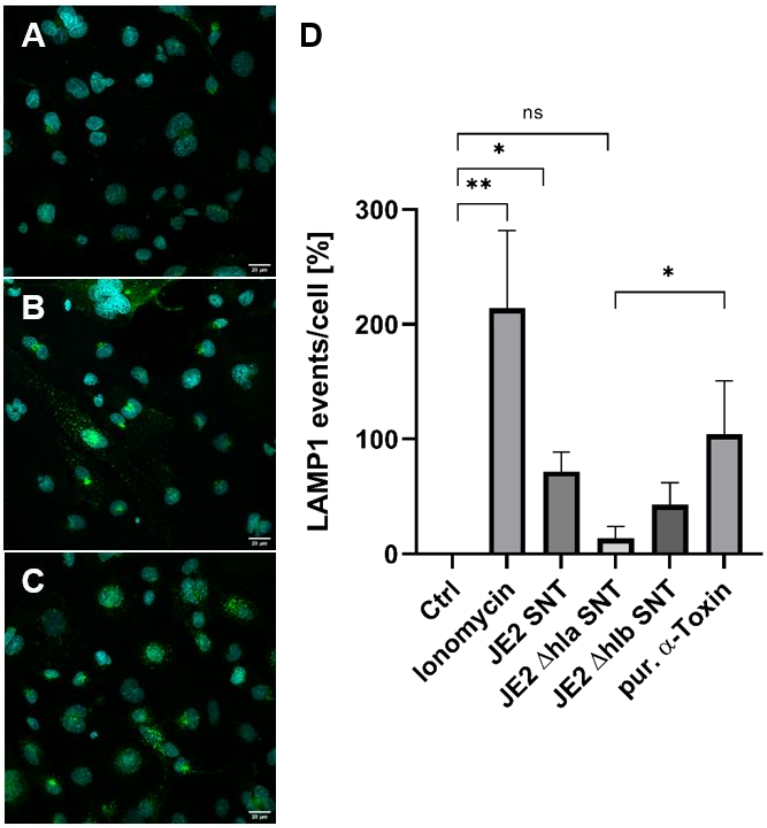

Fig. 37 ***S. aureus induces recruitment of LAMP1 to the plasma membrane***
*HuLEC-5a cells were left untreated (**A**), treated for 30 min with 10 µg/ml purified α-toxin (**B**) or 1 µM of the Ca^{2+} ionophore Ionomycin (**C**). Analysis of fluorescence microscopy demonstrated significantly increased LAMP1 signals for cells treated with either Ionomycin, purified α-toxin or supernatants containing the hemolysin (**D**).*

ASM activity affects numbers of intracellular *S. aureus*

In a previous published study by Peng et al. it was shown that *S. aureus* infected *Asm*-deficient mice or mice treated with Amitriptyline had a higher rate of survival when compared to the parental mouse strain [275]. Mortality rate was even reduced to 0, if *Asm*$^{-/-}$ mice or Amitriptyline treated mice were additionally medicated with either Vancomycin or Methicillin.

The same study indicated a potential connection between *S. aureus* mediated TJ degradation and ASM activity. However, it was not possible to reproduce these results as mentioned beforehand. Indeed, there was no evidence for ASM to be involved in TJP degradation, hence a recruitment to the extracellular space had no impact on cell-cell junction digestion. Anyway, Peng et al. was able to exhibit a correlation between ASM activity and survival *in vivo*. Mice infected with *S. aureus* and treated with Amitriptyline had higher CFU levels in their lungs, but if antibiotics were supplemented to the FIASMA treatment, the CFU count was drastically lowered. Recent reports about a disruption of infection with obligate intracellular pathogens, if cells were treated with FIASMA, might implicate an involvement of ASM in endocytosis of said intracellular pathogens or even *S. aureus*. Survival of mice might not be related to lack of TJP degradation, instead a prolonged exposure of *S. aureus* to antibiotics by decreased invasion leads to an enhanced clearance. To further investigate this hypothesis, HuLEC-5a or an ASM-knock down of HuLEC-5a were infected and CFU/ml was determined. Additionally, cells were treated with Amitriptyline, for a comparison of a potential ASM-knock down effect and Amitriptyline or if an additive effect occurs.

As depicted from Peng et al. data, endothelial cells with an introduced ASM-knock down exhibited a significantly lower CFU/ml count (Fig. 38). This phenotype was further increased, if cells were treated with Amitriptyline until the point where cells were nearly bacteria free.

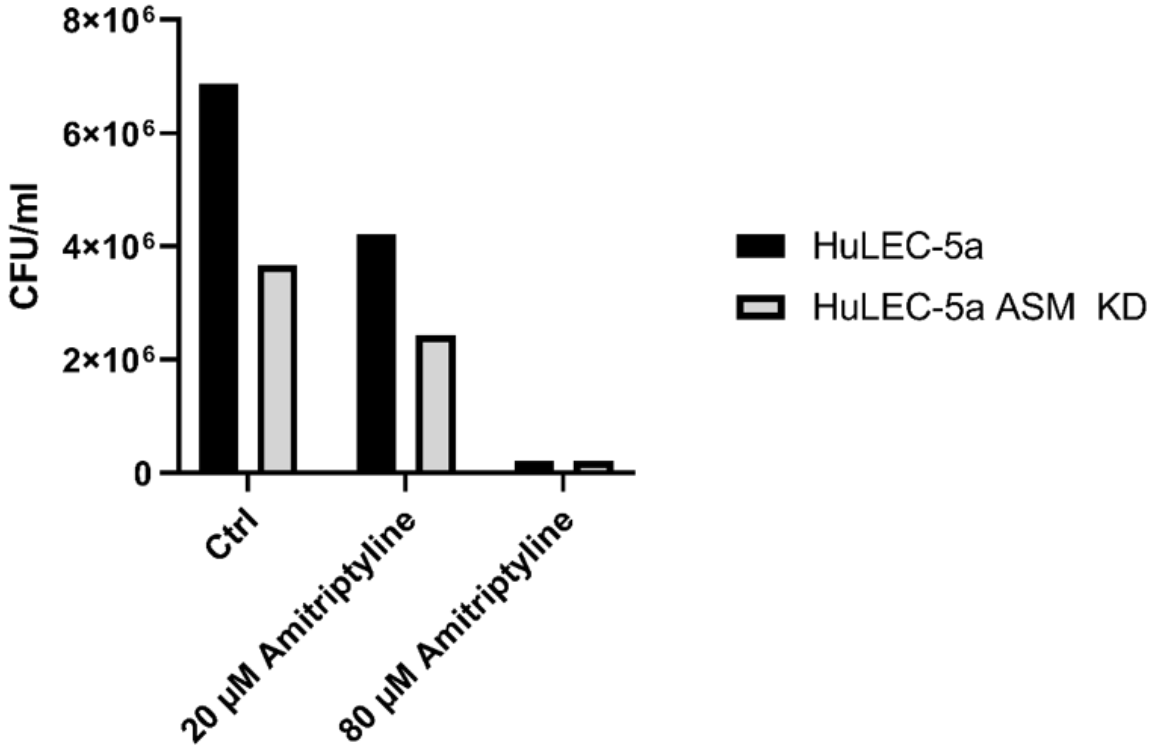

Fig. 38 ***ASM activity affects number of intracellular bacteria***
Wildtype HuLEC-5a or ASM-KD HuLEC-5a were infected with S. aureus JE2 MOI10 for 30 min, before adding Lysostaphin to cell culture medium to lyse extracellular bacteria. Infection was continued for another 90 min before washing cells and lysing them for plating of intracellular bacteria on TSA plates. ASM-KD cells exhibited significant lesser count of intracellular bacteria, whereas ASM inhibition by application of Amitriptyline further decreased intracellular S. aureus numbers.

Quantity of infected cells is scalable to ASM inhibition

In previous experiments, the viability of cells was not further altered if presented with 20 µM of Amitriptyline. This was not excluded for higher concentrations of the FIASMA, therefore murine endothelial cells were subjected to increasing concentrations of Amitriptyline. Except for concentration higher than 80 µM Amitriptyline, no significant cytotoxic effect was detected (Fig. 39**A**). Concurring to this effect, a dose dependent effect of Amitriptyline was exhibited for the quantity of infected cells. Although the decrease of infected cells treated with concentrations higher than 80 µM Amitriptyline was linked to an increased cell death, a dosage of 20 µM Amitriptyline was able to cut the quantity of infected cells by ~50% (Fig. 39**B**). Cells infected with *S. aureus* JE2 or JE2Δ*hla* exhibited comparable effects, for untreated and Amitriptyline treated cells (Fig. 39**C**). Although staphylococcal α-toxin was the driving factor for ASM recruitment depicted in experiments with bacterial supernatants, it could be excluded for this experiment, since this phenotype was independent of JE2 genotype.

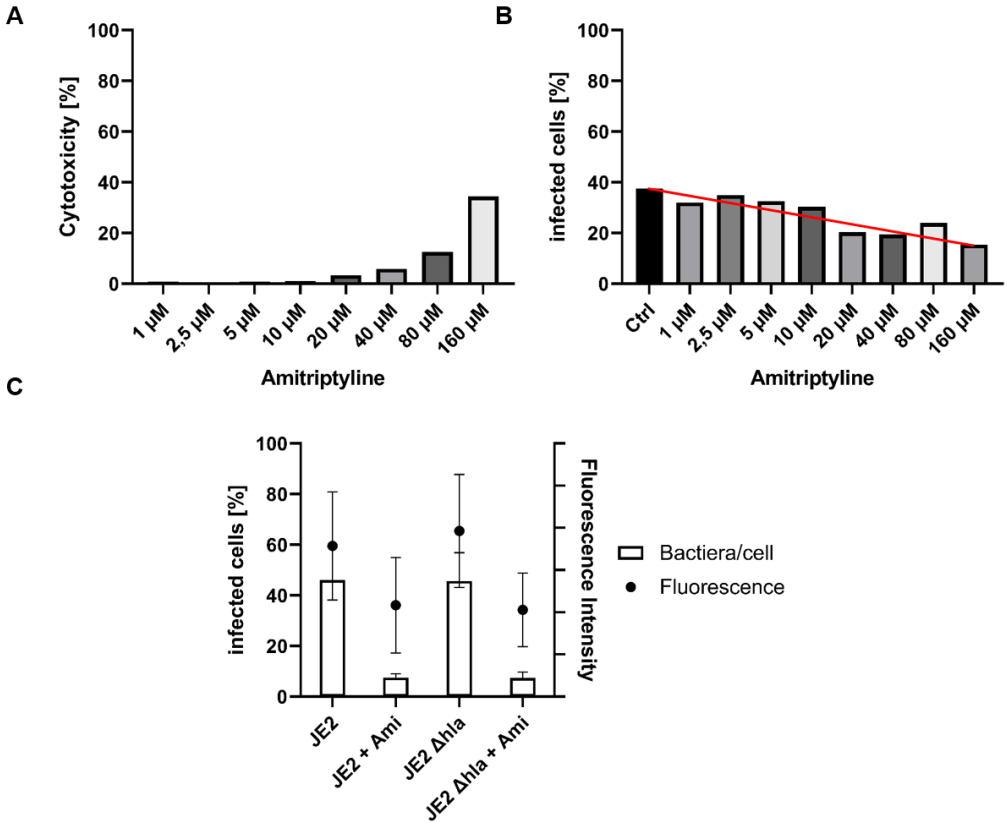

Fig. 39 ***ASM inhibition results in fewer intracellular bacteria in EOMA***
*(**A**) EOMA were incubated with increasing concentrations of Amitriptyline and checked for cytotoxic effects by measuring LDH release. (**B**) EOMA pre-treated with the indicated concentrations of Amitriptyline were infected for 30 min, before extracellular bacteria were lysed by addition of Lysostaphin. Infection continued for another 90 min, after which cells were fixed and analyzed by microscopy assisted counting of intracellular bacteria. (**C**) EOMA were incubated with 20 µM Amitriptyline and infected as described before. Cells were subsequently analyzed for number of intracellular bacteria and total fluorescence by flow cytometry.*

HuLEC-5a treated in a similar manner were displaying an identical phenotype. The quantity of infected cells was reduced if cells were pre-treated with 20 µM Amitriptyline (Fig. 40**A**). Additionally, as observed in EOMA, HuLEC-5a displayed a reduced fluorescence signal when treated with FIASMA. This observation was of most importance, since an analysis of infected cells with a high precision cell sorter led to the identification, that the number of infected cells was only slightly reduced if they were pre-treated with 20 µM Amitriptyline (Fig. 41**A**). Nonetheless the median fluorescence of ASM inhibited cells was reduced as depicted in a previous analysis (Fig. 41**B**). For an increased evaluation of the conflicting results, cells were infected, and intracellular bacteria and cells were counted via an automated Z-Stack image acquisition on a confocal microscope. Images were analyzed by a macro compiled by Dr. Fraunholz using ImageJ software. Utilizing this approach revealed a concurrent Amitriptyline effect for all cell lines tested resulting in a significant decreased bacteria count per cell. For the direct ASM inhibitor ARC39 conflicting results emerged,

depending on the cell type. For the immortalized endothelial cell line HuLEC-5a no difference was detectable (Fig. 42**A**), however the urinary bladder carcinoma cell line T24 carried significant less bacteria per cell after treatment with ARC39 (Fig. 42**B**).

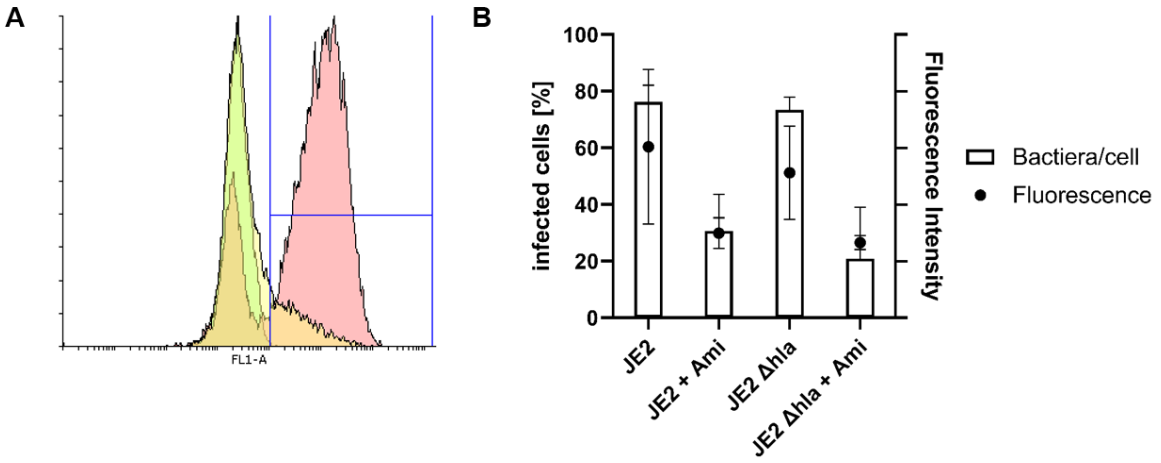

Fig. 40 ***Amitriptyline induced ASM inhibition reduces intracellular bacteria count in HuLEC-5a aswell*** *HuLEC-5a were infected as previously described for EOMA and analyzed by flow cytometry machine BD Accuri C6. (**A**) Population histogram exhibited a significant reduction in mean fluorescence if infected cells were treated with Amitriptyline. Green – uninfected ; Red – JE2 MOI10 ; Yellow – JE2 MOI10 + 20 µM Amitriptyline (**B**) Number of intracellular bacteria was reduced upon treatment with Amitriptyline independent from genotype of S. aureus, which correlates with measured mean fluorescence reduction.*

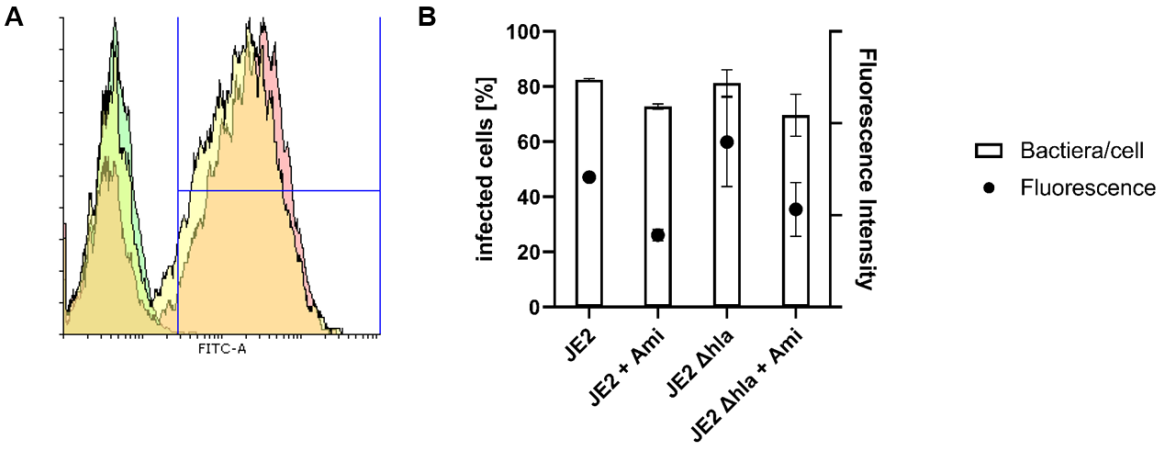

Fig. 41 ***Amitriptyline treated cells exhibit reduced fluorescence if infected with GFP expressing S. aureus*** *HuLEC-5a were infected as previously described for EOMA and analyzed by cell sorting machine BD FACSArias. (**A**) Population histogram is rarely affected by Amitritpyline application on infected cells. Green – uninfected ; Red – JE2 MOI10 ; Yellow – JE2 MOI10 + 20 µM Amitriptyline (**B**) Counting of total number of infected cells did not exhibit a significant difference compared to previous results. Mean fluorescence was still shown to be reduced upon Amitriptyline incubation.*

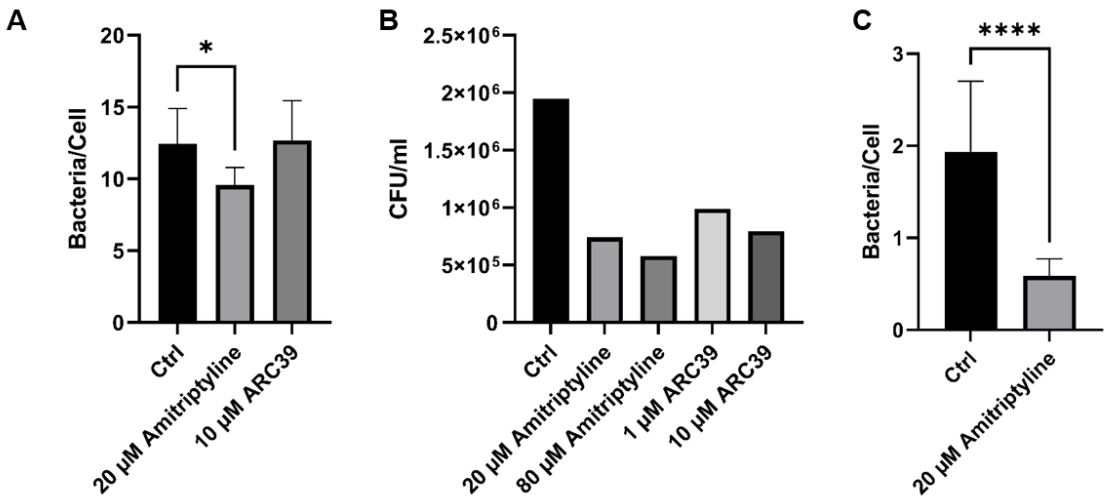

Fig. 42 ***Number of intracellular S. aureus reduced upon ASM inhibition***
HuLEC-5a were infected as previously described and Z-Stack images of 10 different slide positions were taken. Evaluation of intracellular S. aureus count was performed with an ImageJ macro. Intracellular number of S. aureus was reduced in different endothelial cell lines, if ASM inhibitors were applied prior to infection (A – HuLEC-5a ; B – T24 ; C – EOMA). Infection of HuLEC-5a led to a peculiar ASM release.

Similar to a stimulation of endothelial cells with bacterial SNT, HuLEC-5a were infected with *S. aureus* JE2 MOI10 for the indicated time points. Again, ASM activity for cell culture medium (SNT) and cell lysate (LYS) was evaluated and compared for a potential recruitment effect as seen for SNT treatments (Fig. 43). For the infection, a different ASM activity pattern was detected. Enzymatic activity in cell culture medium sharply decreased for the first two time points (5 – 10 min) and stabilized after 20 min at the initial activity. Only after 60 min a significant increase of ASM activity was detectable, increasing by ~ 50% after 120 min compared to Ctrl.

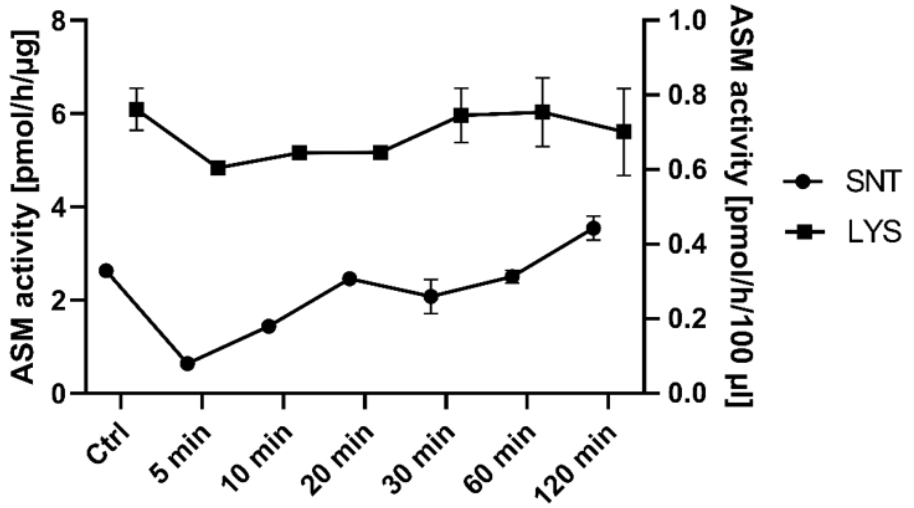

Fig. 43 ***ASM activity during S. aureus infection bares potential limitations***
HuLEC-5a were infected with S. aureus JE2 MOI10 for indicated time points. Analysis of SNT/LYS ASM activity was performed as previously shown. ASM activity pattern did not follow a predictable scheme, revealing potential limitations of this assay.

Contrary to the effects exhibited for bacterial SNT stimulation, where an increased extracellular activity led to a decreased intracellular activity, lysate activity from infected cells was decreased similar as for cell culture medium activity. Nonetheless ASM activity stabilized as seen for SNT after 30 min. After this time point no decisive effect was seen, however after 120 min a trend to a decreased ASM activity was depicted.

S. aureus infection can induce Caspase-8 activation

HuLEC-5a were either treated with differing concentrations of JE2 and JE2Δ*hla* SNT (1 and 10%) or infected with the matching live strains *S. aureus* JE2 and JE2Δ*hla* (MOI 10 and 200) (Fig. 44). Challenging endothelial cells with supernatants did not alter Cas8 activity regardless of α-toxin presence. Infection of HuLEC-5a however induced at the lower MOI an increase of Cas8 activity by ~50%. This effect was significantly increased by infecting cells with a MOI200. Interestingly was this effect independent of the presence of α-toxin, both bacterial strains induced identical effects.

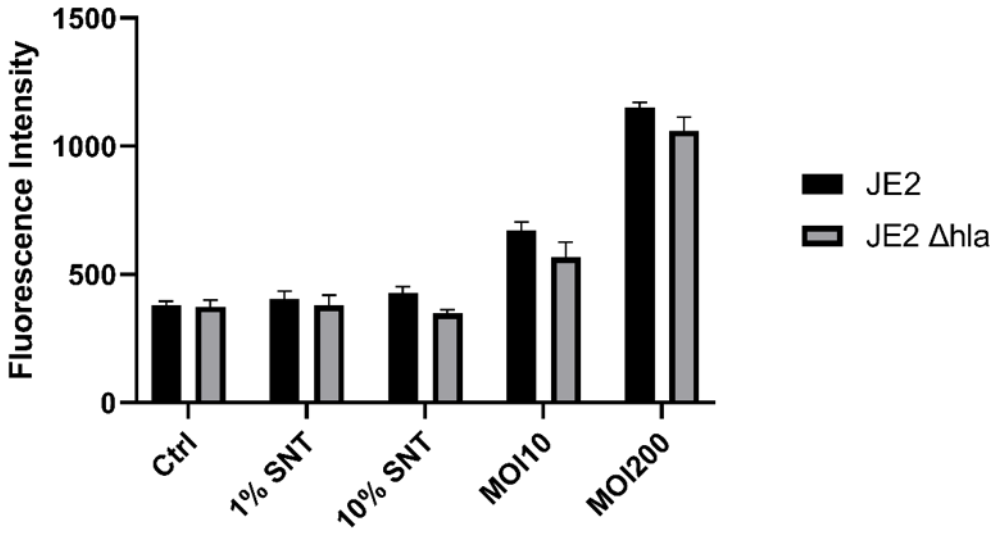

Fig. 44 ***Infection with S. aureus, but not treatment with bacterial culture supernatant, elicit Casp8 activation*** *HuLEC-5a were seeded 8 days prior challenging or infecting with the indicated concentrations for 30 min. Caspase 8 activity was determind with CaspGLOW™ Fluorescein Active Caspase-8 Staining Kit.*

Discussion

Recent findings published by Becker et al. [5] from the cooperating group of Prof. Dr. Gulbins indicate an activation of host cell ASM by staphylococcal α-toxin. This activation was shown to contribute to a disruption of endothelial cell tight junctions. Results from Peng et al. [275] were suggesting, that inhibition of ASM via genetic deficiency or treatment with FIASMA Amitriptyline eventually exhibits a protective mechanism against the degradation of cell-cell connections, further protecting mice from lung oedema and lethal *S. aureus* sepsis. Therefore, the aim of this study was to identify *S. aureus* virulence factors additionally to α-toxin capable to provoke host cell ASM activity. Furthermore, it should be elucidated to which extent *S. aureus* exotoxins affect endothelial tight junction degradation. At least, inhibition of ASM via FIASMA Amitriptyline is proposed to affect *S. aureus* infection mechanisms. Hence, thorough examination of ASM inhibition during *S. aureus* infection should be performed.

Shift in ASM activity indicates plasma membrane repair mechanism

As described in Becker et al. [5], *S. aureus* α-toxin elicits an increase of ASM activity in murine endothelial cells. Therefore, it was of interest, if similar effects may be described for human endothelial cells and more so, which signaling pathways are potentially involved in α-toxin and ASM interaction. Challenging human endothelial cells with purified α-toxin or *S. aureus* supernatants illustrated a significant activity shift for ASM (Fig. 34). Already 30 min after incubation with purified α-toxin or staphylococcal supernatants containing the toxin, HuLEC-5a displayed a significant decline in intracellular and oppositely a significant increase in extracellular ASM activity. Given the narrow time span, it is doubtful that newly generated ASM contributed to this effect, since protein expression of ASM depends on extensive post translational processing [288]. More so, results indicate a recruitment of intracellular ASM to the extracellular space.

This phenotype has not been described so far for S. aureus α-toxin, however, to further promote these findings, a robust method apart from enzyme activity assays for detection of ASM should be employed. This could be verified by measurement of ASM abundance in cell culture medium, yet no reliable antibodies are available for detection of ASM, hence common methods like western blotting or ELISA are currently not consistent enough to deliver significant results. Instead of issuing traditional methods

for protein detection, a direct approach may be used for (live-) tracking ASM in cellular compartments. Direct inhibitors of ASM are known to interact with the enzyme and might be utilized as a reporter system. Modification of e.g., ARC39, which does not hinder interaction of ASM, would be advantageous for tracking by live-cell microscopy or protein detection methods. Although several possibilities are available for detection of ASM, recruitment of ASM after plasma membrane damage through PFT is always accompanied by hallmark events. These mechanisms are not limited to PFT membrane damage, more so, are essential for repair of membrane lesions independent of their source [177,178,289]. However, recruitment of ASM is a phenotype linked to a specific membrane repair mechanism involving ASM activity. One of the additional trademark mechanisms connected to this specific PM repair mechanism is an influx of Ca^{2+} as well as increased surface expression of Lysosome-associated membrane protein 1 (LAMP1) caused by the recruitment of peripheral vesicles [177,221]. Anyhow, all listed studies observing these mechanisms were either using reagents or injury methods, which are known to induce rather large pores, membrane fissures or unnatural circumstances like laser injury method [287], and therefore induce a guaranteed influx of Ca^{2+}. In comparison, at its narrowest point the *S. aureus* α-toxin pore is proposed to be 1,4 nm in diameter [75] and to date Ca^{2+} conductivity of staphylococcal *Hla* pore is still debated [285]. Albeit this discussable topic, it should be investigated, if the observed increase in extracellular ASM activity is caused by the induction of this rather specific PM repair mechanism. Human endothelial cells challenged with α-toxin exhibited a significant increase of intracellular Ca^{2+} concentrations, which was potentiated if supernatants of *S. aureus* strain JE2 were used (Fig. 35). Additionally, contrary to a stimulation with Ionomycin, *S. aureus* SNT as well as purified α-toxin was able to induce an oscillating Ca^{2+} influx. A similar effect has been observed in wound healing processes [161,290]. The second trademark, increased LAMP1 exposure to the cell surface, was observed with an elaborate live-cell antibody staining approach (Fig. 36). Both, a bona fide Ca^{2+} ionophore as well as α-toxin were able to increase exposure of LAMP1 to the cell surface (Fig. 37). In connection to previous results and reports about PM repair mechanisms, it is most likely that staphylococcal *Hla* is able to induce a similar PM repair mechanism involving the recruitment of ASM to the extracellular space. To further emphasize these results, following projects should investigate auxiliary events linked to membrane damage as well as repair. Further downstream signaling involves the phosphorylation of p38

MAPK [286], resulting in the activation of signaling events convoluted in survival pathways, plasma membrane repair and apoptosis [291-295]. It should be of note, that simultaneously to Ca^{2+} influx a K^{+} efflux occurs, and it cannot be disclosed, that the reported p38 phosphorylation under Ca^{2+} omission might be induced for the reason of missing Ca^{2+}. Hereby it should be clarified, how these signaling pathways proceed and link it directly to an interaction of α-toxin and endothelial cells. Hence direct evidence for pore formation by Hla is missing in this project, it might be of high interest to visualize either direct pore formation or key events linked to plasma membrane damage. Regarding the increased exposure of LAMP1 to cell surfaces, it might be advisable to register said recruitment of peripheral vesicles via qualitative than rather quantitative approaches, e.g., live-cell microscopy with transfected cells. Additionally, the recruitment of these vesicles should be investigated since it was not addressed in this project and might give arise to a direct link between Ca^{2+} influx and vesicle recruitment. Further vesicular markers associated to ASM containing vesicles should be observed as well, since their abundance on the cell membrane should transiently increase concomitant to ASM release and LAMP1 exposure. Finally, it should be regarded, that for this project rather high concentrations of α-toxin or *S. aureus* SNT were issued, potential surpassing abundance of the toxin *in vivo*. Since the purity of α-toxin preparations as well as α-toxin concentration in bacterial supernatants were not verified, it should be investigated to challenge endothelial cells with defined concentrations of α-toxin with high purity. Hence the potential concentration of α-toxin could be lower than the deployed concentrations in this project.

Nonetheless it has been shown for the first time, that staphylococcal α-toxin might be able to induce a rather specific membrane repair mechanisms, which was until date linked to membrane damaging events involving greater pore size (SLO ~30 nm, glass beads ~100 nm) [287,296]. In relationship to results of reduced *S. aureus* invasion and findings of other groups [270], this might give inside how *S. aureus* is able to exploit host cell mechanisms to further penetrate cell tissues and reside inside of cells (Fig.45).

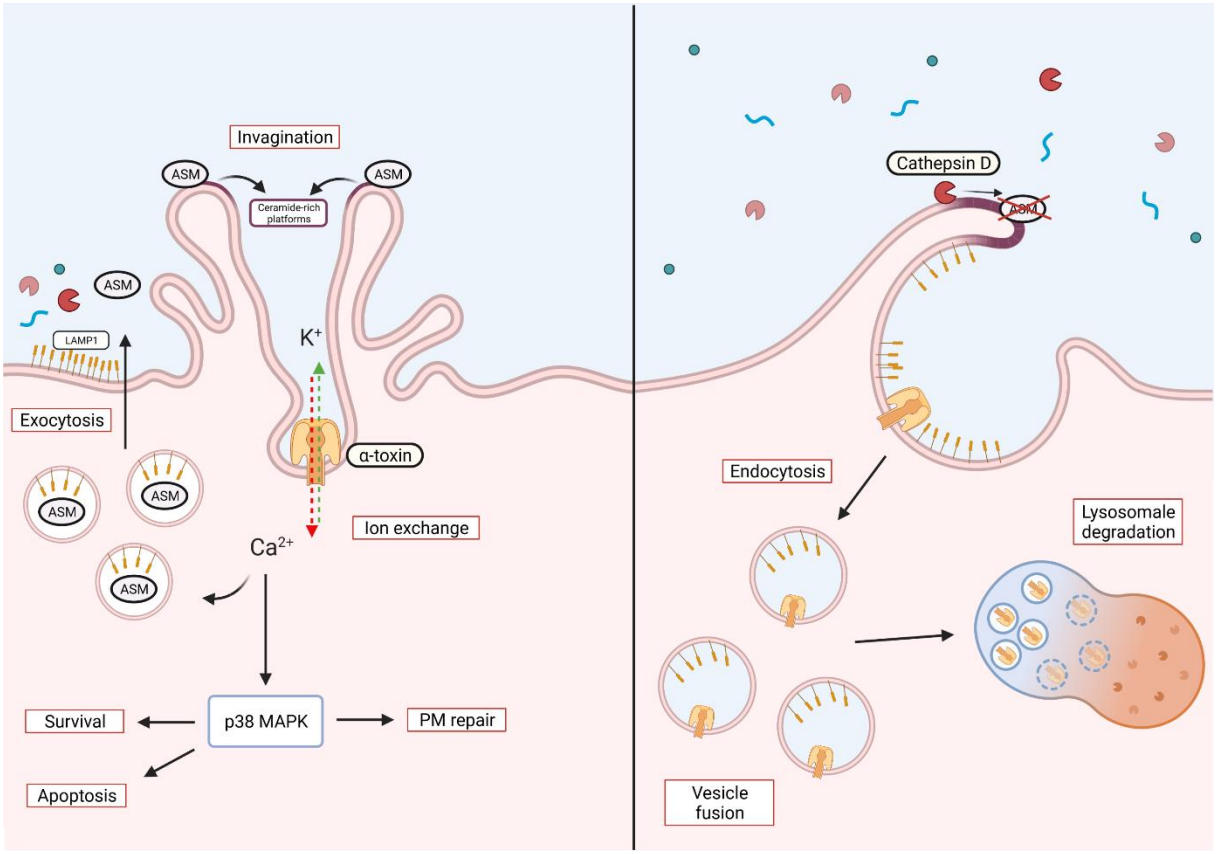

Fig. 45 ***Staphylococcal α-toxin induces ASM activity associated to PM repair***
In this proposed model, membrane damage facilitated via pore formation of Hla leads to an abrupt and uncontrolled ***ion exchange****, initiating differing cellular responses. Either rapid change in Ca^{2+} availability or K^+ absence instigates phosphorylation of p38 MAPK, which enables several signaling pathways including* ***apoptosis*** *or* ***PM repair****. Sudden Ca^{2+} influx recruits peripheral vesicles inducing an* ***exocytosis*** *of lysosomal contents such as ASM or lysozymes. Additionally, intralysosomal proteins like LAMP1 are exposed in large numbers to the cell surface. The activated lysozymes are able to degrade ECM, which interact with the PM facilitating binding of ASM. Conversion of SM to Cer by ASM results in formation of CRD, conducting an* ***invagination*** *at the side of membrane damage. CRD induced invagination enables the cell to* ***endocytose*** *damaged cell membrane parts, engulfing the effector of membrane damage, α-toxin, in a semi-closed compartment. CRD enables binding of Cathepsin D, inducing the degradation of ASM. Once endocytosed compartments are* ***fused into larger endosomal vesicles****, PFT are fully engulfed and ready for* ***lysosomal degradation****.*

TJP degradation mediated by *S. aureus* infection and toxin activity

Studies verified the impact of a plethora of secreted proteins from *S. aureus* on cell barrier integrity [297-299]. A major factor for disrupting junctional integrity is the staphylococcal α-toxin [300,301]. Recently, it has been shown that α-toxin disrupts endothelial cell tight junctions via activation and moreover inhibition of ASM and a depletion of sphingomyelin on plasma membranes was able to mitigate this effect [5,85,275]. Based on Peng et al., it should be investigated if other pathogenic factors of *S. aureus* are able to induce an activation of ASM and further, if a *S. aureus* induced cell barrier disruption may be tempered via reduction of ASM activity. Furthermore, a potential supplementation of ASM activity through bacterial sphingomyelinase activity of *S. aureus* β-toxin should be examined.

The latter was examined in both *S. aureus* JE2 and α-toxin lacking strain JE2Δ*hla,* which were able to express staphylococcal β-toxin, resulting in a robust bacterial sphingomyelinase activity (Fig. 33). Although both strains were able to degrade sphingomyelin, supernatants devoid of α-toxin were not able to induce a degradation of cell barrier proteins per contra to wildtype supernatants (Fig. 24**A**+**E**). Hence it was excluded that staphylococcal β-toxin is involved in cell barrier disruption.

The effect of all other virulence factors listed in Table A.1 should be examined with the murine endothelial cell line EOMA and human microvascular lung endothelial cell line HuLEC-5a. Both endothelial cell lines should be tested based on methods published in previously mentioned publication to further compare potential similarities between reported effects [5,275]. Although culturing methods were described precisely, it was not possible to induce an adequate expression of tight junction proteins like ZO-1 or VE-Cadherin in neither of cell lines (Fig. 13+14). Moreover, described expression of E-Cadherin by Peng et al. is not possible for EOMA since this cell line is of endothelial origin and therefore does not express E-Cadherin [302,303]. Adaptation of cell culture methods, by providing substrate coating and increasing cell growth time was pivotal for sufficient expression of TJP (Fig. 13+14).

Tolerance of EOMA against *S. aureus* infection

Given these information, further investigations regarding the fragmentary expression of TJP after two days led to distinct revelations of EOMA growth conditions and improvement to culturing methods. As depicted in Fig. 13, an improvement in ZO-1 expression was observed, if cells were seeded onto surfaces previously coated with extracellular matrix substrates like collagen or fibronectin. Other publications utilizing EOMA were recommending a standardized cell culture method on pre-coated surfaces as well[304,305]. Observations from own experiments performed as well as publications on this cell line indicate a slow growth for the first three days which accelerates tremendously afterwards [306]. This observation would coincide with results from TJP expression after 2 and 7 days, showing a vastly improved TJP expression on day 7. However, precise data about a time resolved TJP and AJ expression is not available since studies issuing this cell line do not contribute the overall growth time of their models [307-311]. Therefore, it cannot be excluded that technical or methodical factors might contribute to the differential expression of TJP and AJ. Regarding the lack of TJP degradation, there is doubt that the observed loss of signal for TJP and AJ was

caused by *S. aureus* infection. It must be noted that the methods issued for visualization of TJP degradation by Peng et al. likely promote the absorption of reagents by *S. aureus* through interactions with SpA. While SpA exhibits a broad range of affinity against several immunoglobulin subspecies (IgA, IgG, IgM), it possess a high absorption affinity against rabbit IgG antibodies [312]. All antibodies used for immunofluorescence microscopy were raised in rabbits. Additionally, the blocking substance to prevent unspecific binding of antibodies contained 5% FBS. While SpA confers a rather intermediate affinity against bovine IgG, western blot analysis revealed a strong unspecific signal for rabbit antibodies absorbed by SpA if western blots were treated with an equal blocking solution (S-Fig. 5). Unspecific binding of antibodies by SpA could be circumvented if blocking reagent for western blot analysis or immunofluorescence microscopy was substituted with pooled human serum. Samples treated with at least 10% pooled human serum did not exhibit any unspecific binding of antibodies to *S. aureus* (EOMA – Fig. 15+18 ; HuLEC-5a – Fig. 26). Hence a co-staining for nucleic acids is missing for published results by Peng et al., it cannot be verified if the observed degradation of TJP and AJ are caused by *S. aureus* or if the observed fragment signals are antibodies adhered to bacteria. Results from own experiments showed, in contrary to published results, that the murine endothelial cell line displayed a robust resilience against *S. aureus* infection and only exhibited elevated cytotoxic effects after 6h of continuous infection (Fig. 18). For other murine endothelial cell lines or for *in vivo* experiments in mice a disruption of cell barriers after α-toxin treatment was proven [4,5]. Since *in vivo* data from Peng et al. report identical results for tissue damage and overall survivability, the lack of TJP and AJ degradation might be contributed to this specific cell line [313]. Therefore, specific experiments for the overall capability of EOMA need to be undertaken, to further validate their general usefulness for such kind of experiments (e.g., abundance of receptor proteins, expression patterns of endothelial cells markers).

Challenging HuLEC-5a with *S. aureus* toxins

Contrary to the murine endothelial cell line EOMA, a distinct and rapid degradation of cell barrier proteins was depicted in the immortalized humane lung microvascular endothelial cell line HuLEC-5a (Fig. 20). This extent of TJP and AJ degradation would have been expected for EOMA as well since numerous publications provide a significant effect of especially α-toxin on endothelial cells [86,146,314]. In case of HuLEC-5a it was nonessential if cells were treated with staphylococcal supernatants or infected

with *S. aureus*. Regarding a mature expression of cell barrier markers like VE-Cadherin or ZO-1, an increased cell culture time and pre-coating with cell matrix substrate (Collagen, Fibronectin) was of benefit, as stated in several other publications as well [315-317]. However, inhibition of ASM by application of Amitriptyline did not prevent or mitigate the degradation of TJP and AJ (Fig. 23-27), although it was clearly shown that the FIASMA does inhibit enzymatic activity in a time and dose dependent manner (Fig. 9). A single disruption of the *hla* gene locus in *S. aureus* JE2 however abrogated the degradation of TJP and AJ in HuLEC-5a. All other *S. aureus* mutant strains were still able to disrupt cell-cell contacts, rendering α-toxin as a crucial factor for this phenotype. Since supernatants instead of purified α-toxin were issued for these experiments, it could not be ruled out, that a synergistic effect with other virulence factors present in bacterial supernatants contribute to the degradation of VE-Cadherin or ZO-1 in endothelial cells. Other studies do support the hypothesis for α-toxin being the main factor for cell barrier injury [4,86], nonetheless experiments with double knock-out mutant strains lacking α-toxin and an additional virulence factor would be helpful for deeper understanding of a potential interplay of virulence factors present in *S. aureus* supernatants.

Discrepancies in reported and observed ASM phenotype

In summary, published results regarding TJP degradation in EOMA were not reproducible and inhibition of ASM in HuLEC-5a did not mitigate induced TJP degradation. On the other side, both a significant increase as well as decrease in extra- and intracellular ASM activity was measured. Therefore, the question arose, if an increase in ASM activity is required for other *S. aureus* infection mechanisms. This hypothesis should be divided into two separate topics, involving the effect of staphylococcal α-toxin on human endothelial cell ASM activity and the effect of ASM activity on *S. aureus* invasiveness.

S. aureus invasiveness depends on ASM activity

While an involvement of ASM in TJP degradation could not be verified, the performed survival experiments in Peng et al. sparked interest [275]. Mice, if intravenously infected with *S. aureus*, expressing an Asm $^{-/-}$ phenotype or ones treated with Amitriptyline and co-treated with antibiotics had a 100% survival rate, compared to individual treatment with Amitriptyline or antibiotics. These results coincide with reduced lung oedema formation and lesser invasion of neutrophils into lung tissue. The recruitment of

neutrophils as well as their activation contributes eventually to tissue damage and acute lung injury (ALI) [318]. Although recruitment of immune cells is necessary for host defense against bacterial infections, prolonged activity is linked to worse outcome [319-321]. The crucial point between these findings and observations taken in this study is about the role of ASM, regarding its involvement in tissue breakdown, sphingolipid turnover and the survival of *S. aureus*. While it was shown that ASM may not be involved in TJP degradation *in vitro*, global inhibition of ASM *in vivo* may contribute to lesser tissue damage indirectly. Reduced ASM activity not only contributes to sphingolipid storage disorder, but it also influences signaling pathways for numerous cell types. Albeit an increased concentration of cytokines, some of which are especially responsible for the recruitment and chemoattraction of neutrophils (IL-6 ; MCP-1 ; S-1-P [322] ; IL-8 [323] ; MIP-2 [324]) can be detected in *Asm*$^{-/-}$ mice, there is major evidence for a disrupted or rather dysfunctional immune signaling, which might be the cause for a decreased influx of neutrophils. In case of ALI development a chronic inflammation leads to tissue damage, caused by the aggregation of foamy macrophages in alveolar space, hence the alleviated cytokine concentrations[325].

Asm$^{-/-}$ mice exhibit an increased vascular permeability and high numbers of neutrophils in alveolar space, while induction of sterile sepsis leads to a reduction of neutrophils numbers in lungs, steering these immune cells to the vascular system [326]. In summary it can be questioned, if genetical or chemical inhibition of ASM directly diminishes tissue damage, less it may be an indirect effect of dysfunctional immune cell recruitment and their activation [327]. Yet a benefit for the survival of mice, ASM activation might be a major element in transmigration of *S. aureus* from the vascular system to the alveolar space. As reported for other pathogens, the invasion of especially intracellular bacteria relies on ASM activity [270,328,329]. Considering the results of mice protected from lethal *S. aureus* induced sepsis, if treated with ASM inhibitors and antibiotics, and an involvement of ASM in the uptake of bacteria in host cells, it was hypothesized that *S. aureus* uptake into host cells was directly linked to ASM activity. Therefore, invasion assays were performed on several cell lines (human and murine) which were genetically modified, or treated with two distinct ASM inhibitors, and the ability of *S. aureus* to infect these cells was asserted. As hypothesized, a decrease in intracellular bacteria was observed, if ASM activity was decreased by genetical modifications or chemically inhibition (Fig. 38+39). In this case not the overall number of infected cells was reduced, but the bacterial load per cell

decreased, which was verified via microscopic count and flow cytometer fluorescence analysis (Fig. 40-42). Reduction of intracellular bacteria was scalable with the dose of inhibitor used, although high concentrations of Amitriptyline induced cytotoxicity in host cells (Fig. 39**A**+**B**). If these results are taken into consideration with findings from Peng and colleagues, it can be stated that the increased survivability of mice after *S. aureus* induced sepsis may be based on faster clearance of bacteria from the vascular system. The decreased ability of *S. aureus* to transmigrate cell barriers as a result ASM inhibition, which leads to a reduced uptake in host cells, leaves them vulnerable to antibiotics injected intravenously as well. Lesser transmigration of bacteria to the alveolar space additionally leads to a reduced invasion of immune cells like neutrophils, limiting tissue damage from bacterial and inflammatory sources. Evidence for this hypothesis needs to be collected in future projects, nonetheless, results of this project provide sufficient evidence to disclose a direct involvement of ASM in TJP degradation, but rather its essential role as a key factor for bacterial uptake in host cells.

As for an analysis of ASM activity in infected endothelial cells, results were conflicting with initial results from supernatant challenged HuLEC-5a, although this may not disagree with the hypothesis stated above. As shown in Fig. 43, a sharp decrease can be detected for the first 5 min of infection for both extra- as well as intracellular ASM activity, which gradually increases for the onset of infection. After 120 min infection time extracellular ASM activity exceeds the initial threshold, whereas intracellular activity depicts a downwards trend. At this point it cannot be disclosed if the experimental layout for infection of endothelial cells or ASM activity measurement need to be adapted to yield significant data on ASM activity during *S. aureus* infection. The initial threshold of ASM activity might be different since cells are centrifuged for eight minutes prior to the start of infection. During this time frame ASM activity might already change, as assays for infection could already show a sharp change within five minutes. Furthermore, infection with live bacteria involves more complex interactions than incubating endothelial cells with *S. aureus* supernatants. Although supernatants contain a variety of toxins, antigens or exoenzymes, live *S. aureus* express a myriad of potential surface interaction proteins, like SpA or Fibronectin binding protein (FnBP), which in return might interfere with the deployed ASM activity assay [184,278]. Moreover, it has to be disclosed, how *S. aureus* enables the recruitment of ASM or how the activity changes the interaction between bacteria and host cells.

Independent of ASM activity results from infection experiments, ASM inhibition interferes with the ability of *S. aureus* to infect human endothelial cells. This novel phenotype has not been reported yet giving insight into *S. aureus* infection mechanisms. Hence in future projects it should be disclosed, how *S. aureus* is able to exploit host cell ASM activity regarding its interaction with cell surface proteins and further signaling pathways. A potential manipulation of ASM activity could give rise to pathways in reducing *S. aureus* infectivity or tissue penetration. For a broader summary, a list of future projects will be discussed in the following chapter.

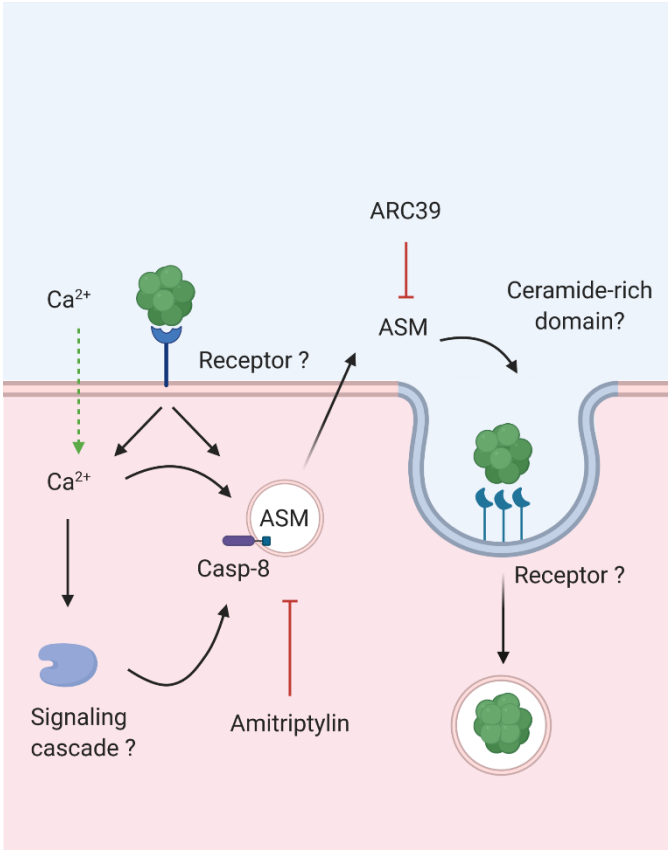

Fig. 46 ***Potential pathways involved in ASM mediated S. aureus invasion***
Infection of endothelial cells diminished in ASM activity were exhibiting a reduced number intracellular S. aureus. First control experiments about inhibitor kinetics revealed a significant implication of lysosomal derived ASM. Hence the hypothesis was proposed that S. aureus is able to recruit lysosomal ASM, which elicits an increased endocytosis.

Detection of acid sphingomyelinase

For deletion of *Smpd1* in murine hemangioendothelioma and human lung endothelial cells, a standardized CRISPR approach published by Ann Ran et al. [279] was chosen (see chapter 2.2.3). Transfection of EOMA successfully led to ablation of ASM expression (Fig. 7**A**+**B**). However, the deletion was lost shortly after although transfection was controlled by GFP reporter and knock-out was verified via genome sequencing as well as Western blot. Albeit flow cytometry-based cell sorting methods

were performed for a single cell sorting per vessel, EOMA have shown to be highly adhesive and even thorough incubation in dissociation buffer left cells at times in duplets/triplets. This characteristic most probably led to an overgrowth with contaminant wildtype cells, which by chance resulted in a loss of *Smpd1* knock-out. (Fig. 6**C**+**D** ; S-Fig. 1). Further explanation for loss of Smpd1 knock-out supporting the overgrowth hypothesis can be found in literature reports for mice models lacking *Smpd1*, highlighting the significance of ASM for cell vitality and homeostasis. Horinouchi et al. created mice models resembling NPD type A and B [232]. Most notably *Smpd1*-/- mice had less than half of body weight compared to their heterozygous littermates. Size and volume of organs were decreased as well with the highest disparity in brain volume. ASM ubiquitous involvement in cell growth and homeostasis was observed in, cells carrying *Smpd1* knock-out [330-332]. Single cell clones of EOMA had significant growth impairments, delaying the establishment of confluent cell monolayers. While single wildtype cells were able to regrow fully confluent cell monolayers in approximately two weeks, knock-out cells took at least four to six weeks until a confluent cell monolayer was established.

For the human endothelial cell line HuLEC-5a an identical mutagenesis approach was performed. After adapting sgRNA templates to *SMPD1,* transfection as well as cell sorting was conducted as described for EOMA. After transfection with the knock-out construct and subsequent single cell sorting, HuLEC-5a were drastically impaired in cell growth, taking three to four weeks to establish a cell colony consisting of a few hundred cells. As in EOMA, this growth impairment might implicate a successful mutagenesis of *SMPD1*, however without analysis of DNA or protein material this remains an assumption. Both, growth impairment and lack of evidence for knock-out, were detrimental for further experiments, therefore the approach of modifying genes via CRIPSCas9 was discarded.

Since the deletion of *SMPD1* via CRISPRCas9 was rather challenging and time consuming, altering expression of ASM by introduction of a knock-down was performed. Introduction of *SMPD1* knock-down constructs was performed by lentiviral transduction of knock-down-vector pLVTHM-Pm_LAMP1-YFP_Spe-shRNA-ASM1 and was verified by green fluorescence reporter in target cells (establishment and verification done by Kerstin Paprotka). HuLEC-5a were transfected with two distinct constructs (see Table A.2) and were investigated for their cell growth as well as ability to convert sphingomyelin.

In comparison to knock-out variants, knock-down cells did not exhibit a major cell growth impairment, rather displayed viability comparable to wildtype cells. Furthermore, knock-down cells showed no phenotypic changes and were able to be conducted to ASM activity assays. As depicted in Fig. 7, the quality of ASM inhibition differed between the issued constructs, whereat construct ASM KD#1 excelled the inhibitory potential of the second construct. Although ASM activity was reduced by ~50% for cells transfected with construct 1, the inhibitory effect of both knock-down variants was inferior to application of the chemical inhibitors Amitriptyline or ARC39. The apparent advantage of mentioned inhibitors is their fast application time as well as high inhibitory effects [236,270,333]. Additionally, if used in short term experiments (< 4 hours) the contribution of lysosomal and secreted ASM can be distinguished. Whereas Amitriptyline induces a rapid inhibition of lysosomal ASM activity, ARC39 offers a direct inhibition of secreted ASM (Fig. 8+9). Both inhibitors do not exhibit cytotoxic effects on either EOMA or HuLEC-5a at the given concentrations (Fig. 10), labelling them a convenient tool for ASM activity investigation [333]. However, the knock-down cells still pose to be useful since Amitriptyline and ARC39 introduce other implications if utilized *in vitro.* Functional inhibition of ASM by Amitriptyline occurs at high concentrations in lysosomes. This selective accumulation via acid trapping leads to a detachment of ASM from the inner lysosomal membrane, targeting the protein for degradation [237,238]. Hence detachment is induced by protonation of lysosomes, other proteins like acid ceramidase are detached and degraded as well [236]. Therefore, it may be questionable to attribute phenotypical changes to a decrease of ASM activity, if Amitriptyline was applied during any timepoint. Hence, experiments performed with Amitriptyline should be carefully controlled by overlapping experiments, since observed changes could be contributed through a degradation of other lysosomal proteins. While ARC39 is a highly effective direct inhibitor of ASM, cells exhibit a low uptake because of its potent negative charge in physiological pH environments. Furthermore, it cannot be used in *in vivo* experiments, due to a high absorption by bone surfaces [333,334]. However, near total inhibition may be achieved *in vitro* by continuous application of ARC39 for 12-24 hours. Early measurement of cytotoxicity did not impact cell viability (Fig.10), therefore labelling ARC39 the most potent ASM inhibitor, given the assumption long time incubation leads to a near total inhibition.

Tracking cellular localization of ASM

Besides quantitative measurements of ASM expressions as well as enzymatic activity, an approach for qualitative tracking of ASM expression and kinetic was employed by transfection of HuLEC-5a with a mCherry conjugated ASM protein. Furthermore, another construct was introduced, which was carrying a non-functional variant of ASM, resembling an ASM variant in NPD patients. First experiments revealed issues, rendering both constructs unfitting for this project (Fig. 11). HuLEC-5a transfected with the NPD variant exhibited a distribution of ASM in intracellular networks (most probably endoplasmatic reticulum), indicating a non-functional distribution of ASM. Challenging cells with α-toxin did not impact this distribution, which led to the assumption, that ASM might be trapped. Although a single gene is responsible for ASM expression, two distinct forms can be detected – the lysosomal (L-ASM) and secretory (S-ASM) form [261,335]. Distribution to its distinct destinations, either secretion via the constitutive secretion pathway into the extracellular space (S-ASM) or shuttling to lysosomes (L-ASM), depends on post-translational processing upon entering the ER [332]. Hence neither specific signals in the NPD variant for lysosomal nor Golgi-apparatus distribution was detected, the apparent assumption for a faltering distribution can be taken. Distribution of wildtype ASM constructs was resembling the depiction in literature, but upon release of the enzyme into the extracellular space by application of any known trigger, the fluorescent tag was immediately lost. Further analysis of cell lysates revealed a loss of the mCherry tag from the ASM protein (Fig. 11). As for the NPD variant, additional processing of ASM occurs inside of lysosomes, which is most likely the cause for loss of the fluorescent reporter protein [336]. Given these implications, no further efforts were taken to establish an ASM reporter for microscopic purposes. Processing of ASM occurs in multiple steps and several organelles, which involves transformation at the core, N- and C-terminus, making it difficult to apply a reporter to the protein without influencing correct transport, protein folding or loss of the reporter. Nonetheless, the wildtype ASM construct may be used as an extracellular reporter system, in which the fluorescence yield of extracellular medium can be investigated to indirectly measure the release of ASM from cells.

Methods implemented for ASM activity detection

With poor results from attempting to knock-out *SMPD1* and all commercially available antibodies raised against ASM performing weak in western blots as well as

immunofluorescence microscopy, a method had to be established, to distinguish both ASM expression and activity. For this purpose, a commercial enzymatic activity test kit and a published activity protocol had been issued. Work with the commercial test kit was discontinued out of economic reasoning (highly expensive reagents) and for its assay structure. Measurement of sphingomyelinase activity with this kit is based on the subsequent degradation of ceramide into other substrates, which finally yield Resorufin. In theory, measurement of fluorometric product Resorufin enables a calculation to the initial ceramide concentration. However, conversion of ceramide to Resorufin depends on alkaline phosphatase, choline oxidase and horseradish peroxidase activity [337]. *S. aureus* expresses similar enzymes [338], may degrade substrates essential for this assay kit [339] or is able to inhibit enzymatic activity respectively enzyme substrates [340]. Samples containing bacterial lysate or supernatants were not reacting to this testing kit, further supporting potential interference from *S. aureus* contents.

Since other commercial available kits were either relying on identical enzymatic reactions or included similar highly expensive reagents, ASM activity testing was performed after methods published by C.Mühle and J.Kornhuber [282]. First results from this assay were indicating an impact of staphylococcal supernatant on ASM activity, however results could not be replicated by means of high variances. Further investigations revealed three major implications in measuring ASM activity:

Material: As briefly discussed in C.Mühle and J.Kornhuber upon disclosure of BSA or low protein concentrations, the sphingomyelin substrate used in this assay may adhere to plastic surfaces. As suggested for this issues, polypropylene reaction vessels were used at any time. Nonetheless, thorough testing revealed significant and quantifiable carryover of samples from pipet tips or sample retention in reaction vessels (Fig. 29-31). Replacement materials instead of standard pipet tips were tested, but none were providing any significant improvement. Since the carryover were reproducible with different samples, it was assumed as a standard error and considered for each individual measurement. The major issue for high variance was sample retention by high volatility of the $CHCl_3$/MeOH solution, which affected the volume of sample that was extractable from reaction vessels. Therefore, the sample preparation described in this protocol was adapted to 20 µl total volume to ensure for exact application of 10 µl volume for each sample.

Fetal bovine serum: ASM is commonly present in blood serum and represents a hallmark biomarker for several diseases [341-343]. Not only in humans but other mammals as cows, ASM can be detected in serum samples [344]. Hence mentioned ASM of bovine origin generated a high background enzymatic activity, it was not possible to elucidate ASM activity from treated host cell cultures (Fig. 32**A**). To eliminate residual bovine ASM activity, FBS was heat inactivated for 30 min 55°C as for inactivation of the complement system [345]. Anyhow, even after heat treatment a significant residual ASM activity was detected (Fig. 32**A**). FBS could not be omitted from cell culture medium since serum contents are essential for inhibition of staphylococcal PSMs [346,347]. Lack of FBS in cell culture medium led to significant and high cytotoxicity (S-Fig. 3). Alternative, a heat treatment was implemented, which was able to eliminate residual ASM activity while containing inhibitory capabilities against PSMs from staphylococcal supernatants (Fig. 32**B** ; S-Fig. 3). Therefore, FSB was treated for 1 hour at 70°C. Another approach would have been the employment of *S. aureus* strains lacking PSM expression. However, it cannot be excluded that PSMs might impact ASM activity, hence the prior option was chosen.

Bacterial Sphingomyelinase: As a potential factor in *S. aureus* infectious mechanism, staphylococcal β-toxin was a major focus point for this project. Previous studies indicated that α-toxin may induce ASM activity [274]. Apathogenic *S. aureus* strains like RN4220 are unable to express α-hemolysin, however they are known for their high secretion of β-hemolysin [348]. Hence staphylococcal β-toxin is a bacterial sphingomyelinase, the induction of host cell ASM through α-toxin may be supplemented by high expression of β-toxin which might enable host cell sphingolipid manipulation independent from host cell ASM. As a result of bacteriophage induced lysogeny, β-toxin expression in *S. aureus* strain JE2 is inactivated [107,108]. Yet recent publications delivered evidence for a common production of β-toxin in *S. aureus* strains carrying the specific bacteriophage responsible for β-hemolysin ablation[108]. A comparison of staphylococcal strains for their ability to degrade sphingomyelin exhibited a significant bacterial sphingomyelinase activity in *S. aureus* JE2, although β-toxin inactivating bacteriophage δSa3 was previously detected in strains used for this project (Data not shown – Experiment performed by Julian Scherer)(Fig. 33). Stress stimuli like antibiotics are able to induce an excision of φSa3, resulting in expression of β-toxin [110]. In contrast to natural β-hemolysin secreting strains like *S. aureus* RN4220 or 6850, the activity of JE2 appears minuscule, however even low

expression sufficed to introduce major variances in ASM activity assays. Therefore *S. aureus* strain JE2Δ*hlb* was introduced to experiments investigating ASM activity for validation of results independent of left-over bacterial sphingomyelinase activity in cell culture medium. Additionally, all results from experiments issuing JE2 strains still carrying bacteriophage φSa3 were verified by inclusion of *S. aureus* strain JE2Δ*hlb*. Since *S. aureus* JE2 harbors another gene for expression of a phospholipase C capable of modifying sphingolipids, an additional knock-out strain was introduced to investigate its involvement in sphingomyelinase activity (S-Fig. 4; JE2Δ*plc*). This strain still exhibited significant bSMase activity, disclosing an involvement of *plc* in this context.

All the above taken steps helped to establish a robust and reproducible ASM activity assay for this project. By measuring ASM activity for both cell lysate as well as cell culture medium, it was possible to display a shift of ASM from the intra- to extracellular space. However, direct measurement or ASM abundancy via western blot or more preferably ELISA would be direct evidence for recruitment of ASM, yet high qualitative antibodies for this purpose are not available. Since short time spans were investigated for ASM activity, production of fresh ASM protein were negligible [349]. Equal reactions to other bacterial PFTs have been reported previously, which led to the assumption, that similar mechanisms were involved in this process [350,351]. Further explanations and results provided in the following chapters will promote this hypothesis.

Prospects

This project provided interesting revelations of how *S. aureus* manipulates host cell ASM activity. Thereby several aspects can be brought up to further analyze the interaction of *S. aureus* with endothelial cells and how ASM activity influences infection mechanisms.

For future projects, the scaffold around ASM activity assays and detection should be improved. As depicted above, analysis of ASM activity in simple experimental setups (e.g., SNT challenge) is working as intended, however presence of live bacteria might be influencing said assays. It should be observed, how these interactions might influence this assay and hence improvements undertaken to further analyze *S. aureus* ability to induce ASM recruitment. As for the detection of ASM via microscopy or western blot, intensive work needs to be invested. A collaboration with groups specialized on protein modification or tracking methods might be beneficial at this point.

As for the observations regarding a recruitment of ASM and plasma membrane repair mechanism, it has been noted that essential events for this phenotype were verified, nonetheless further proof would reinforce this hypothesis. Experiments could provide evidence for an essential role of α-toxin; however, pore formation should be investigated. Hence methods should be introduced, which revolve around Influx markers (e.g., Fluorescein diacetate staining) or excitable markers reacting to sudden changes in ion concentrations (e.g., K^+ indicator). A more elegant approach would be the transfection of endothelial cells with different fluorescent Annexin variants as shown in the publication of Draeger et al. [167]. As Ca^{2+} sensing proteins, Annexins are known to be recruited to the side of plasma membrane damage for resealing purposes [167]. Size and type of a membrane leak determine which type of Annexin is recruited [352]. In this context the general impact of Ca^{2+} should be further investigated. The putative source of ASM, peripheral vesicles, are probably recruited by to the sudden change of intracellular Ca^{2+} concentration. Associated with this process are Soluble NSD attachment proteins Receptor (SNARE), essential for vesicle budding with the plasma membrane and probably required for the recruitment of ASM [353,354]. In return, chelating intracellular as well as removing extracellular Ca^{2+} would give insight into p38 MAPK phosphorylation dynamics. Blocking of Ca^{2+} signaling could be combined with investigation in further downstream signaling as a result of p38 MAPK phosphorylation, e.g. apoptosis markers like caspase activation [355]. Regarding an identification of ASM carrying vesicles, both vesicular proteins excreted and associated with LAMP1 vesicles were detected. Associated to a release of ASM are proteases like cathepsin B, D and L, whose catalytic activity could be verified in cell culture medium [178]. Recruitment itself could be observed by issuing vesicle loading dyes (e.g., Lysotracker) or with dual reporter systems associated to LAMP1, which change in fluorescence emission pattern depending on pH value. At last, it might be of interest, if an uptake of the Hla pore is dependent on ASM activity. This project provided support for the hypothesis of ASM dependent release after α-toxin treatment, nonetheless these results provide a solid foundation for further projects, which could settle these observations.

The most promising as well as interesting findings surround the reduced invasion of *S. aureus* in endothelial cells if ASM activity was inhibited. While results were indicating a significant change in infection kinetics, many questions are still left unanswered. Other studies already provide a correlation between host cell sphingolipid metabolism

and the ability of pathogens to exploit the enzymatic activity to gain access to intracellular compartments [270,329,356]. For *S. aureus* this evidence was shown so far, for which reason additional attempts should be taken to further elucidate the role of ASM in staphylococcal infection mechanisms. Beside the difficulties around ASM activity assays with live bacteria samples, it should be clarified if *S. aureus* induces an identical process as observed for experiments performed with bacterial SNT and α-toxin. This would involve identical questions regarding a potential Ca^{2+} influx and LAMP1 exposure to cell surfaces after infection. In case of SNT experiments, both events could be pinpointed to pore formation caused by α-toxin. In case of staphylococcal infection this process might be more delicate and elaborate, since beside PFT interaction with host cell membrane, *S. aureus* might induce identical effects by interaction with cell surface proteins. One cell surface protein, which is depending on ASM activity[357] and might as well interact with *S. aureus,* is the Tumor necrosis factor receptor superfamily member 1A (TNFRSA1) [131,358]. A critical factor for the recruitment of ASM via TNFRSA1 interaction is the cysteine-aspartic acid protease 8 (Casp8) [359]. Preliminary data was indicating an increase in Casp8 activity if endothelial cells were infected with *S. aureus* JE2 but not challenged with SNT of similar strains (Fig. 44). Interestingly was this increase independent of *S. aureus* genotype. Wildtype JE2 and Δ*hla* strain were able to induce a comparable Casp8 activity. Further, *S. aureus* SNT was unable to induce protease activity, raising the question if staphylococcal SNT might induce a different effect than infection with live bacteria. Hereby the question arises, if the same receptor interaction with *S. aureus* is responsible for extracellular ASM recruitment and the uptake inside the cell. One receptor found to be involved in *S. aureus* internalization is $\alpha_5\beta_1$ integrin, which is also found to be endocytosed depending on cholesterol and sphingolipids present in the plasma membrane [360]. With the results provided it remains elusive, how *S. aureus* exploits host cell ASM activity, however a hypothesis was proposed involving experimental as well as published findings (Fig. 46) that in return could serve for future projects. As an outcome of increased ASM activity, ceramide-rich domains pose to be another interesting topic that should be investigated. As already shown by Peters et al., *N. meningitidis* induces formation of pathogen-engulfing ceramide-rich platforms (CRP) [329]. As well as for further investigations regarding α-toxin interactions and effects of live bacteria on host cells, it would be beneficial to investigate similar mechanisms induced by *S. aureus.*

Many more aspects are still unanswered (PKCδ involvement, ASM effect on intracellular *S. aureus* replication), however this project was able to provide novel evidence for the involvement of ASM activity in *S. aureus* ability to invade human endothelial cells. Introducing supplemental projects in the future would give insight into *S. aureus* ability to infect human endothelial cells, stimulate their uptake in host cells and the contribution of this pathway to *S. aureus* persistence in humans. Undoubtedly this situation is more complex *in vivo*, nonetheless provided this initial data evidence how to further trace *S. aureus* ability to persist in its host environment and evade immune reactions.

This project gave valuable insight into *S. aureus* infection mechanisms and promising opportunities for future research. As already mentioned, *S. aureus* specific interaction with host ASM seems to be the most promising prospect of this project. Recent research into pathogen – host cell ASM interaction may indicate, that manipulation of host sphingolipid metabolism offers a universal route for entry into host cells. Even for the current topic of Severe Acute Respiratory Syndrome-Coronavirus-type 2 (SARS-CoV-2) initial studies hint at the involvement of ASM in infection mechanism [361-363]. Especially the diversity of different pathogens utilizing this pathway is staggering and should be motivation for further research into the dynamics of *S. aureus* and host cell sphingolipid interaction.

Bibliography

[1] Hannun, Y.A. and L.M. Obeid, *Sphingolipids and their metabolism in physiology and disease.* Nat Rev Mol Cell Biol, 2018. **19**(3): p. 175-191.

[2] A.Schartendorff, G.H.a., *S.aureus - Electron microscopy*, R2009-04_01_S_aureus_010_TIF, Editor. 2014, Robert-Koch Institut: Web Page.

[3] Tanaka, Y., et al., *2-Methyl-2,4-pentanediol induces spontaneous assembly of staphylococcal alpha-hemolysin into heptameric pore structure.* Protein Sci, 2011. **20**(2): p. 448-56.

[4] Inoshima, I., et al., *A Staphylococcus aureus pore-forming toxin subverts the activity of ADAM10 to cause lethal infection in mice.* Nat Med, 2011. **17**(10): p. 1310-4.

[5] Becker, K.A., et al., *Staphylococcus aureus Alpha-Toxin Disrupts Endothelial-Cell Tight Junctions via Acid Sphingomyelinase and Ceramide.* Infect Immun, 2018. **86**(1).

[6] Sturtzel, C., *Endothelial Cells.* Adv Exp Med Biol, 2017. **1003**: p. 71-91.

[7] Domigan, C.K. and M.L. Iruela-Arispe, *Recent advances in vascular development.* Curr Opin Hematol, 2012. **19**(3): p. 176-83.

[8] McColl, B.K., S.A. Stacker, and M.G. Achen, *Molecular regulation of the VEGF family -- inducers of angiogenesis and lymphangiogenesis.* APMIS, 2004. **112**(7-8): p. 463-80.

[9] Mickoleit, M., et al., *High-resolution reconstruction of the beating zebrafish heart.* Nat Methods, 2014. **11**(9): p. 919-22.

[10] Haack, T. and S. Abdelilah-Seyfried, *The force within: endocardial development, mechanotransduction and signalling during cardiac morphogenesis.* Development, 2016. **143**(3): p. 373-86.

[11] Cong, X. and W. Kong, *Endothelial tight junctions and their regulatory signaling pathways in vascular homeostasis and disease.* Cell Signal, 2020. **66**: p. 109485.

[12] Chiba, H., et al., *Transmembrane proteins of tight junctions.* Biochim Biophys Acta, 2008. **1778**(3): p. 588-600.

[13] Furuse, M., *Molecular basis of the core structure of tight junctions.* Cold Spring Harb Perspect Biol, 2010. **2**(1): p. a002907.

[14] Gonzalez-Mariscal, L., R. Tapia, and D. Chamorro, *Crosstalk of tight junction components with signaling pathways.* Biochim Biophys Acta, 2008. **1778**(3): p. 729-56.

[15] Wolburg, H. and A. Lippoldt, *Tight junctions of the blood-brain barrier: development, composition and regulation.* Vascul Pharmacol, 2002. **38**(6): p. 323-37.

[16] Rahimi, N., *Defenders and Challengers of Endothelial Barrier Function.* Front Immunol, 2017. **8**: p. 1847.

[17] Zihni, C., et al., *Tight junctions: from simple barriers to multifunctional molecular gates.* Nat Rev Mol Cell Biol, 2016. **17**(9): p. 564-80.

[18] Fanning, A.S. and J.M. Anderson, *Zonula occludens-1 and -2 are cytosolic scaffolds that regulate the assembly of cellular junctions.* Ann N Y Acad Sci, 2009. **1165**: p. 113-20.

[19] Ebnet, K., et al., *Junctional adhesion molecules (JAMs): more molecules with dual functions?* J Cell Sci, 2004. **117**(Pt 1): p. 19-29.

[20] Furuse, M., et al., *Occludin: a novel integral membrane protein localizing at tight junctions.* J Cell Biol, 1993. **123**(6 Pt 2): p. 1777-88.

[21] Tsukita, S. and M. Furuse, *The structure and function of claudins, cell adhesion molecules at tight junctions.* Ann N Y Acad Sci, 2000. **915**: p. 129-35.

[22] Citi, S., et al., *Cingulin: characterization and localization.* J Cell Sci, 1989. **93 (Pt 1)**: p. 107-22.

[23] Riazuddin, S., et al., *Tricellulin is a tight-junction protein necessary for hearing.* Am J Hum Genet, 2006. **79**(6): p. 1040-51.

[24] Gonzalez-Mariscal, L., et al., *Tight junctions and the regulation of gene expression.* Semin Cell Dev Biol, 2014. **36**: p. 213-23.

[25] Garrido-Urbani, S., P.F. Bradfield, and B.A. Imhof, *Tight junction dynamics: the role of junctional adhesion molecules (JAMs).* Cell Tissue Res, 2014. **355**(3): p. 701-15.

[26] Tornavaca, O., et al., *ZO-1 controls endothelial adherens junctions, cell-cell tension, angiogenesis, and barrier formation.* J Cell Biol, 2015. **208**(6): p. 821-38.

[27] McSherry, E.A., et al., *Breast cancer cell migration is regulated through junctional adhesion molecule-A-mediated activation of Rap1 GTPase.* Breast Cancer Res, 2011. **13**(2): p. R31.

[28] Itoh, M., et al., *Involvement of ZO-1 in cadherin-based cell adhesion through its direct binding to alpha catenin and actin filaments.* J Cell Biol, 1997. **138**(1): p. 181-92.

[29] Bauer, H., et al., *The dual role of zonula occludens (ZO) proteins.* J Biomed Biotechnol, 2010. **2010**: p. 402593.

[30] Xu, J., et al., *Early embryonic lethality of mice lacking ZO-2, but Not ZO-3, reveals critical and nonredundant roles for individual zonula occludens proteins in mammalian development.* Mol Cell Biol, 2008. **28**(5): p. 1669-78.

[31] Stevenson, B.R., et al., *Phosphorylation of the tight-junction protein ZO-1 in two strains of Madin-Darby canine kidney cells which differ in transepithelial resistance.* Biochem J, 1989. **263**(2): p. 597-9.

[32] Chen, W., et al., *Propofol improved hypoxia-impaired integrity of blood-brain barrier via modulating the expression and phosphorylation of zonula occludens-1.* CNS Neurosci Ther, 2019. **25**(6): p. 704-713.

[33] Rochfort, K.D. and P.M. Cummins, *Cytokine-mediated dysregulation of zonula occludens-1 properties in human brain microvascular endothelium.* Microvasc Res, 2015. **100**: p. 48-53.

[34] Giannotta, M., M. Trani, and E. Dejana, *VE-cadherin and endothelial adherens junctions: active guardians of vascular integrity.* Dev Cell, 2013. **26**(5): p. 441-54.

[35] *CDH5 cadherin 5 [Homo sapiens (human)]*. 2021, NCBI: https://www.ncbi.nlm.nih.gov/gene?Db=gene&Cmd=ShowDetailView&TermToSearch=1003.

[36] Vittet, D., et al., *Embryonic stem cells differentiate in vitro to endothelial cells through successive maturation steps.* Blood, 1996. **88**(9): p. 3424-31.

[37] Breier, G., et al., *Molecular cloning and expression of murine vascular endothelial-cadherin in early stage development of cardiovascular system.* Blood, 1996. **87**(2): p. 630-41.

[38] Lampugnani, M.G., et al., *CCM1 regulates vascular-lumen organization by inducing endothelial polarity.* J Cell Sci, 2010. **123**(Pt 7): p. 1073-80.

[39] Strilic, B., et al., *The molecular basis of vascular lumen formation in the developing mouse aorta.* Dev Cell, 2009. **17**(4): p. 505-15.

[40] Gaengel, K., et al., *The sphingosine-1-phosphate receptor S1PR1 restricts sprouting angiogenesis by regulating the interplay between VE-cadherin and VEGFR2.* Dev Cell, 2012. **23**(3): p. 587-99.

[41] Lenard, A., et al., *In vivo analysis reveals a highly stereotypic morphogenetic pathway of vascular anastomosis.* Dev Cell, 2013. **25**(5): p. 492-506.

[42] Navarro, P., L. Ruco, and E. Dejana, *Differential localization of VE- and N-cadherins in human endothelial cells: VE-cadherin competes with N-cadherin for junctional localization.* J Cell Biol, 1998. **140**(6): p. 1475-84.

[43] Takeichi, M., *The cadherins: cell-cell adhesion molecules controlling animal morphogenesis.* Development, 1988. **102**(4): p. 639-55.

[44] Guipaud, O., et al., *The importance of the vascular endothelial barrier in the immune-inflammatory response induced by radiotherapy.* Br J Radiol, 2018. **91**(1089): p. 20170762.

[45] Ley, K., et al., *Getting to the site of inflammation: the leukocyte adhesion cascade updated.* Nat Rev Immunol, 2007. **7**(9): p. 678-89.

[46] Vestweber, D., *Relevance of endothelial junctions in leukocyte extravasation and vascular permeability.* Ann N Y Acad Sci, 2012. **1257**: p. 184-92.

[47] Lemichez, E., et al., *Breaking the wall: targeting of the endothelium by pathogenic bacteria.* Nat Rev Microbiol, 2010. **8**(2): p. 93-104.

[48] Dictionary.com. *Word definition - Staphylococcus*. [Online Dictionary] 2021 [cited 2021 19.02.2021]; Dictionary]. Available from: https://www.dictionary.com/browse/staphylococcus.

[49] Lexico.com. *Word definition - Staphylococcus*. [Online Dictionary] 2021 [cited 2021; Available from: https://www.lexico.com/definition/staphylococcus.

[50] Sejvar, J.J., *Neuroinfections (What Do I Do Now?).* Emerging Infectious Diseases, 2013. **19**(9): p. 1553-1553.

[51] Chambers, H.F., *Community-associated MRSA--resistance and virulence converge.* N Engl J Med, 2005. **352**(14): p. 1485-7.

[52] Boucher, H.W. and G.R. Corey, *Epidemiology of methicillin-resistant Staphylococcus aureus.* Clin Infect Dis, 2008. **46 Suppl 5**: p. S344-9.

[53] Taylor, T.A. and C.G. Unakal, *Staphylococcus Aureus*, in *StatPearls*. 2020: Treasure Island (FL).

[54] Lowy, F.D., *Staphylococcus aureus infections.* N Engl J Med, 1998. **339**(8): p. 520-32.

[55] Liu, C.M., et al., *Staphylococcus aureus and the ecology of the nasal microbiome.* Sci Adv, 2015. **1**(5): p. e1400216.

[56] Uehara, Y., et al., *Bacterial interference among nasal inhabitants: eradication of Staphylococcus aureus from nasal cavities by artificial implantation of Corynebacterium sp.* J Hosp Infect, 2000. **44**(2): p. 127-33.

[57] Robert-Koch-Institut. *Staphylokokken-Erkrankungen, insbesondere Infektionen durch MRSA*. 2016 [cited 2021 18.02.2021].

[58] Haag, A.F., J.R. Fitzgerald, and J.R. Penades, *Staphylococcus aureus in Animals.* Microbiol Spectr, 2019. **7**(3).

[59] Barber, M. and M. Rozwadowska-Dowzenko, *Infection by penicillin-resistant staphylococci.* Lancet, 1948. **2**(6530): p. 641-4.

[60] Kirby, W.M., *Extraction of a Highly Potent Penicillin Inactivator from Penicillin Resistant Staphylococci.* Science, 1944. **99**(2579): p. 452-3.

[61] Rountree, P.M. and B.M. Freeman, *Infections caused by a particular phage type of Staphylococcus aureus.* Med J Aust, 1955. **42**(5): p. 157-61.

[62] Barber, M., *Methicillin-resistant staphylococci.* J Clin Pathol, 1961. **14**: p. 385-93.

[63] Jevons, M.P. and M.T. Parker, *The Evolution of New Hospital Strains of Staphylococcus Aureus.* J Clin Pathol, 1964. **17**: p. 243-50.

[64] Organisation, W.H. <*Critically Important Antimicrobials for Human Medicine - 6th Revision.pdf*>. 2019 [cited 2021.

[65] Hiramatsu, K., et al., *Dissemination in Japanese hospitals of strains of Staphylococcus aureus heterogeneously resistant to vancomycin.* Lancet, 1997. **350**(9092): p. 1670-3.

[66] Weigel, L.M., et al., *Genetic analysis of a high-level vancomycin-resistant isolate of Staphylococcus aureus.* Science, 2003. **302**(5650): p. 1569-71.

[67] Centers for Disease, C. and Prevention, *Vancomycin-resistant Staphylococcus aureus--New York, 2004.* MMWR Morb Mortal Wkly Rep, 2004. **53**(15): p. 322-3.

[68] Robert-Koch-Institut. <*Infektionsepidemiologisches Jahrbuch meldepflichtiger Krankheiten für 2019 - RKI.pdf*>. 2020 [cited 2021 18.02.2021].

[69] Chambers, H.F. and F.R. Deleo, *Waves of resistance: Staphylococcus aureus in the antibiotic era.* Nat Rev Microbiol, 2009. **7**(9): p. 629-41.

[70] Gonzalez, B.E., et al., *Pulmonary manifestations in children with invasive community-acquired Staphylococcus aureus infection.* Clin Infect Dis, 2005. **41**(5): p. 583-90.

[71] Gonzalez, B.E., et al., *Severe Staphylococcal sepsis in adolescents in the era of community-acquired methicillin-resistant Staphylococcus aureus.* Pediatrics, 2005. **115**(3): p. 642-8.

[72] Miller, L.G., et al., *Necrotizing fasciitis caused by community-associated methicillin-resistant Staphylococcus aureus in Los Angeles.* N Engl J Med, 2005. **352**(14): p. 1445-53.

[73] OECD. <*AMR-Tackling-the-Burden-in-the-EU-OECD-ECDC-Briefing-Note-2019.pdf*>. 2019.

[74] Deutschland, B. <*Deutscher Bundestag - Drucksache 19-12409.pdf*>. 2019 [cited 2021; Antwort der Bundesregierung auf die Kleine Anfrage der Abgeordneten Dr. Andrew Ullmann, Michael Theurer, Grigorios Aggelidis, weiterer Abgeordneter und der Fraktion der FDP – Drucksache 19/12045 – Bekämpfung von antimikrobiellen Resistenzen].

[75] Song, L., et al., *Structure of staphylococcal alpha-hemolysin, a heptameric transmembrane pore.* Science, 1996. **274**(5294): p. 1859-66.

[76] Christmas, D., *Recherches expérimentales sur la suppuration.* Annales de l'Institut Pasteur, 1888. **2**: p. 469.

[77] Leber, V., *Uber die entstehung der entzundung und die wirkung der entzundungserregenden schadlichkeiten.* Fortschr. Med, 1888. **6**: p. 460.

[78] Akers, H. and S. Porter, *Bundaberg's Gethsemane: the tragedy of the inoculated children*. Vol. 20. 2008: Copyright Agency. 261–278.

[79] Glenny, A.T. and M.F. Stevens, *Staphylococcus toxins and antitoxins.* The Journal of Pathology and Bacteriology, 1935. **40**(2): p. 201-210.

[80] Kumar, S., et al., *The Characterization of Staphylococcal Toxins : Ii. The Isolation and Characterization of a Homogeneous Staphylococcal Protein Possessing Alpha Hemolytic, Dermonecrotic, Lethal, and Leucocidal Activities.* J Exp Med, 1962. **115**(6): p. 1107-15.

[81] Bernheimer, A.W. and L.L. Schwartz, *Isolation and composition of staphylococcal alpha toxin.* J Gen Microbiol, 1963. **30**: p. 455-68.

[82] Wilke, G.A. and J. Bubeck Wardenburg, *Role of a disintegrin and metalloprotease 10 in Staphylococcus aureus alpha-hemolysin-mediated cellular injury.* Proc Natl Acad Sci U S A, 2010. **107**(30): p. 13473-8.

[83] Schwiering, M., et al., *Lipid and phase specificity of alpha-toxin from S. aureus.* Biochim Biophys Acta, 2013. **1828**(8): p. 1962-72.

[84] Galdiero, S. and E. Gouaux, *High resolution crystallographic studies of alpha-hemolysin-phospholipid complexes define heptamer-lipid head group interactions: implication for understanding protein-lipid interactions.* Protein Sci, 2004. **13**(6): p. 1503-11.

[85] Ziesemer, S., et al., *Sphingomyelin Depletion from Plasma Membranes of Human Airway Epithelial Cells Completely Abrogates the Deleterious Actions of S. aureus Alpha-Toxin.* Toxins (Basel), 2019. **11**(2).

[86] Powers, M.E., et al., *ADAM10 mediates vascular injury induced by Staphylococcus aureus alpha-hemolysin.* J Infect Dis, 2012. **206**(3): p. 352-6.

[87] Belmonte, G., et al., *Pore formation by Staphylococcus aureus alpha-toxin in lipid bilayers. Dependence upon temperature and toxin concentration.* Eur Biophys J, 1987. **14**(6): p. 349-58.

[88] Bhakdi, S. and J. Tranum-Jensen, *Alpha-toxin of Staphylococcus aureus.* Microbiol Rev, 1991. **55**(4): p. 733-51.

[89] Cho, J.S., et al., *Neutrophil-derived IL-1beta is sufficient for abscess formation in immunity against Staphylococcus aureus in mice.* PLoS Pathog, 2012. **8**(11): p. e1003047.

[90] Haugwitz, U., et al., *Pore-forming Staphylococcus aureus alpha-toxin triggers epidermal growth factor receptor-dependent proliferation.* Cell Microbiol, 2006. **8**(10): p. 1591-600.

[91] Ezepchuk, Y.V., et al., *Staphylococcal toxins and protein A differentially induce cytotoxicity and release of tumor necrosis factor-alpha from human keratinocytes.* J Invest Dermatol, 1996. **107**(4): p. 603-9.

[92] Gillespie, W.A. and V.G. Alder, *Control of an outbreak of staphylococcal infection in a hospital.* Lancet, 1957. **272**(6969): p. 632-4.

[93] Rountree, P.M. and M.A. Beard, *Further observations on infection with phage type 80 staphylococci in Australia.* Med J Aust, 1958. **45**(24): p. 789-95.

[94] Montgomery, C.P., et al., *Comparison of virulence in community-associated methicillin-resistant Staphylococcus aureus pulsotypes USA300 and USA400 in a rat model of pneumonia.* J Infect Dis, 2008. **198**(4): p. 561-70.

[95] DeLeo, F.R., et al., *Molecular differentiation of historic phage-type 80/81 and contemporary epidemic Staphylococcus aureus.* Proc Natl Acad Sci U S A, 2011. **108**(44): p. 18091-6.

[96] Bubeck Wardenburg, J., R.J. Patel, and O. Schneewind, *Surface proteins and exotoxins are required for the pathogenesis of Staphylococcus aureus pneumonia.* Infect Immun, 2007. **75**(2): p. 1040-4.

[97] Kennedy, A.D., et al., *Targeting of alpha-hemolysin by active or passive immunization decreases severity of USA300 skin infection in a mouse model.* J Infect Dis, 2010. **202**(7): p. 1050-8.

[98] Bayer, A.S., et al., *Hyperproduction of alpha-toxin by Staphylococcus aureus results in paradoxically reduced virulence in experimental endocarditis: a host defense role for platelet microbicidal proteins.* Infect Immun, 1997. **65**(11): p. 4652-60.

[99] Doery, H.M., et al., *The properties of phospholipase enzymes in staphylococcal toxins.* J Gen Microbiol, 1965. **40**(2): p. 283-96.

[100] Katayama, Y., et al., *Beta-hemolysin promotes skin colonization by Staphylococcus aureus.* J Bacteriol, 2013. **195**(6): p. 1194-203.

[101] Walev, I., et al., *Selective killing of human monocytes and cytokine release provoked by sphingomyelinase (beta-toxin) of Staphylococcus aureus.* Infect Immun, 1996. **64**(8): p. 2974-9.

[102] Huseby, M., et al., *Structure and biological activities of beta toxin from Staphylococcus aureus.* J Bacteriol, 2007. **189**(23): p. 8719-26.

[103] Projan, S.J., et al., *Nucleotide sequence: the beta-hemolysin gene of Staphylococcus aureus.* Nucleic Acids Res, 1989. **17**(8): p. 3305.

[104] Huseby, M.J., et al., *Beta toxin catalyzes formation of nucleoprotein matrix in staphylococcal biofilms.* Proc Natl Acad Sci U S A, 2010. **107**(32): p. 14407-12.

[105] Flores-Diaz, M., et al., *Bacterial Sphingomyelinases and Phospholipases as Virulence Factors.* Microbiol Mol Biol Rev, 2016. **80**(3): p. 597-628.

[106] Aarestrup, F.M., et al., *Frequency of alpha- and beta-haemolysin in Staphylococcus aureus of bovine and human origin. A comparison between pheno- and genotype and variation in phenotypic expression.* APMIS, 1999. **107**(4): p. 425-30.

[107] Tran, P.M., et al., *varphiSa3mw Prophage as a Molecular Regulatory Switch of Staphylococcus aureus beta-Toxin Production.* J Bacteriol, 2019. **201**(14).

[108] Salgado-Pabon, W., et al., *Staphylococcus aureus beta-toxin production is common in strains with the beta-toxin gene inactivated by bacteriophage.* J Infect Dis, 2014. **210**(5): p. 784-92.

[109] Goerke, C., et al., *Extensive phage dynamics in Staphylococcus aureus contributes to adaptation to the human host during infection.* Mol Microbiol, 2006. **61**(6): p. 1673-85.

[110] Goerke, C., J. Koller, and C. Wolz, *Ciprofloxacin and trimethoprim cause phage induction and virulence modulation in Staphylococcus aureus.* Antimicrob Agents Chemother, 2006. **50**(1): p. 171-7.

[111] Aman, M.J., et al., *Structural model of the pre-pore ring-like structure of Panton-Valentine leukocidin: providing dimensionality to biophysical and mutational data.* J Biomol Struct Dyn, 2010. **28**(1): p. 1-12.

[112] Yamashita, K., et al., *Crystal structure of the octameric pore of staphylococcal gamma-hemolysin reveals the beta-barrel pore formation mechanism by two components.* Proc Natl Acad Sci U S A, 2011. **108**(42): p. 17314-9.

[113] Yoong, P. and V.J. Torres, *The effects of Staphylococcus aureus leukotoxins on the host: cell lysis and beyond.* Curr Opin Microbiol, 2013. **16**(1): p. 63-9.

[114] Shukla, S.K., et al., *Virulence genes and genotypic associations in nasal carriage, community-associated methicillin-susceptible and methicillin-resistant USA400 Staphylococcus aureus isolates.* J Clin Microbiol, 2010. **48**(10): p. 3582-92.

[115] Dumont, A.L., et al., *Characterization of a new cytotoxin that contributes to Staphylococcus aureus pathogenesis.* Mol Microbiol, 2011. **79**(3): p. 814-25.

[116] Alonzo, F., 3rd, et al., *Staphylococcus aureus leucocidin ED contributes to systemic infection by targeting neutrophils and promoting bacterial growth in vivo.* Mol Microbiol, 2012. **83**(2): p. 423-35.

[117] Alonzo, F., 3rd, et al., *CCR5 is a receptor for Staphylococcus aureus leukotoxin ED.* Nature, 2013. **493**(7430): p. 51-5.

[118] Gillet, Y., et al., *Association between Staphylococcus aureus strains carrying gene for Panton-Valentine leukocidin and highly lethal necrotising pneumonia in young immunocompetent patients.* Lancet, 2002. **359**(9308): p. 753-9.

[119] Lina, G., et al., *Involvement of Panton-Valentine leukocidin-producing Staphylococcus aureus in primary skin infections and pneumonia.* Clin Infect Dis, 1999. **29**(5): p. 1128-32.

[120] Mehlin, C., C.M. Headley, and S.J. Klebanoff, *An inflammatory polypeptide complex from Staphylococcus epidermidis: isolation and characterization.* J Exp Med, 1999. **189**(6): p. 907-18.

[121] Peschel, A. and M. Otto, *Phenol-soluble modulins and staphylococcal infection.* Nat Rev Microbiol, 2013. **11**(10): p. 667-73.

[122] Rautenberg, M., et al., *Neutrophil responses to staphylococcal pathogens and commensals via the formyl peptide receptor 2 relates to phenol-soluble modulin release and virulence.* FASEB J, 2011. **25**(4): p. 1254-63.

[123] Wang, R., et al., *Identification of novel cytolytic peptides as key virulence determinants for community-associated MRSA.* Nat Med, 2007. **13**(12): p. 1510-4.

[124] McCarthy, A.J. and J.A. Lindsay, *Genetic variation in Staphylococcus aureus surface and immune evasion genes is lineage associated: implications for vaccine design and host-pathogen interactions.* BMC Microbiol, 2010. **10**: p. 173.

[125] Foster, T.J., et al., *Adhesion, invasion and evasion: the many functions of the surface proteins of Staphylococcus aureus.* Nat Rev Microbiol, 2014. **12**(1): p. 49-62.

[126] Genome, N., *Staphylococcus aureus*. NCBI: https://www.ncbi.nlm.nih.gov/genome/?term=Staphylococcus%20aureus[Organism]&cmd=DetailsSearch.

[127] Hammer, N.D. and E.P. Skaar, *Molecular mechanisms of Staphylococcus aureus iron acquisition.* Annu Rev Microbiol, 2011. **65**: p. 129-47.

[128] McAleese, F.M., et al., *Loss of clumping factor B fibrinogen binding activity by Staphylococcus aureus involves cessation of transcription, shedding and cleavage by metalloprotease.* J Biol Chem, 2001. **276**(32): p. 29969-78.

[129] Bischoff, M., et al., *Microarray-based analysis of the Staphylococcus aureus sigmaB regulon.* J Bacteriol, 2004. **186**(13): p. 4085-99.

[130] Sun, Y., et al., *Staphylococcal Protein A Contributes to Persistent Colonization of Mice with Staphylococcus aureus.* J Bacteriol, 2018. **200**(9).

[131] Gomez, M.I., et al., *Staphylococcus aureus protein A activates TNFR1 signaling through conserved IgG binding domains.* J Biol Chem, 2006. **281**(29): p. 20190-6.

[132] Edwards, A.M., et al., *Staphylococcus aureus extracellular adherence protein triggers TNFalpha release, promoting attachment to endothelial cells via protein A.* PLoS One, 2012. **7**(8): p. e43046.

[133] Silverman, G.J. and C.S. Goodyear, *Confounding B-cell defences: lessons from a staphylococcal superantigen.* Nat Rev Immunol, 2006. **6**(6): p. 465-75.

[134] Mascari, L.M. and J.M. Ross, *Quantification of staphylococcal-collagen binding interactions in whole blood by use of a confocal microscopy shear-adhesion assay.* J Infect Dis, 2003. **188**(1): p. 98-107.

[135] O'Seaghdha, M., et al., *Staphylococcus aureus protein A binding to von Willebrand factor A1 domain is mediated by conserved IgG binding regions.* FEBS J, 2006. **273**(21): p. 4831-41.

[136] Zong, Y., et al., *A 'Collagen Hug' model for Staphylococcus aureus CNA binding to collagen.* EMBO J, 2005. **24**(24): p. 4224-36.

[137] Kang, M., et al., *Collagen-binding microbial surface components recognizing adhesive matrix molecule (MSCRAMM) of Gram-positive bacteria inhibit complement activation via the classical pathway.* J Biol Chem, 2013. **288**(28): p. 20520-31.

[138] Valotteau, C., et al., *Single-Cell and Single-Molecule Analysis Unravels the Multifunctionality of the Staphylococcus aureus Collagen-Binding Protein Cna.* ACS Nano, 2017. **11**(2): p. 2160-2170.

[139] Lopes, J.D., M. dos Reis, and R.R. Brentani, *Presence of laminin receptors in Staphylococcus aureus.* Science, 1985. **229**(4710): p. 275-7.

[140] Zhang, Z., et al., *The alpha v beta 1 integrin functions as a fibronectin receptor but does not support fibronectin matrix assembly and cell migration on fibronectin.* J Cell Biol, 1993. **122**(1): p. 235-42.

[141] Sinha, B., et al., *Fibronectin-binding protein acts as Staphylococcus aureus invasin via fibronectin bridging to integrin alpha5beta1.* Cell Microbiol, 1999. **1**(2): p. 101-17.

[142] Maali, Y., et al., *Identification and Characterization of Staphylococcus delphini Internalization Pathway in Nonprofessional Phagocytic Cells.* Infect Immun, 2020. **88**(5).

[143] Rozalska, B. and T. Wadstrom, *Interaction of fibronectin and fibronectin binding protein (FnBP) of Staphylococcus aureus with murine phagocytes and lymphocytes.* FEMS Microbiol Immunol, 1992. **4**(6): p. 305-15.

[144] Menzies, B.E., *The role of fibronectin binding proteins in the pathogenesis of Staphylococcus aureus infections.* Curr Opin Infect Dis, 2003. **16**(3): p. 225-9.

[145] Kramko, N., et al., *Early Staphylococcus aureus-induced changes in endothelial barrier function are strain-specific and unrelated to bacterial translocation.* Int J Med Microbiol, 2013. **303**(8): p. 635-44.

[146] Menzies, B.E. and I. Kourteva, *Staphylococcus aureus alpha-toxin induces apoptosis in endothelial cells.* FEMS Immunol Med Microbiol, 2000. **29**(1): p. 39-45.

[147] Buerke, M., et al., *Staphylococcus aureus alpha toxin mediates polymorphonuclear leukocyte-induced vasocontraction and endothelial dysfunction.* Shock, 2002. **17**(1): p. 30-5.

[148] Herrera, A., et al., *Staphylococcal beta-Toxin Modulates Human Aortic Endothelial Cell and Platelet Function through Sphingomyelinase and Biofilm Ligase Activities.* mBio, 2017. **8**(2).

[149] Lubkin, A., et al., *Staphylococcus aureus Leukocidins Target Endothelial DARC to Cause Lethality in Mice.* Cell Host Microbe, 2019. **25**(3): p. 463-470 e9.

[150] Li, L., et al., *Phenol-soluble modulin alpha4 mediates Staphylococcus aureus-associated vascular leakage by stimulating heparin-binding protein release from neutrophils.* Sci Rep, 2016. **6**: p. 29373.

[151] Fisher, J. and A. Linder, *Heparin-binding protein: a key player in the pathophysiology of organ dysfunction in sepsis.* J Intern Med, 2017. **281**(6): p. 562-574.

[152] Lin, Q., et al., *Increased plasma levels of heparin-binding protein in patients with acute respiratory distress syndrome.* Crit Care, 2013. **17**(4): p. R155.

[153] Bentzer, P., et al., *Heparin-binding protein is important for vascular leak in sepsis.* Intensive Care Med Exp, 2016. **4**(1): p. 33.

[154] Maurer, K., et al., *Autophagy mediates tolerance to Staphylococcus aureus alpha-toxin.* Cell Host Microbe, 2015. **17**(4): p. 429-40.

[155] Gutierrez, M.G., et al., *Autophagy is a defense mechanism inhibiting BCG and Mycobacterium tuberculosis survival in infected macrophages.* Cell, 2004. **119**(6): p. 753-66.

[156] Bauckman, K.A., N. Owusu-Boaitey, and I.U. Mysorekar, *Selective autophagy: xenophagy.* Methods, 2015. **75**: p. 120-7.

[157] Escobar, D.A., et al., *Sepsis-Induced Autophagy is a Protective Mechanism against Cell Death*, in *Autophagy: Cancer, Other Pathologies, Inflammation, Immunity, Infection, and Aging*. 2014. p. 247-268.

[158] Andrews, N.W. and M. Corrotte, *Plasma membrane repair.* Curr Biol, 2018. **28**(8): p. R392-R397.

[159] Opitz, B., et al., *Extra- and intracellular innate immune recognition in endothelial cells.* Thromb Haemost, 2007. **98**(2): p. 319-26.

[160] Cooper, S.T. and P.L. McNeil, *Membrane Repair: Mechanisms and Pathophysiology.* Physiol Rev, 2015. **95**(4): p. 1205-40.

[161] Reddy, A., E.V. Caler, and N.W. Andrews, *Plasma membrane repair is mediated by Ca(2+)-regulated exocytosis of lysosomes.* Cell, 2001. **106**(2): p. 157-69.

[162] Lariccia, V., et al., *Massive calcium-activated endocytosis without involvement of classical endocytic proteins.* J Gen Physiol, 2011. **137**(1): p. 111-32.

[163] Clapham, D.E., *The mother of all endocytosis.* Elife, 2013. **2**: p. e01738.

[164] Bi, G.Q., J.M. Alderton, and R.A. Steinhardt, *Calcium-regulated exocytosis is required for cell membrane resealing.* J Cell Biol, 1995. **131**(6 Pt 2): p. 1747-58.

[165] Mellgren, R.L., et al., *Calpain is required for the rapid, calcium-dependent repair of wounded plasma membrane.* J Biol Chem, 2007. **282**(4): p. 2567-75.

[166] Han, R., et al., *Dysferlin-mediated membrane repair protects the heart from stress-induced left ventricular injury.* J Clin Invest, 2007. **117**(7): p. 1805-13.

[167] Draeger, A., K. Monastyrskaya, and E.B. Babiychuk, *Plasma membrane repair and cellular damage control: the annexin survival kit.* Biochem Pharmacol, 2011. **81**(6): p. 703-12.

[168] Bouter, A., et al., *Review: Annexin-A5 and cell membrane repair.* Placenta, 2015. **36 Suppl 1**: p. S43-9.

[169] Bendix, P.M., et al., *Interdisciplinary Synergy to Reveal Mechanisms of Annexin-Mediated Plasma Membrane Shaping and Repair.* Cells, 2020. **9**(4).

[170] Terasaki, M., K. Miyake, and P.L. McNeil, *Large plasma membrane disruptions are rapidly resealed by Ca2+-dependent vesicle-vesicle fusion events.* J Cell Biol, 1997. **139**(1): p. 63-74.

[171] Davenport, N.R. and W.M. Bement, *Cell repair: Revisiting the patch hypothesis.* Commun Integr Biol, 2016. **9**(6): p. e1253643.

[172] Togo, T., T.B. Krasieva, and R.A. Steinhardt, *A decrease in membrane tension precedes successful cell-membrane repair.* Mol Biol Cell, 2000. **11**(12): p. 4339-46.

[173] Corrotte, M. and T. Castro-Gomes, *Lysosomes and plasma membrane repair.* Curr Top Membr, 2019. **84**: p. 1-16.

[174] Miao, Y., et al., *A TRP Channel Senses Lysosome Neutralization by Pathogens to Trigger Their Expulsion.* Cell, 2015. **161**(6): p. 1306-19.

[175] Ireton, K., H. Van Ngo, and M. Bhalla, *Interaction of microbial pathogens with host exocytic pathways.* Cell Microbiol, 2018. **20**(8): p. e12861.

[176] Tancini, B., et al., *Lysosomal Exocytosis: The Extracellular Role of an Intracellular Organelle.* Membranes (Basel), 2020. **10**(12).

[177] Tam, C., et al., *Exocytosis of acid sphingomyelinase by wounded cells promotes endocytosis and plasma membrane repair.* J Cell Biol, 2010. **189**(6): p. 1027-38.

[178] Castro-Gomes, T., et al., *Plasma Membrane Repair Is Regulated Extracellularly by Proteases Released from Lysosomes.* PLoS One, 2016. **11**(3): p. e0152583.

[179] Draeger, A., et al., *Dealing with damage: plasma membrane repair mechanisms.* Biochimie, 2014. **107 Pt A**: p. 66-72.

[180] Atanassoff, A.P., et al., *Microvesicle shedding and lysosomal repair fulfill divergent cellular needs during the repair of streptolysin O-induced plasmalemmal damage.* PLoS One, 2014. **9**(2): p. e89743.

[181] Hamill, R.J., J.M. Vann, and R.A. Proctor, *Phagocytosis of Staphylococcus aureus by cultured bovine aortic endothelial cells: model for postadherence events in endovascular infections.* Infect Immun, 1986. **54**(3): p. 833-6.

[182] Fowler, T., et al., *Cellular invasion by Staphylococcus aureus involves a fibronectin bridge between the bacterial fibronectin-binding MSCRAMMs and host cell beta1 integrins.* Eur J Cell Biol, 2000. **79**(10): p. 672-9.

[183] Agerer, F., et al., *Integrin-mediated invasion of Staphylococcus aureus into human cells requires Src family protein-tyrosine kinases.* J Biol Chem, 2003. **278**(43): p. 42524-31.

[184] Josse, J., F. Laurent, and A. Diot, *Staphylococcal Adhesion and Host Cell Invasion: Fibronectin-Binding and Other Mechanisms.* Front Microbiol, 2017. **8**: p. 2433.

[185] Thwaites, G.E. and V. Gant, *Are bloodstream leukocytes Trojan Horses for the metastasis of Staphylococcus aureus?* Nat Rev Microbiol, 2011. **9**(3): p. 215-22.

[186] Fowler, V.G., Jr., et al., *Clinical identifiers of complicated Staphylococcus aureus bacteremia.* Arch Intern Med, 2003. **163**(17): p. 2066-72.

[187] Khatib, R., et al., *Persistence in Staphylococcus aureus bacteremia: incidence, characteristics of patients and outcome.* Scand J Infect Dis, 2006. **38**(1): p. 7-14.

[188] Khatib, R., et al., *Persistent Staphylococcus aureus bacteremia: incidence and outcome trends over time.* Scand J Infect Dis, 2009. **41**(1): p. 4-9.

[189] Li, C., et al., *Staphylococcus aureus Survives in Cystic Fibrosis Macrophages, Forming a Reservoir for Chronic Pneumonia.* Infect Immun, 2017. **85**(5).

[190] Lehar, S.M., et al., *Novel antibody-antibiotic conjugate eliminates intracellular S. aureus.* Nature, 2015. **527**(7578): p. 323-8.

[191] Raineri, E.J.M., et al., *Time-resolved analysis of Staphylococcus aureus invading the endothelial barrier.* Virulence, 2020. **11**(1): p. 1623-1639.

[192] Sandberg, A., et al., *Intracellular activity of antibiotics against Staphylococcus aureus in a mouse peritonitis model.* Antimicrob Agents Chemother, 2009. **53**(5): p. 1874-83.

[193] Abu-Humaidan, A.H., et al., *Persistent Intracellular Staphylococcus aureus in Keratinocytes Lead to Activation of the Complement System with Subsequent Reduction in the Intracellular Bacterial Load.* Front Immunol, 2018. **9**: p. 396.

[194] Clement, S., et al., *Evidence of an intracellular reservoir in the nasal mucosa of patients with recurrent Staphylococcus aureus rhinosinusitis.* J Infect Dis, 2005. **192**(6): p. 1023-8.

[195] Proctor, R.A., et al., *Small colony variants: a pathogenic form of bacteria that facilitates persistent and recurrent infections.* Nat Rev Microbiol, 2006. **4**(4): p. 295-305.

[196] Proctor, R.A., et al., *Persistent and relapsing infections associated with small-colony variants of Staphylococcus aureus.* Clin Infect Dis, 1995. **20**(1): p. 95-102.

[197] Melter, O. and B. Radojevic, *Small colony variants of Staphylococcus aureus--review.* Folia Microbiol (Praha), 2010. **55**(6): p. 548-58.

[198] Horn, J., et al., *Inside job: Staphylococcus aureus host-pathogen interactions.* Int J Med Microbiol, 2018. **308**(6): p. 607-624.

[199] Giese, B., et al., *Staphylococcal alpha-toxin is not sufficient to mediate escape from phagolysosomes in upper-airway epithelial cells.* Infect Immun, 2009. **77**(9): p. 3611-25.

[200] Bewley, M.A., et al., *A cardinal role for cathepsin d in co-ordinating the host-mediated apoptosis of macrophages and killing of pneumococci.* PLoS Pathog, 2011. **7**(1): p. e1001262.

[201] Bera, A., et al., *Why are pathogenic staphylococci so lysozyme resistant? The peptidoglycan O-acetyltransferase OatA is the major determinant for lysozyme resistance of Staphylococcus aureus.* Mol Microbiol, 2005. **55**(3): p. 778-87.

[202] Karavolos, M.H., et al., *Role and regulation of the superoxide dismutases of Staphylococcus aureus.* Microbiology (Reading), 2003. **149**(Pt 10): p. 2749-2758.

[203] Hybiske, K. and R.S. Stephens, *Exit strategies of intracellular pathogens.* Nat Rev Microbiol, 2008. **6**(2): p. 99-110.

[204] Klein, M., M. Kronke, and O. Krut, *Expression of lysostaphin in HeLa cells protects from host cell killing by intracellular Staphylococcus aureus.* Med Microbiol Immunol, 2006. **195**(3): p. 159-63.

[205] Burlak, C., et al., *Global analysis of community-associated methicillin-resistant Staphylococcus aureus exoproteins reveals molecules produced in vitro and during infection.* Cell Microbiol, 2007. **9**(5): p. 1172-90.

[206] Blattner, S., et al., *Staphylococcus aureus Exploits a Non-ribosomal Cyclic Dipeptide to Modulate Survival within Epithelial Cells and Phagocytes.* PLoS Pathog, 2016. **12**(9): p. e1005857.

[207] Kubica, M., et al., *A potential new pathway for Staphylococcus aureus dissemination: the silent survival of S. aureus phagocytosed by human monocyte-derived macrophages.* PLoS One, 2008. **3**(1): p. e1409.

[208] Grosz, M., et al., *Cytoplasmic replication of Staphylococcus aureus upon phagosomal escape triggered by phenol-soluble modulin alpha.* Cell Microbiol, 2014. **16**(4): p. 451-65.

[209] Kahl, B.C., et al., *Staphylococcus aureus RN6390 replicates and induces apoptosis in a pulmonary epithelial cell line.* Infect Immun, 2000. **68**(9): p. 5385-92.

[210] Haslinger-Loffler, B., et al., *Multiple virulence factors are required for Staphylococcus aureus-induced apoptosis in endothelial cells.* Cell Microbiol, 2005. **7**(8): p. 1087-97.

[211] Baran, J., et al., *Apoptosis of monocytes and prolonged survival of granulocytes as a result of phagocytosis of bacteria.* Infect Immun, 1996. **64**(10): p. 4242-8.

[212] Alexander, E.H., et al., *Staphylococcus aureus and Salmonella enterica serovar Dublin induce tumor necrosis factor-related apoptosis-inducing ligand expression by normal mouse and human osteoblasts.* Infect Immun, 2001. **69**(3): p. 1581-6.

[213] Wesson, C.A., et al., *Apoptosis induced by Staphylococcus aureus in epithelial cells utilizes a mechanism involving caspases 8 and 3.* Infect Immun, 2000. **68**(5): p. 2998-3001.

[214] Scaffidi, C., et al., *Two CD95 (APO-1/Fas) signaling pathways.* EMBO J, 1998. **17**(6): p. 1675-87.

[215] Weglarczyk, K., et al., *Caspase-8 activation precedes alterations of mitochondrial membrane potential during monocyte apoptosis induced by phagocytosis and killing of Staphylococcus aureus.* Infect Immun, 2004. **72**(5): p. 2590-7.

[216] Accarias, S., et al., *Pyroptosis of resident macrophages differentially orchestrates inflammatory responses to Staphylococcus aureus in resistant and susceptible mice.* Eur J Immunol, 2015. **45**(3): p. 794-806.

[217] Munoz-Planillo, R., et al., *A critical role for hemolysins and bacterial lipoproteins in Staphylococcus aureus-induced activation of the Nlrp3 inflammasome.* J Immunol, 2009. **183**(6): p. 3942-8.

[218] Kobayashi, S.D., et al., *Rapid neutrophil destruction following phagocytosis of Staphylococcus aureus.* J Innate Immun, 2010. **2**(6): p. 560-75.

[219] Stelzner, K., et al., *Intracellular Staphylococcus aureus Perturbs the Host Cell Ca(2+) Homeostasis To Promote Cell Death.* mBio, 2020. **11**(6).

[220] Flannagan, R.S., B. Heit, and D.E. Heinrichs, *Intracellular replication of Staphylococcus aureus in mature phagolysosomes in macrophages precedes host cell death, and bacterial escape and dissemination.* Cell Microbiol, 2016. **18**(4): p. 514-35.

[221] Andrews, N.W., P.E. Almeida, and M. Corrotte, *Damage control: cellular mechanisms of plasma membrane repair.* Trends Cell Biol, 2014. **24**(12): p. 734-42.

[222] Folch, J., *Isolation of brain diphosphoinositide, a new phosphatide containing inositol meta diphosphate as a constituent.* Fed Proc, 1946. **5**(1 Pt 2): p. 134.

[223] Niemann, A., *Ein unbekanntes Krankheitsbild. In: Jahrbuch für Kinderheilkunde*. Vol. 79. 1914.

[224] Cassiman, D., et al., *Cause of death in patients with chronic visceral and chronic neurovisceral acid sphingomyelinase deficiency (Niemann-Pick disease type B and B variant): Literature review and report of new cases.* Mol Genet Metab, 2016. **118**(3): p. 206-213.

[225] Barnholz, Y., A. Roitman, and S. Gatt, *Enzymatic hydrolysis of sphingolipids. II. Hydrolysis of sphingomyelin by an enzyme from rat brain.* J Biol Chem, 1966. **241**(16): p. 3731-7.

[226] Schneider, P.B. and E.P. Kennedy, *Sphingomyelinase in normal human spleens and in spleens from subjects with Niemann-Pick disease.* J Lipid Res, 1967. **8**(3): p. 202-9.

[227] Schuchman, E.H., *Acid sphingomyelinase, cell membranes and human disease: lessons from Niemann-Pick disease.* FEBS Lett, 2010. **584**(9): p. 1895-900.

[228] Uz, E., et al., *Niemann-Pick disease type B presenting with hepatosplenomegaly and thrombocytopenia.* South Med J, 2008. **101**(11): p. 1188.

[229] McGovern, M.M., et al., *Morbidity and mortality in type B Niemann-Pick disease.* Genet Med, 2013. **15**(8): p. 618-23.

[230] OMIM. *Online Mendelian Inheritance in Man, OMIM®. Johns Hopkins University, Baltimore, MD. MIM Number:257220:052620:https://www.omim.org/entry/257220#*. [Online human gene compendium] 2020 26.05.2020 [cited 2021 18.02.2021]; Niemann-Pick Disease, Type C1; NPC1].

[231] Stroke, N.I.o.N.D.a. *Niemann-Pick Disease Information Page*. [Neurological Disorder Database] 2020 [cited 2021 18.02.2021].

[232] Horinouchi, K., et al., *Acid sphingomyelinase deficient mice: a model of types A and B Niemann-Pick disease.* Nat Genet, 1995. **10**(3): p. 288-93.

[233] Smith, E.L. and E.H. Schuchman, *The unexpected role of acid sphingomyelinase in cell death and the pathophysiology of common diseases.* FASEB J, 2008. **22**(10): p. 3419-31.

[234] Albouz, S., et al., *Tricyclic antidepressants induce sphingomyelinase deficiency in fibroblast and neuroblastoma cell cultures.* Biomedicine, 1981. **35**(7-8): p. 218-20.

[235] Kornhuber, J., et al., *Identification of new functional inhibitors of acid sphingomyelinase using a structure-property-activity relation model.* J Med Chem, 2008. **51**(2): p. 219-37.

[236] Kornhuber, J., et al., *Functional Inhibitors of Acid Sphingomyelinase (FIASMAs): a novel pharmacological group of drugs with broad clinical applications.* Cell Physiol Biochem, 2010. **26**(1): p. 9-20.

[237] Trapp, S., et al., *Quantitative modeling of selective lysosomal targeting for drug design.* Eur Biophys J, 2008. **37**(8): p. 1317-28.

[238] Kolzer, M., N. Werth, and K. Sandhoff, *Interactions of acid sphingomyelinase and lipid bilayers in the presence of the tricyclic antidepressant desipramine.* FEBS Lett, 2004. **559**(1-3): p. 96-8.

[239] Arenz, C., *Small molecule inhibitors of acid sphingomyelinase.* Cell Physiol Biochem, 2010. **26**(1): p. 1-8.

[240] Popik, W., T.M. Alce, and W.C. Au, *Human immunodeficiency virus type 1 uses lipid raft-colocalized CD4 and chemokine receptors for productive entry into CD4(+) T cells.* J Virol, 2002. **76**(10): p. 4709-22.

[241] Grassme, H., et al., *Acidic sphingomyelinase mediates entry of N. gonorrhoeae into nonphagocytic cells.* Cell, 1997. **91**(5): p. 605-15.

[242] Gault, C.R., L.M. Obeid, and Y.A. Hannun, *An overview of sphingolipid metabolism: from synthesis to breakdown.* Adv Exp Med Biol, 2010. **688**: p. 1-23.

[243] Schnaar, R.L. and T. Kinoshita, *Glycosphingolipids*, in *Essentials of Glycobiology*, rd, et al., Editors. 2015: Cold Spring Harbor (NY). p. 125-135.

[244] Yamashita, T., et al., *A vital role for glycosphingolipid synthesis during development and differentiation.* Proc Natl Acad Sci U S A, 1999. **96**(16): p. 9142-7.

[245] Laviad, E.L., et al., *Characterization of ceramide synthase 2: tissue distribution, substrate specificity, and inhibition by sphingosine 1-phosphate.* J Biol Chem, 2008. **283**(9): p. 5677-84.

[246] Lahiri, S., et al., *Kinetic characterization of mammalian ceramide synthases: determination of K(m) values towards sphinganine.* FEBS Lett, 2007. **581**(27): p. 5289-94.

[247] Venkataraman, K., et al., *Upstream of growth and differentiation factor 1 (uog1), a mammalian homolog of the yeast longevity assurance gene 1 (LAG1), regulates N-stearoyl-sphinganine (C18-(dihydro)ceramide) synthesis in a fumonisin B1-independent manner in mammalian cells.* J Biol Chem, 2002. **277**(38): p. 35642-9.

[248] Spassieva, S.D., et al., *Disruption of ceramide synthesis by CerS2 down-regulation leads to autophagy and the unfolded protein response.* Biochem J, 2009. **424**(2): p. 273-83.

[249] Kalo, D. and Z. Roth, *Involvement of the sphingolipid ceramide in heat-shock-induced apoptosis of bovine oocytes.* Reprod Fertil Dev, 2011. **23**(7): p. 876-88.

[250] Lin, X., Z. Fuks, and R. Kolesnick, *Ceramide mediates radiation-induced death of endothelium.* Crit Care Med, 2000. **28**(4 Suppl): p. N87-93.

[251] Obeid, L.M., et al., *Programmed cell death induced by ceramide.* Science, 1993. **259**(5102): p. 1769-71.

[252] Grosch, S., S. Schiffmann, and G. Geisslinger, *Chain length-specific properties of ceramides.* Prog Lipid Res, 2012. **51**(1): p. 50-62.

[253] Mesicek, J., et al., *Ceramide synthases 2, 5, and 6 confer distinct roles in radiation-induced apoptosis in HeLa cells.* Cell Signal, 2010. **22**(9): p. 1300-7.

[254] Ogretmen, B., et al., *Biochemical mechanisms of the generation of endogenous long chain ceramide in response to exogenous short chain ceramide in the A549 human lung adenocarcinoma cell line. Role for endogenous ceramide in mediating the action of exogenous ceramide.* J Biol Chem, 2002. **277**(15): p. 12960-9.

[255] Sot, J., F.M. Goni, and A. Alonso, *Molecular associations and surface-active properties of short- and long-N-acyl chain ceramides.* Biochim Biophys Acta, 2005. **1711**(1): p. 12-9.

[256] Schwiebs, A., et al., *Cancer-induced inflammation and inflammation-induced cancer in colon: a role for S1P lyase.* Oncogene, 2019. **38**(24): p. 4788-4803.

[257] Moruno Manchon, J.F., et al., *Cytoplasmic sphingosine-1-phosphate pathway modulates neuronal autophagy.* Sci Rep, 2015. **5**: p. 15213.

[258] UniProt. *Sphingomyelin phosphodiesterase - SMPD1*. [Protein Database] 1990 [cited 2021 18.02.2021]; Sphingomyelin phosphodiesterase].

[259] Schissel, S.L., et al., *The cellular trafficking and zinc dependence of secretory and lysosomal sphingomyelinase, two products of the acid sphingomyelinase gene.* J Biol Chem, 1998. **273**(29): p. 18250-9.

[260] Jenkins, R.W., et al., *A novel mechanism of lysosomal acid sphingomyelinase maturation: requirement for carboxyl-terminal proteolytic processing.* J Biol Chem, 2011. **286**(5): p. 3777-88.

[261] Jenkins, R.W., et al., *Regulated secretion of acid sphingomyelinase: implications for selectivity of ceramide formation.* J Biol Chem, 2010. **285**(46): p. 35706-18.

[262] Marathe, S., et al., *Human vascular endothelial cells are a rich and regulatable source of secretory sphingomyelinase. Implications for early atherogenesis and ceramide-mediated cell signaling.* J Biol Chem, 1998. **273**(7): p. 4081-8.

[263] Billich, A. and T. Baumruker, *Sphingolipid metabolizing enzymes as novel therapeutic targets.* Subcell Biochem, 2008. **49**: p. 487-522.

[264] Wong, M.L., et al., *Acute systemic inflammation up-regulates secretory sphingomyelinase in vivo: a possible link between inflammatory cytokines and atherogenesis.* Proc Natl Acad Sci U S A, 2000. **97**(15): p. 8681-6.

[265] Kobayashi, K., et al., *Increase in secretory sphingomyelinase activity and specific ceramides in the aorta of apolipoprotein E knockout mice during aging.* Biol Pharm Bull, 2013. **36**(7): p. 1192-6.

[266] Claus, R.A., et al., *Role of increased sphingomyelinase activity in apoptosis and organ failure of patients with severe sepsis.* FASEB J, 2005. **19**(12): p. 1719-21.

[267] Haimovitz-Friedman, A., et al., *Lipopolysaccharide induces disseminated endothelial apoptosis requiring ceramide generation.* J Exp Med, 1997. **186**(11): p. 1831-41.

[268] Jbeily, N., et al., *Hyperresponsiveness of mice deficient in plasma-secreted sphingomyelinase reveals its pivotal role in early phase of host response.* J Lipid Res, 2013. **54**(2): p. 410-24.

[269] Simonis, A. and A. Schubert-Unkmeir, *The role of acid sphingomyelinase and modulation of sphingolipid metabolism in bacterial infection.* Biol Chem, 2018. **399**(10): p. 1135-1146.

[270] Cockburn, C.L., et al., *Functional inhibition of acid sphingomyelinase disrupts infection by intracellular bacterial pathogens.* Life Sci Alliance, 2019. **2**(2).

[271] Meiners, J., et al., *Intestinal Acid Sphingomyelinase Protects From Severe Pathogen-Driven Colitis.* Front Immunol, 2019. **10**: p. 1386.

[272] Slotte, J.P., et al., *Rapid turn-over of plasma membrane sphingomyelin and cholesterol in baby hamster kidney cells after exposure to sphingomyelinase.* Biochim Biophys Acta, 1990. **1030**(2): p. 251-7.

[273] Cohen, R. and Y. Barenholz, *Correlation between the thermotropic behavior of sphingomyelin liposomes and sphingomyelin hydrolysis by sphingomyelinase of Staphylococcus aureus.* Biochim Biophys Acta, 1978. **509**(1): p. 181-7.

[274] Ma, J., et al., *Staphylococcus aureus alpha-Toxin Induces Inflammatory Cytokines via Lysosomal Acid Sphingomyelinase and Ceramides.* Cell Physiol Biochem, 2017. **43**(6): p. 2170-2184.

[275] Peng, H., et al., *Acid sphingomyelinase inhibition protects mice from lung edema and lethal Staphylococcus aureus sepsis.* J Mol Med (Berl), 2015. **93**(6): p. 675-89.

[276] Corrotte, M., et al., *Toxin pores endocytosed during plasma membrane repair traffic into the lumen of MVBs for degradation.* Traffic, 2012. **13**(3): p. 483-94.

[277] Fernandes, M.C., et al., *Trypanosoma cruzi subverts the sphingomyelinase-mediated plasma membrane repair pathway for cell invasion.* J Exp Med, 2011. **208**(5): p. 909-21.

[278] *Staphylococcus aureus subsp. aureus USA300_FPR3757*

f g x - functional genomics explorer. 2012.

[279] Ran, F.A., et al., *Genome engineering using the CRISPR-Cas9 system.* Nat Protoc, 2013. **8**(11): p. 2281-2308.

[280] *CHOPCHOP CRISPR/Cas9 web tool*. 2019.

[281] Labun, K., et al., *CHOPCHOP v3: expanding the CRISPR web toolbox beyond genome editing.* Nucleic Acids Res, 2019. **47**(W1): p. W171-W174.

[282] Muhle, C. and J. Kornhuber, *Assay to measure sphingomyelinase and ceramidase activities efficiently and safely.* J Chromatogr A, 2017. **1481**: p. 137-144.

[283] Ades, E.W., et al., *HMEC-1: establishment of an immortalized human microvascular endothelial cell line.* J Invest Dermatol, 1992. **99**(6): p. 683-90.

[284] al, K.e., *Staphylococcus aureus α-toxin induces acid sphingomyelinase release from a human endothelial cell line.* Frontiers in Microbiology, 2021. **tbd**.

[285] von Hoven, G., et al., *Staphylococcus aureus alpha-toxin: small pore, large consequences.* Biol Chem, 2019. **400**(10): p. 1261-1276.

[286] Eiffler, I., et al., *Staphylococcus aureus alpha-toxin-mediated cation entry depolarizes membrane potential and activates p38 MAP kinase in airway epithelial cells.* Am J Physiol Lung Cell Mol Physiol, 2016. **311**(3): p. L676-85.

[287] Corrotte, M., et al., *Approaches for plasma membrane wounding and assessment of lysosome-mediated repair responses.* Methods Cell Biol, 2015. **126**: p. 139-58.

[288] Jenkins, R.W., D. Canals, and Y.A. Hannun, *Roles and regulation of secretory and lysosomal acid sphingomyelinase.* Cell Signal, 2009. **21**(6): p. 836-46.

[289] Defour, A., et al., *Dysferlin regulates cell membrane repair by facilitating injury-triggered acid sphingomyelinase secretion.* Cell Death Dis, 2014. **5**: p. e1306.

[290] Justet, C., S. Chifflet, and J.A. Hernandez, *Calcium Oscillatory Behavior and Its Possible Role during Wound Healing in Bovine Corneal Endothelial Cells in Culture.* Biomed Res Int, 2019. **2019**: p. 8647121.

[291] Niaudet, C., et al., *Plasma membrane reorganization links acid sphingomyelinase/ceramide to p38 MAPK pathways in endothelial cells apoptosis.* Cell Signal, 2017. **33**: p. 10-21.

[292] Kloft, N., et al., *Pore-forming toxins activate MAPK p38 by causing loss of cellular potassium.* Biochem Biophys Res Commun, 2009. **385**(4): p. 503-6.

[293] Kao, C.Y., et al., *Global functional analyses of cellular responses to pore-forming toxins.* PLoS Pathog, 2011. **7**(3): p. e1001314.

[294] Husmann, M., et al., *Differential role of p38 mitogen activated protein kinase for cellular recovery from attack by pore-forming S. aureus alpha-toxin or streptolysin O.* Biochem Biophys Res Commun, 2006. **344**(4): p. 1128-34.

[295] Choi, H.H., et al., *Endoplasmic reticulum stress response is involved in Mycobacterium tuberculosis protein ESAT-6-mediated apoptosis.* FEBS Lett, 2010. **584**(11): p. 2445-54.

[296] Stewart, S.E., et al., *Assembly of streptolysin O pores assessed by quartz crystal microbalance and atomic force microscopy provides evidence for the formation of anchored but incomplete oligomers.* Biochim Biophys Acta, 2015. **1848**(1 Pt A): p. 115-26.

[297] Basler, K., et al., *Biphasic influence of Staphylococcus aureus on human epidermal tight junctions.* Ann N Y Acad Sci, 2017. **1405**(1): p. 53-70.

[298] Murphy, J., et al., *Staphylococcus Aureus V8 protease disrupts the integrity of the airway epithelial barrier and impairs IL-6 production in vitro.* Laryngoscope, 2018. **128**(1): p. E8-E15.

[299] Martens, K., et al., *Staphylococcus aureus enterotoxin B disrupts nasal epithelial barrier integrity.* Clin Exp Allergy, 2021. **51**(1): p. 87-98.

[300] von Hoven, G., et al., *Dissecting the role of ADAM10 as a mediator of Staphylococcus aureus alpha-toxin action.* Biochem J, 2016. **473**(13): p. 1929-40.

[301] Kwak, Y.K., et al., *The Staphylococcus aureus alpha-toxin perturbs the barrier function in Caco-2 epithelial cell monolayers by altering junctional integrity.* Infect Immun, 2012. **80**(5): p. 1670-80.

[302] Boller, K., D. Vestweber, and R. Kemler, *Cell-adhesion molecule uvomorulin is localized in the intermediate junctions of adult intestinal epithelial cells.* J Cell Biol, 1985. **100**(1): p. 327-32.

[303] Tegoshi, T., et al., *E-cadherin and cadherin-associated cytoplasmic proteins are expressed in murine mast cells.* Lab Invest, 2000. **80**(10): p. 1571-81.

[304] Tsuneki, M. and J.A. Madri, *Adhesion molecule-mediated hippo pathway modulates hemangioendothelioma cell behavior.* Mol Cell Biol, 2014. **34**(24): p. 4485-99.

[305] Watanabe, T., et al., *Paracellular barrier and tight junction protein expression in the immortalized brain endothelial cell lines bEND.3, bEND.5 and mouse brain endothelial cell 4.* Biol Pharm Bull, 2013. **36**(3): p. 492-5.

[306] Ilan, N., A. Tucker, and J.A. Madri, *Vascular endothelial growth factor expression, beta-catenin tyrosine phosphorylation, and endothelial proliferative behavior: a pathway for transformation?* Lab Invest, 2003. **83**(8): p. 1105-15.

[307] Rutkowski, J.M., et al., *Differential transendothelial transport of adiponectin complexes.* Cardiovasc Diabetol, 2014. **13**: p. 47.

[308] Wang, L., et al., *Enhancement of endothelial permeability by free fatty acid through lysosomal cathepsin B-mediated Nlrp3 inflammasome activation.* Oncotarget, 2016. **7**(45): p. 73229-73241.

[309] Zhou, X., et al., *Aspirin alleviates endothelial gap junction dysfunction through inhibition of NLRP3 inflammasome activation in LPS-induced vascular injury.* Acta Pharm Sin B, 2019. **9**(4): p. 711-723.

[310] Chen, Y., et al., *Instigation of endothelial Nlrp3 inflammasome by adipokine visfatin promotes inter-endothelial junction disruption: role of HMGB1.* J Cell Mol Med, 2015. **19**(12): p. 2715-27.

[311] Zhang, Y., et al., *Aloe emodin relieves Ang II-induced endothelial junction dysfunction via promoting ubiquitination mediated NLRP3 inflammasome inactivation.* J Leukoc Biol, 2020. **108**(6): p. 1735-1746.

[312] KGaA, M. *Protein G and protein A bind to different IgG*. 2021 [cited 2021 19.02.2021]; Available from: https://www.sigmaaldrich.com/technical-documents/articles/biology/affinity-chromatography-antibodies/protein-a-g-binding.html.

[313] Becker, K., *EOMA TJP Degradation*. 2020.

[314] Berube, B.J. and J. Bubeck Wardenburg, *Staphylococcus aureus alpha-toxin: nearly a century of intrigue.* Toxins (Basel), 2013. **5**(6): p. 1140-66.

[315] Hermanns, M.I., et al., *Primary human coculture model of alveolo-capillary unit to study mechanisms of injury to peripheral lung.* Cell Tissue Res, 2009. **336**(1): p. 91-105.

[316] Hensen, L., et al., *HA-Dependent Tropism of H5N1 and H7N9 Influenza Viruses to Human Endothelial Cells Is Determined by Reduced Stability of the HA, Which Allows the Virus To Cope with Inefficient Endosomal Acidification and Constitutively Expressed IFITM3.* J Virol, 2019. **94**(1).

[317] Hewett, P.W. and J.C. Murray, *Human lung microvessel endothelial cells: isolation, culture, and characterization.* Microvasc Res, 1993. **46**(1): p. 89-102.

[318] Mokra, D. and P. Kosutova, *Biomarkers in acute lung injury.* Respir Physiol Neurobiol, 2015. **209**: p. 52-8.

[319] Grommes, J. and O. Soehnlein, *Contribution of neutrophils to acute lung injury.* Mol Med, 2011. **17**(3-4): p. 293-307.

[320] Shasby, D.M., et al., *Granulocytes mediate acute edematous lung injury in rabbits and in isolated rabbit lungs perfused with phorbol myristate acetate: role of oxygen radicals.* Am Rev Respir Dis, 1982. **125**(4): p. 443-7.

[321] Lee, W.L. and G.P. Downey, *Neutrophil activation and acute lung injury.* Curr Opin Crit Care, 2001. **7**(1): p. 1-7.

[322] von Bismarck, P., et al., *IKK NBD peptide inhibits LPS induced pulmonary inflammation and alters sphingolipid metabolism in a murine model.* Pulm Pharmacol Ther, 2012. **25**(3): p. 228-35.

[323] Yu, H., et al., *Defective acid sphingomyelinase pathway with Pseudomonas aeruginosa infection in cystic fibrosis.* Am J Respir Cell Mol Biol, 2009. **41**(3): p. 367-75.

[324] Dhami, R., et al., *Analysis of the lung pathology and alveolar macrophage function in the acid sphingomyelinase--deficient mouse model of Niemann-Pick disease.* Lab Invest, 2001. **81**(7): p. 987-99.

[325] Manabe, T., et al., *Ultrastructural changes in the lung in Niemann-Pick type C mouse.* Virchows Arch, 1995. **427**(1): p. 77-83.

[326] Reiss, L.K., et al., *Reevaluation of Lung Injury in TNF-Induced Shock: The Role of the Acid Sphingomyelinase.* Mediators Inflamm, 2020. **2020**: p. 3650508.

[327] Ploppa, A., et al., *The inhibition of human neutrophil phagocytosis and oxidative burst by tricyclic antidepressants.* Anesth Analg, 2008. **107**(4): p. 1229-35.

[328] Simonis, A., et al., *Differential activation of acid sphingomyelinase and ceramide release determines invasiveness of Neisseria meningitidis into brain endothelial cells.* PLoS Pathog, 2014. **10**(6): p. e1004160.

[329] Peters, S., et al., *Neisseria meningitidis Type IV Pili Trigger Ca(2+)-Dependent Lysosomal Trafficking of the Acid Sphingomyelinase To Enhance Surface Ceramide Levels.* Infect Immun, 2019. **87**(8).

[330] Wasserstein, M.P. and E.H. Schuchman, *Acid Sphingomyelinase Deficiency*, in *GeneReviews((R))*, M.P. Adam, et al., Editors. 1993: Seattle (WA).

[331] Henry, B., et al., *Acid sphingomyelinase.* Handb Exp Pharmacol, 2013(215): p. 77-88.

[332] Kornhuber, J., et al., *Secretory sphingomyelinase in health and disease.* Biol Chem, 2015. **396**(6-7): p. 707-36.

[333] Naser, E., et al., *Characterization of the small molecule ARC39, a direct and specific inhibitor of acid sphingomyelinase in vitro.* J Lipid Res, 2020. **61**(6): p. 896-910.

[334] Lin, J.H., *Bisphosphonates: a review of their pharmacokinetic properties.* Bone, 1996. **18**(2): p. 75-85.

[335] Schissel, S.L., et al., *Zn2+-stimulated sphingomyelinase is secreted by many cell types and is a product of the acid sphingomyelinase gene.* J Biol Chem, 1996. **271**(31): p. 18431-6.

[336] Erickson, A.H. and G. Blobel, *Carboxyl-terminal proteolytic processing during biosynthesis of the lysosomal enzymes beta-glucuronidase and cathepsin D.* Biochemistry, 1983. **22**(22): p. 5201-5.

[337] Abnova, *Abnova Sphingomyelinase Assay Kit*. Abnova: https://www.abnova.com/protocol_pdf/KA1374.pdf.

[338] Danikowski, K.M. and T. Cheng, *Colorimetric Analysis of Alkaline Phosphatase Activity in S. aureus Biofilm.* J Vis Exp, 2019(146).

[339] Song, Y., et al., *Additional routes to Staphylococcus aureus daptomycin resistance as revealed by comparative genome sequencing, transcriptional profiling, and phenotypic studies.* PLoS One, 2013. **8**(3): p. e58469.

[340] Painter, K.L., et al., *Staphylococcus aureus adapts to oxidative stress by producing H2O2-resistant small-colony variants via the SOS response.* Infect Immun, 2015. **83**(5): p. 1830-44.

[341] Yoshida, S., et al., *Elevation of Serum Acid Sphingomyelinase Activity in Children with Acute Respiratory Syncytial Virus Bronchiolitis.* Tohoku J Exp Med, 2017. **243**(4): p. 275-281.

[342] Muhle, C., et al., *Secretory Acid Sphingomyelinase in the Serum of Medicated Patients Predicts the Prospective Course of Depression.* J Clin Med, 2019. **8**(6).

[343] Leonetti, D., et al., *Secretion of Acid Sphingomyelinase and Ceramide by Endothelial Cells Contributes to Radiation-Induced Intestinal Toxicity.* Cancer Res, 2020. **80**(12): p. 2651-2662.

[344] Spence, M.W., et al., *A new Zn2+-stimulated sphingomyelinase in fetal bovine serum.* J Biol Chem, 1989. **264**(10): p. 5358-63.

[345] Triglia, R.P. and W.D. Linscott, *Titers of nine complement components, conglutinin and C3b-inactivator in adult and fetal bovine sera.* Mol Immunol, 1980. **17**(6): p. 741-8.

[346] Hommes, J.W., et al., *High density lipoproteins mediate in vivo protection against staphylococcal phenol-soluble modulins.* Sci Rep, 2021. **11**(1): p. 15357.

[347] Surewaard, B.G., et al., *Inactivation of staphylococcal phenol soluble modulins by serum lipoprotein particles.* PLoS Pathog, 2012. **8**(3): p. e1002606.

[348] Gaskin, D.K., et al., *Purification of Staphylococcus aureus beta-toxin: comparison of three isoelectric focusing methods.* Protein Expr Purif, 1997. **9**(1): p. 76-82.

[349] Alberts B, J.A., Lewis J, et al., *Molecular Biology of the Cell. 4th edition.* Vol. 4th Edition. 2002, New York: Garland Science.

[350] Tam, C., A.R. Flannery, and N. Andrews, *Live imaging assay for assessing the roles of Ca2+ and sphingomyelinase in the repair of pore-forming toxin wounds.* J Vis Exp, 2013(78): p. e50531.

[351] Schoenauer, R., et al., *Down-regulation of acid sphingomyelinase and neutral sphingomyelinase-2 inversely determines the cellular resistance to plasmalemmal injury by pore-forming toxins.* FASEB J, 2019. **33**(1): p. 275-285.

[352] Boye, T.L. and J. Nylandsted, *Annexins in plasma membrane repair.* Biol Chem, 2016. **397**(10): p. 961-9.

[353] Jahn, R., T. Lang, and T.C. Sudhof, *Membrane fusion.* Cell, 2003. **112**(4): p. 519-33.

[354] Bonifacino, J.S. and B.S. Glick, *The mechanisms of vesicle budding and fusion.* Cell, 2004. **116**(2): p. 153-66.

[355] Grab, J. and J. Rybniker, *The Expanding Role of p38 Mitogen-Activated Protein Kinase in Programmed Host Cell Death.* Microbiol Insights, 2019. **12**: p. 1178636119864594.

[356] Faulstich, M., et al., *Neutral sphingomyelinase 2 is a key factor for PorB-dependent invasion of Neisseria gonorrhoeae.* Cell Microbiol, 2015. **17**(2): p. 241-53.

[357] Lin, T., et al., *Role of acidic sphingomyelinase in Fas/CD95-mediated cell death.* J Biol Chem, 2000. **275**(12): p. 8657-63.

[358] Gomez, M.I., et al., *Staphylococcus aureus protein A induces airway epithelial inflammatory responses by activating TNFR1.* Nat Med, 2004. **10**(8): p. 842-8.

[359] Sawada, M., et al., *Acid sphingomyelinase activation requires caspase-8 but not p53 nor reactive oxygen species during Fas-induced apoptosis in human glioma cells.* Exp Cell Res, 2002. **273**(2): p. 157-68.

[360] Tsuda, K., et al., *Functional analysis of alpha5beta1 integrin and lipid rafts in invasion of epithelial cells by Porphyromonas gingivalis using fluorescent beads coated with bacterial membrane vesicles.* Cell Struct Funct, 2008. **33**(1): p. 123-32.

[361] Padmanabhan, P., R. Desikan, and N.M. Dixit, *Targeting TMPRSS2 and Cathepsin B/L together may be synergistic against SARS-CoV-2 infection.* PLoS Comput Biol, 2020. **16**(12): p. e1008461.

[362] Katopodis, P., et al., *Pancancer analysis of transmembrane protease serine 2 and cathepsin L that mediate cellular SARSCoV2 infection leading to COVID-19.* Int J Oncol, 2020. **57**(2): p. 533-539.

[363] Schloer, S., et al., *Targeting the endolysosomal host-SARS-CoV-2 interface by clinically licensed functional inhibitors of acid sphingomyelinase (FIASMA) including the antidepressant fluoxetine.* Emerg Microbes Infect, 2020. **9**(1): p. 2245-2255.

[364] Kreiswirth, B.N., et al., *The toxic shock syndrome exotoxin structural gene is not detectably transmitted by a prophage.* Nature, 1983. **305**(5936): p. 709-12.

[365] Haukenes, G., *Serological Typing of Staphylococcus Aureus. 6. Antibodies of Immune Sera to Strains Cowan I, Cowan Ii, Cowan Iii, Wood 46, 670, 830, 1015, 5687, and 6376.* Acta Pathol Microbiol Scand, 1964. **61**: p. 415-26.

[366] Fey, P.D., et al., *A genetic resource for rapid and comprehensive phenotype screening of nonessential Staphylococcus aureus genes.* mBio, 2013. **4**(1): p. e00537-12.

[367] Vann, J.M. and R.A. Proctor, *Ingestion of Staphylococcus aureus by bovine endothelial cells results in time- and inoculum-dependent damage to endothelial cell monolayers.* Infect Immun, 1987. **55**(9): p. 2155-63.

[368] Fraunholz, M., et al., *Complete Genome Sequence of Staphylococcus aureus 6850, a Highly Cytotoxic and Clinically Virulent Methicillin-Sensitive Strain with Distant Relatedness to Prototype Strains.* Genome Announc, 2013. **1**(5).

[369] Rosenstein, R., et al., *Genome analysis of the meat starter culture bacterium Staphylococcus carnosus TM300.* Appl Environ Microbiol, 2009. **75**(3): p. 811-22.

[370] Schoch, C.L., et al., *NCBI Taxonomy: a comprehensive update on curation, resources and tools.* Database (Oxford), 2020. **2020**.

[371] Liese, J., et al., *Intravital two-photon microscopy of host-pathogen interactions in a mouse model of Staphylococcus aureus skin abscess formation.* Cell Microbiol, 2013. **15**(6): p. 891-909.

[372] Pedelacq, J.D., et al., *Engineering and characterization of a superfolder green fluorescent protein.* Nat Biotechnol, 2006. **24**(1): p. 79-88.

[373] Wiznerowicz, M. and D. Trono, *Conditional suppression of cellular genes: lentivirus vector-mediated drug-inducible RNA interference.* J Virol, 2003. **77**(16): p. 8957-61.

[374] Gee, P., et al., *Extracellular nanovesicles for packaging of CRISPR-Cas9 protein and sgRNA to induce therapeutic exon skipping.* Nat Commun, 2020. **11**(1): p. 1334.

[375] Bachi, B., *Physical mapping of the BglI, BglII, PstI and EcoRI restriction fragments of staphylococcal phage phi 11 DNA.* Mol Gen Genet, 1980. **180**(2): p. 391-8.

[376] Bon, J., N. Mani, and R.K. Jayaswal, *Molecular analysis of lytic genes of bacteriophage 80 alpha of Staphylococcus aureus.* Can J Microbiol, 1997. **43**(7): p. 612-6.

[377] García, P., et al., *Functional genomic analysis of two Staphylococcus aureus phages isolated from the dairy environment.* Applied and environmental microbiology, 2009. **75**(24): p. 7663-7673.

Appendix A

List of cell lines, bacterial strains, and plasmids

Table A. 1: Details of bacterial strains used in this study

Strain	Description	Reference
Escherichia coli		
DH5α	K-12 derivate, F^-, *end*A1, *hsd*R17 (r_k^-, m_k^-), *sup*E44, *thi*-1, *rec*A1, *Gyr*A96, *rel*A1, λ^-, Δ(*lacZYA-argF*)U169, Φ80*dlac*Z ΔM15, *deo*R, *nup*G	BRL Life Technology
Staphylococcus aureus		
RN4220	Non-haemolytic derivative of NCTC 8325-4, *sau1*-, *hsdR* developed for cloning and laboratory studies. Reference Genome: NCTC 8325, NCBI Accession: NC_007795	[364]
Cowan	NCTC 8530, isolated from septic arthritis, *agr* dysfunction, low expression of toxins and proteases	[365]
JE2	Plasmid-cured derivative of USA300 LAC.	[366]
JE2 Δ*hla*	JE2 with targeted deletion of *hla* gene coding for α-toxin	This study
NE1354	JE2 transposon insertion mutant within *hla*, locus ID: SAUSA300_1058	[366]
NE1261	JE2 transposon insertion mutant within *hlb*, locus ID: SAUSA300_1973	[366]
NE678	JE2 transposon insertion mutant within *plc,* locus ID: SAUSA300_0099	[366]
NE1848	JE2 transposon insertion mutant within *LukS-PV*, locus ID: SAUSA300_1382	[366]
NE558	JE2 transposon insertion mutant within *LukE*, locus ID: SAUSA300_1769	[366]
NE1386	JE2 transposon insertion mutant within *LukA/LukG*, locus ID: SAUSA300_1974	[366]
NE1682	JE2 transposon insertion mutant within *hlgB*, locus ID: SAUSA300_2367	[366]
NE286	JE2 transposon insertion mutant within *spa*, locus ID: SAUSA300_0113	[366]
NE1532	JE2 transposon insertion mutant within *agrA*, locus ID: SAUSA300_1992	[366]
NE10	JE2 transposon insertion mutant within locus ID:SAUSA300_2129	[366]
6850	MSSA but *O*-lactam resistant, *spa* type t185, ST50, no CC (Singleton). Isolated from a patient with a skin abscess, progressed to bacteraemia, osteomyelitis, septic arthritis and multiple systemic abscesses.	[367,368]
6850 NE1261	6850 transposon insertion mutant within *hlb*, locus ID: SAUSA300_1973	

Staphylococcus carnosus		**Reference**
TM300	Known as Staphylococcus carnosus, these non-pathogenic bacteria are used to allow the fermentation and ripening process to be carried out under controlled conditions	**[369]**

Table A. 2: Details of plasmids used in this study

Plasmid	**Description**	**Reference**
pSpCas9(BB)-2A-GFP	Cas9 from S. pyogenes with 2A-EGFP, and cloning backbone for sgRNA	**[279]** Addgene plasmid # 48138
pJL74-SarAP1 GFP	vector expressing GFP, Erm^R	[370,371]
pGFPsf	Superfolder GFP expressing plasmid	[372]
pLVTHM-Pm_YFPCWT_Spe_shRNA_ASM1KP	pLVTHM plasmid issued for SMPD1 knock-down	[373] Addgene plasmid #12247
pVSV-G	pVSV-G plasmid for virus production in HEK293T	[374] Addgene plasmid #138479
psPAX2	psPAX plasmid for virus production in HEK293T	psPAX2 was a gift from Didier Trono Addgene plasmid #12260

Table A. 3: Details of cell lines used in this study

Cell line	**Description**	**Reference**
EOMA	EOMA cells exhibit characteristic endothelial cell properties, such as rearrangement into tubelike structures on Matrigel and retention of cobblestone morphology at confluence. They behave in vitro in a manner similar to microvascular endothelial cells	ATCC® CRL-2586™
HuLEC-5a	CRL-3244, HULEC-5a, has been shown to retain many of the characteristics of endothelial cells. These immortalized cells, because they are a continuously renewable source of human endothelial microvascular cells, can be used as a replacement for primary human lung endothelial cells for many research studies	ATCC® CRL-3244™
HEK-293	Epithelial cell lines issued for virus replication	ATCC® CRL-1573™
Defibrinated Sheep blood	Sheep blood deprived of coagulation factors for haemolysis assays and addition in sheep blood agar	Fiebig Nährstofftechnik, Germany

Table A. 4: Details of bacteriophages used in this study

Phages	Description	Reference
S. aureus bacteriophage Φ11	Lytic bacteriophage issued for transposon transduction	[375]
S. aureus bacteriophage Φ80a	Lytic bacteriophage issued for transposon transduction	[376]
S. aureus bacteriophage Φ86	Lytic bacteriophage issued for transposon transduction	[377]

Appendix B

List of oligonucleotides

Table B. 1: List of oligonucleotides used in this study. Synthesis of all oligonucleotides was performed by Sigma-Aldrich Chemie GmbH, Germany.

ID	Name	% GC	TM (°C)	Length (bp)	Sequence (5'-3')
358	ITR-F	54,5	76,8	33	ACAGGTTGGCTGATAAGTCCCCGGTCTCTAGAC
359	ITR-R	54,5	76,8	33	GTCTAGAGACCGGGGACTTATCAGCCAACCTGT
1072	mSmpd1-ko-f	60	69,8	20	GGCAGGAACCCAAAGAACCG
1073	mSmpd1-ko-r	50	75,8	28	AAACCGGTTCTTTGGGTTCCTGCCTTTC
1074	mSmpd2-ko-f	60	71,5	20	TGTGGCCCAAGCTTGGGAAC
1075	mSmpd2-ko-r	50	77,4	28	AAACGTTCCCAAGCTTGGGCCACATTTC
1076	mSmpd1-test-r	45,4	59,4	22	GGTTGAGAGCAGTGAATAAGAC
1077	mSmpd1-test-f	54,5	60,9	22	CAGAGACTGGAGAGGTCCTTAC
1081	mSmpd1_1-fwd	58,3	76,6	24	CACCAGAAGGAGCCCAATGTGGCA
1082	mSmpd1_1-rev	50	71,4	24	AAACTGCCACATTGGGCTCCTTCT
1083	mSmpd1_2-fwd	54,1	73,5	24	CACCAGGCTTTCTAGCGTTCGCAA
1084	mSmpd1_2-rev	45,8	68,7	24	AAACTTGCGAACGCTAGAAAGCCT
1085	mSmpd2_1-fwd	62,5	76,7	24	CACCTGTGGCCCAAGCTTGGGAAC
1086	mSmpd2_1-rev	54,1	76,2	24	AAACGTTCCCAAGCTTGGGCCACA
1087	mSmpd2_2-fwd	54,1	68,6	24	CACCTCTAAGTGGACTGGTGCTCA
1088	mSmpd2_2-rev	45,8	65	24	AAACTGAGCACCAGTCCACTTAGA
1089	NE 1261_1386-test	43,4	63,2	23	GCAAAAGGTACAATTGGTAGTGG
1090	NE 10_test	52,1	64,3	23	GTCCAACCTATCCAACCACCTAC
1091	NE 1682_test	45,8	62,5	24	CATCTTGTCTGTGTGATAGTACGC
1092	NE 1848_test	42,3	68,2	26	CTTATCGGAATCTGATGTTGCAGTTG
1093	NE 1354_test	45,8	65,5	24	GTTGAAGTCCAGTGCAATTGGTAG

1094	NE 678_test	47,6	63,3	21	GGATTCGCATTACTTCCTGTG
1095	NE 558_test	40	63,7	25	CCAGGATTAGTTTCTTTAGAATCCG
1148	Smpd1-KO Test	59	72,1	22	GCAAGCCACAAGCCTCTGATGG
1161	Adam10-KOsgRNA 1-fwd	62,9	79,7	27	CACCCATAAATACGGCCCACAGGGGGG
1162	Adam10-KOsgRNA 1-rev	53,8	75,2	26	AAACCCCCCCTGTGGGCCGTATTTAT
1163	Adam10-KOsgRNA 2-fwd	55,5	75,7	27	CACCCAAACGAGCAGTCTCACATGAGG
1164	Adam10-KOsgRNA 2-rev	48,1	72,5	27	AAACCCTCATGTGAGACTGCTCGTTTG
1165	Asah1-KOsgRNA 1-fwd	59,2	80,9	27	CACCATTGGCTCAAAAGGCACCAGCGG
1166	Asah1-KOsgRNA 1-rev	51,8	78,1	27	AAACCCGCTGGTGCCTTTTGAGCCAAT
1167	Asah1-KOsgRNA 2-fwd	55,5	70,6	27	CACCCCTCTAGGTAACGTACACCTTGC
1168	Asah1-KOsgRNA 2-rev	48,1	68,4	27	AAACGCAAGGTGTACGTTACCTAGAGG
1169	mTnfrsf1a-KOsgRNA 1-fwd	59,2	78,5	27	CACCGATGGGGATACATCCATCAGGGG
1170	mTnfrsf1a-KOsgRNA 1-rev	51,8	74,7	27	AAACCCCCTGATGGATGTATCCCCATC
1171	mTnfrsf1a-KOsgRNA 2-fwd	55,5	79,2	27	CACCCCGCTTGCAAATGTCACAAACCC
1172	mTnfrsf1a-KOsgRNA 2-rev	48,1	77	27	AAACGGGTTTGTGACATTTGCAAGCGG
1173	mCtsb-KOsgRNA 1-fwd	62,9	81,4	27	CACCCAATGGCCGAGTCAACGTGGAGG
1174	mCtsb-KOsgRNA 1-rev	55,5	78,3	27	AAACCCTCCACGTTGACTCGGCCATTG
1175	mCtsb-KOsgRNA 2-fwd	66,6	82,2	27	CACCCCGTCCCCCATGCACTGGAGAAG
1176	mCtsb-KOsgRNA 2-rev	59,2	79,1	27	AAACCTTCTCCAGTGCATGGGGGACGG
1177	hCTSB-KOsgRNA (1-fwd)	51,8	75,2	27	CACCATGGCCGAGATCTACAAAAACGG
1178	hCTSB-KOsgRNA (1-rev)	44,4	72,6	27	AAACCCGTTTTTGTAGATCTCGGCCAT
1179	hCTSB-KOsgRNA (2-fwd)	55,5	76,2	27	CACCCCGACCTACAAACAGGACAAGCA
1180	hCTSB-KOsgRNA (2-rev)	48,1	71,2	27	AAACTGCTTGTCCTGTTTGTAGGTCGG
2067	hTNFRSF1a-KO sgRNA 1-fwd	62,9	78,9	27	CACCTACAATGACTGTCCAGGCCCGGG
2068	hTNFRSF1a-KO sgRNA 1-rev	55,5	77,6	27	AAACCCCGGGCCTGGACAGTCATTGTA
2069	hTNFRSF1a-KO sgRNA 2-fwd	74	87,9	27	CACCGCATGCTGGCGACCTGGAGGCGG

2070	hTNFRSF1a-KO sgRNA 2-rev	66,6	84,1	27	AAACCCGCCTCCAGGTCGCCAGCATGC
2071	hTNFRSF1a-KO sgRNA 3-fwd	51,8	71,8	27	CACCTAATGTATCGCTACCAACGGTGG
2072	hTNFRSF1a-KO sgRNA 3-rev	44,4	70,7	27	AAACCCACCGTTGGTAGCGATACATTA

Appendix C

List of reagents and media

Table C. 1: List of reagents and media used in this study

Labeling	Description	Manufacturer
Bacterial culture media and supplements		
Lysogeny Broth (LB)	Tryptone (10 g/l) Sodium Chloride (10 g/l) Bacto™ Yeast extract (5 g/l)	Oxoid, UK VWR, Germany Becton Dickinson
LB Agar	LB broth, 500 ml GC Agar Base (15 g/l)	Oxoid, UK
Brain Heart Infusion Broth (BHI)		Sigma Aldrich, USA
BHI Agar	BHI (37,5 g/l) GC Agar Base (15 g/l)	Sigma-Aldrich Oxoid, UK
Tryptic Soy Broth (TSB)		Sigma Aldrich
Tryptic Soy Broth w/o Dextrose		Sigma Aldrich
Tryptic Soy Agar (TSA)	TSB w/o Dextrose (30 g/l) GC Agar Base (15 g/l)	Sigma-Aldrich Oxoid, UK
Colombia Blood Agar	BDColumbia CNA Agar with 5% Sheep Blood	Becton Dickinson, USA
Cryo-preservation buffer	50% Glycerol (v/v)	Carl-Roth, Germany
Phage buffer	LB broth, 50 ml $CaCl^2$ (20 mM)	Carl-Roth, Germany
Phage Soft Agar	LB broth, 200 ml GC Agar Base (1.,2 g) $CaCl^2$ (5 mM)	Oxoid, UK Carl-Roth, Germany
Phage Citrate Agar	LB broth, 200 ml GC Agar Base (1.,2 g) Na-citrate (20 mM)	Oxoid, UK Carl-Roth, Germany
Toxins		
S. aureus α-toxin	Purified α-toxin produced in *S. aureus*	Merck, Germany
S. aureus β-toxin	Purified β-toxin produced in *S. aureus*	Merck, Germany
Antibiotics		
Erythromycin	Erythromycin powder (10 mg/ml) 99% Ethanol	Sigma-Aldrich, USA Carl-Roth, Germany
Chloramphenicol	Chloramphenicol powder (10 mg/ml) 99% Ethanol	Sigma-Aldrich, USA Carl-Roth, Germany
Tissue culture and supplements		

Calcium Measurement medium	RPMI 1640, Glutamax Fluo-3AM (4 µM)	Thermo Scientific, USA Invitrogen, USA
DMEM full medium	DMEM Fetal bovine serum (10% v/v) Penicillin-Streptomycin (1000 U/ml – 1 mg/ml)	Sigma-Aldrich, USA Sigma-Aldrich, USA Thermo Scientific, USA
DMEM infection medium	DMEM Fetal bovine serum (10% v/v)	Sigma-Aldrich, USA Sigma-Aldrich, USA
MCDB 131 full medium	MDCB 131, no glutamine Fetal bovine serum (5% v/v) GlutaMAX™ Supplement (2 mM) Hydrocortisol (2.,76 µM) Epidermal Growth Factor, human (0,01 ng/ml) Microvascular Growth Supplement, 1x Penicillin-Streptomycin (1000 U/ml – 1 mg/ml)	Thermo Scientific, USA Sigmal-Adlrich, USA Thermo Scientific, USA Sigma-Aldrich, USA Sigma-Aldrich, USA Thermo Scientific, USA Thermo Scientific, USA
MCDB 131 infection medium	MDCB 131, no glutamine Fetal bovine serum (5% v/v) GlutaMAX™ Supplement (2 mM) Hydrocortisol (2.,76 µM) Epidermal Growth Factor, human (0,.01 ng/ml) Microvascular Growth Supplement, 1x	Thermo Scientific, USA Sigmal-Adlrich, USA Thermo Scientific, USA Sigma-Aldrich, USA Sigma-Aldrich, USA Thermo Scientific, USA
ASM measurement medium	MDCB 131, no glutamine FBS (5% v/v), 70°C heat inactivated GlutaMAX™ Supplement (2 mM) Hydrocortisol (2,.76 µM) Epidermal Growth Factor, human (0.,01 ng/ml) Microvascular Growth Supplement, 1x	Thermo Scientific, USA Sigmal-Adlrich, USA Thermo Scientific, USA Sigma-Aldrich, USA Sigma-Aldrich, USA Thermo Scientific, USA
Cell freezing medium	Fetal Bovine serum (90% v/v) Dimethylsulfoxide (DMSO) (10% v/v)	Sigma-Aldrich, USA Carl-Roth, Germany
Transfection buffer	OptiMem Medium	Thermo Scientific, USA

Buffers & Solutions

Dulbecco's Phosphate Buffer Saline (DPBS), 1x	Cell culture grade, sterile and individually bottled	Thermo Scientific, USA
TrypLE™ Express Enzyme (1X), no phenol red	Cell culture dissociation buffer	Thermo Scientific, USA
Radioimmunoprecipitation Assay buffer (RIPA)	NaCl (150 mM) EDTA pH 8.,0 (5 mM) TRIS pH 8.,0 (50 mM) NP-40 (IGEPAL) (1% v/v) Sodium deoxycholate (0.,5 % v/v) SDS (0.,1% v/v)	Carl-Roth, Germany Carl-Roth, Germany Carl-Roth, Germany Carl-Roth, Germany Carl-Roth, Germany Carl-Roth, Germany
Laemmli buffer (2x)	TRIS HCl pH 6.,8 (100 mM) SDS (4% w/v) Glycerol (20 % v/v) β-mercaptoethanol (1.,5% v/v) bromphenol blue (0.,004% v/v)	Carl-Roth, Germany Carl-Roth, Germany Carl-Roth, Germany Sigma-Aldrich, USA Carl-Roth, Germany
SDS solution, 10%	SDS pellets (0.,1g /ml)	Carl-Roth, Germany
SDS-PAGE buffer, 10x	Glycine (1.,92 M) TRIS Base (250 mM) Adjust to pH 8.,5	Sigma-Aldrich, USA Carl-Roth, Germany
Blotting buffer, 10x	Glycine (1.,92 M) TRIS Base (250 mM) SDS (0.,2 % v/v)	Sigma-Aldrich, USA Carl-Roth, Germany Carl-Roth, Germany
TAE buffer, 50x	EDTA (50 mM) TRIS Base (2 M) Acetic Acid (1 M)	Carl-Roth, Germany Carl-Roth, Germany Carl-Roth, Germany
TRIS buffered saline, 10x	TRIS Base (500 mM) NaCl (1.,5 M) Adjust to pH 7.,5	Carl-Roth, Germany Carl-Roth, Germany

TBS-T	TBS, 10x Tween20 (0,01% v/v)	Carl-Roth, Germany
Blocking reagent	Pooled human serum/BSA/skim milk (5%) TBS-T	Sigma-Aldrich, USA
ECL Solution 1	TRIS HCl (100 mM) Luminol (2.,5 mM) Coumaric acid (0.,4 mM)	Carl-Roth, Germany Carl-Roth, Germany Sigma-Aldrich, USA
ECL Solution 2	TRIS HCl (100 mM) 33% H_2O_2 (0.,02% v/v)	Carl-Roth, Germany Carl-Roth, Germany
Silver Staining Fixing solution	Ethanol (50% v/v) Acetic acid (12% v/v) 37 % Formaldehyde (0.,05% v/v)	Carl-Roth, Germany Carl-Roth, Germany Morphisto, Germany
Silver Staining Sensitizer Stock	$Na_2S_2O_3$ x 5 H_2O (25 mg/ml)	Carl-Roth, Germany
Silver stain	$AgNO_3$ (0.02 ng/ml) 37% Formaldehyde (0.,075%)	Carl-Roth, Germany Morphisto, Germany
Silver Staining Developer	Na_2CO_3 (0.,06 g/ml) $Na_2S_2O_3$ x 5 H_2O (4 µg/ml) 37% Formaldehyde (0.,05% v/v)	Carl-Roth, Germany Carl-Roth, Germany Morphisto, Germany
Silver Staining Stop solution	Glycine (1% w/v)	Carl-Roth, Germany
ASM Lysis buffer	Na-acetate pH 5,0 (250 mM) Nonidet P40 (0.,1% v/v) EDTA (1.,3 mM) Roche complete Protease inhibitor (1x) Adjust to pH 5.,0	Carl-Roth, Germany Carl-Roth, Germany Carl-Roth, Germany Merck, Germany
ASM Lysate buffer	Na-acetate pH 5,0 (200 mM) NaCl (500 mM) Nonidet P-40 (0.,2% v/v) BODIPY-FL-C_{12} (58 pM)	Carl-Roth, Germany Carl-Roth, Germany Carl-Roth, Germany Thermo Scientific, USA
ASM Supernatant buffer	Na-acetate pH 5,0 (200 mM) NaCl (500 mM) Nonidet P-40 (0.,2% v/v) $ZnCl_2$ (500 µM) BODIPY-FL-C_{12} (58 pM) Lysostaphin (20% v/v)	Carl-Roth, Germany Carl-Roth, Germany Carl-Roth, Germany Carl-Roth, Germany Thermo Scientific, USA AMBI, USA
Bacterial lysis buffer	TRIS Base pH 8 (2% v/v) Triton X-100 (1.,2% v/v) RNAse A (0.,8 % v/v) 0.,5 M EDTA (0.,4% v/v)	Carl-Roth, Germany Carl-Roth, Germany Qiagen, Germany Carl-Roth, Germany
ROTI® GelStain	Fluorogenic dye for nucleic acid staining	Carl-Roth, Germany
DNA Gel Loading Dye (6x)	Sample preparation for gel electrophoresis	Thermo Scientific, USA
Inhibitors		
Amitriptyline hydrochloride		Sigma-Aldrich, USA
ARC39	We thank Prof. Dr. Arenz and Zain Ahmed for providing us with the ASM specific inhibitor ARC39	
Enzymes		
Exonuclease V (RecBCD)		NEB, USA
FastDigest BpiI		Invitrogen, USA

Phusion DNA polymerase	Phusion High-Fidelity DNA-directed DNA polymerase	Invitrogen, USA
Proteinase K	A non-specific peptidase from *Tritirachium album*	Carl-Roth, Germany
Recombinant Human SMPD1 Protein		R&D, USA
Sphingomyelinase from Staphylococcus aureus		Sigma-Aldrich, USA
T4 DNA Ligase		Invitrogen, USA
T4 Polynucleotide Kinase		Invitrogen, USA

Antibodies

Goat anti-rat IgG	Secondary antibody, NL637-conjugated	R&D, USA
Goat anti-rabbit IgG	Secondary antibody, Cy2 conjugated	Dianova, Germany
Goat anti-mouse IgG	Secondary antibody, Cy2 conjugated	Dianova, Germany
Goat anti-rabbit IgG	Secondary antibody, Cy3 conjugated	Dianova, Germany
Goat anti-mouse IgG	Secondary antibody, Cy3 conjugated	Dianova, Germany
Goat anti-rabbit IgG	Secondary antibody, Cy5 conjugated	Dianova, Germany
Goat anti-mouse IgG	Secondary antibody, Cy5 conjugated	Dianova, Germany
Goat anti-rabbit IgG	Secondary antibody, HRP conjugated	Santa Cruz, USA
Goat anti-mouse IgG	Secondary antibody, HRP conjugated	Santa Cruz, USA
Mouse anti-β Actin	mAb AC-15 : A5441	Merck, Germany
Mouse anti-human LAMP1	mAb H4A3 : sc-20011	Santa Cruz, USA
Mouse anti-human VE-Cadherin	mAb 123413 : MAB9381	R&D, USA
Mouse anti-human Caspase 8	mAb 1C12 : #9746	Cell Signalling, USA
Rabbit anti-human E-Cadherin	mAb 24E10 : #3195	Cell Signalling, USA
Rabbit anti-sheep IgG	Secondary antibody, HRP conjugated	Thermo Scientific, USA
Rabbit anit-human ZO-1	mAb D7D12 : #8193	Cell Signalling, USA
Rabbit anti-human ZO-2	pAb : #2847	Cell Signalling, USA
Rabbit anti-human ASM	pAb : #3687	Cell Signalling, USA
Rabbit anti-human ASM	pAb : SAB2102244	Merck, Germany

Rabbit anti-human ASM	pAb H-181 : sc-11352	Santa Cruz, USA
Rabbit anti-RFP	pAb ab62341	Abcam, USA
Rat anti-mouse VE-Cadherin	mAb eBioBV13 : # 14-1441-82	Thermo Scientific, USA
Tight Junction Antibody Sampler Kit	#8683	Cell Signalling, USA

Appendix D

List of instruments, commercial kits and consumables

Table D. 1 List of instruments, commercial kits and consumables used in this study

Labeling	Description	Manufacturer
Instruments		
Bench centrifuge(refrigerated)	HeraeusTM MegafugeTM 1.0. Medium bench centrifuge with swinging bucket rotor, max. 6.,240 xg	Thermo Scientific, USA
BSL-2 sterile hood	HerasafeTM KS (NSF) Class II, Type A2 Biological Safety cabinets	Thermo Scientific, USA
Chemiluminescence imager	INTAS Cooled CCD Sensorwith ChemoStar imaging software	INTAS Science Imaging Instruments GmbH, Germany
Cell counting chamber	Neubauer Cell Counting Chamber	Hartenstein, Germany
Cell sorter	BD FACSAria™ III Cell Sorter	BD, USA
CO_2 incubator	Heracell™ 150i CO_2 Incubator	Thermo Scientific, USA
Confocal microscopy	Leica TCS SP5	Leica, Germany
Electrophoresis power supplies	Peqlab EV202 for PAGE & CONSORT microcomputer for Agarose gels	Peqlab, Germany and Consort, Belgium
Flow cytometer	BD Accuri C6 flow cytometer and software v2.3 with standard optical filters	BD, USA
Gel imager	BiostepDark hood DH-40/50 with Argus X1 gel documentation software v7.6	Biostep GmbH, Germany
Laboratory refrigerators	Refrigerators with freezers (4°C and -20°C)	Liebherr, Germany
Laser scanning unit	Amersham Typhoon 9200 Imager	Amersham, UK
Light microscope	DMIL light microscope	Leica, Germany
Microcentrifuge (nonrefrigerated)	Hettich MIKRO 200 centrifuge with fixed angle rotor, max. 18.,000 xg	Hettich Lab tech., USA
Microcentrifuge (refrigerated)	Hitachi himac CT15RE centrifuge with fixed angle rotor, max. 21.,500 xg	Hitachi-Koki, Japan
Microcentrifuge (refrigerated)	Eppendorf® microcentrifuge 5417	Merck, Germany
Multimode microplate reader	TECAN InfiniteM200 with i-control 1.10 reader software	TECAN, Switzerland
Multimode microplate reader	TECAN MPLEX with Magellan software	TECAN, Switzerland
PCR Thermocycler	PEQLAB peqSTAR 96x universal gradient thermal cycler	VWR International, Germany
Pipettes	Eppendorf Pipettes 0,1 – 1000 µl	Eppendorf, Germany

Sonication device, Bath type	Biorupturr Plus, Auto-revolving, uniform wave, bath type	Diagenode, Belgium
Thermal mixing unit	Eppendorf Thermomixer compact 5350	Eppendorf, Germany
Ultra low temperature freezers	New BrunswickTM Innovar upright freezer U535	Eppendorf, Germany
UV-VisMicro spectrophotometer	NanoDrop 1000 with ND-1000 software v3.7	Thermo Scientific, USA
Vacuum concentrator	Eppendorf Vacufuge Concentrator	Eppendorf, Germany
Western blotting device	PerfectBlue™ 'Semi-Dry'-Electro-blotter	Peqlab, Germany
Consumables		
Cell culture T-flasks	Corningr sterile cell culture grade (T-25, T-75 and T-150), Polystyrene	Corning, USA
Centrifuge tubes	Falconr Centrifuge Tubes (50ml, 15ml), Polypropylene, Sterile	Corning, USA
Cryo tubes	CryoPure Code platelets, colour mixture	Sarstedt, Germany
Disposable Combitips	Eppendorf CombiTips (5, 10ml) Polypropylene, Sterile	Eppendorf, Germany
Electroporation cuvettes	Sterile and disposable, Gap: 2 mm, Volume capacity: 400 µl	VWR, Germany
Disposable Pipettes	Sterile cell culture grade (1 ml, 5 ml, 10 ml and 25 ml), Polystyrene	Sarstedt, Germany
Electroporation cuvettes	Sterile and disposable, Gap: 2 mm, Volume capacity: 400 µl	VWR, Germany
Inoculation loop	Inoculation loops 1 – 10 µl white	Sarstedt, Germany
Live-cell microwell plates	micro-Plate 24 well ibiTreat, sterile	Ibidi, Germany
Microcentrifuge tubes	Micro tube (1.5 ml, 2 ml) with attached EASY CAP, Polypropylene	Sarstedt, Germany
Multiple Well Microplates	Multiple Well Microplates 6/12/24/48/96 well clear TC-treated, sterile	Corning, USA
Serological pipettes	Greiner serological pipettes (1-50 ml), sterile	Greiner, Germany
Sterile filter	Filtropur S, 0.2 / 0.,45 µm	Sarstedt, Germany
Syringes	Syringes: 1 - 50ml Luer-Lock	VWR, Germany
TLC sheets	ALU*GRAM*® Xtra SIL G aluminium sheets	Thermo Scientific, USA
Glass ware		
Cover slips	Cover Glass Round Ø 12-24 mm	VWR, Germany
Object slides	Objektträger, SuperFrost® plus	Hartenstein, Germany

Erlenmeyer flasks	Duran® graduated glass flasks (1000 ml, 500 ml, 250 ml, 100 ml)	DURAN Group GmbH
Glass bottles	Duran® graduated glass bottles (1000 ml, 500 ml, 250 ml, 100 ml)	DURAN Group GmbH
Test tubes	5 ml capacity with metal caps	A. Hartenstein GmbH
Commercial Kits		
Amplex™ Red Sphingomyelinase Assay Kit	Kit for measurement of sphingomyelinase activity in cell culture supernatants and cell lysate, used according to manufacturer's instructions	Invitrogen, USA
CaspGLOW™ Fluorescein Active Caspase-8 Staining Kit	Kit for measurement of Caspase 8 activity in cell lysates, used according to manufacturer's instructions	Thermo Scientific, USA
Cytotoxicity detection kit^{PLUS}	Kit for measurement of lactate dehydrogenase (LDH) activity released from the cytosol of damaged cells into the supernatant, used according to manufacturer's instructions	Roche, Switzerland
Lipofectamine® 3000 Transfection Reagent	Kit used for cell transfection, used according to manufacturer's instructions	Thermo Scientific, USA
PureLink® Quick Plasmid Miniprep kit	Kit for plasmid DNA extraction by centrifugation, used according to manufacturer's instructions	Invitrogen, USA
QIAprep SpinMiniprep kit	Kit for plasmid DNA extraction by centrifugation, used according to manufacturer's instructions	QIAGEN, Germany
QIAGEN PlasmidMini kit	Kit for plasmid DNA extraction by anion-exchange on gravity flow columns, used according to manufacturer's instructions	QIAGEN, Germany
Qiagen Blood Mini Kit gDNA	Kit for plasmid DNA extraction by anion-exchange on gravity flow columns, used according to manufacturer's instructions	QIAGEN, Germany

Appendix E

Supplemental figures

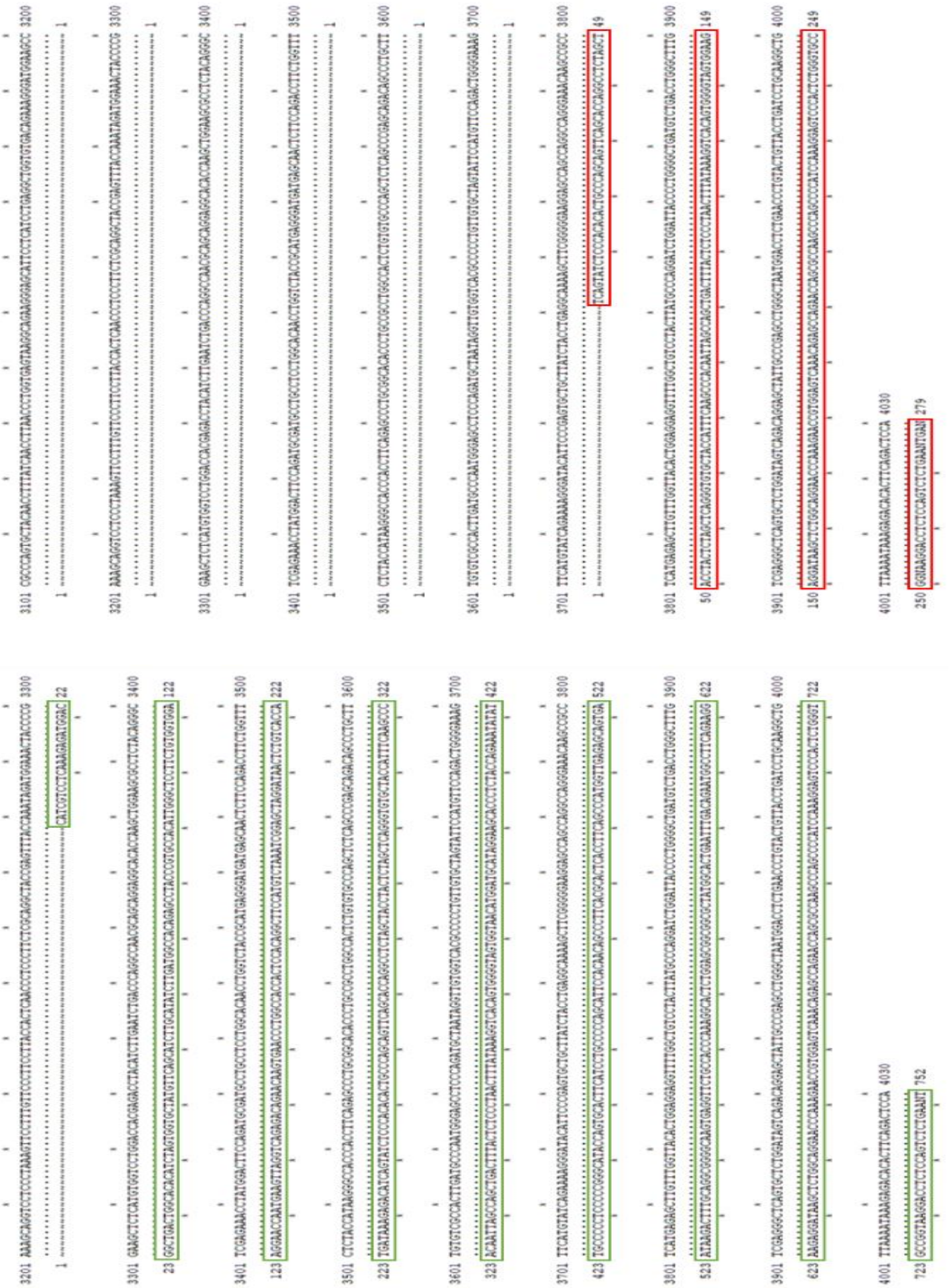

S-Fig. 1 ***Successful Smpd1 knock-out in EOMA***
EOMA were treated after the described CRISPRCas9 method and single-cell sorted. Analysis of a positive Knock-out PCR sample was confirmed by sequence analysis. Green – wildtype control ; red – deletion in Smpd1 gene locus.

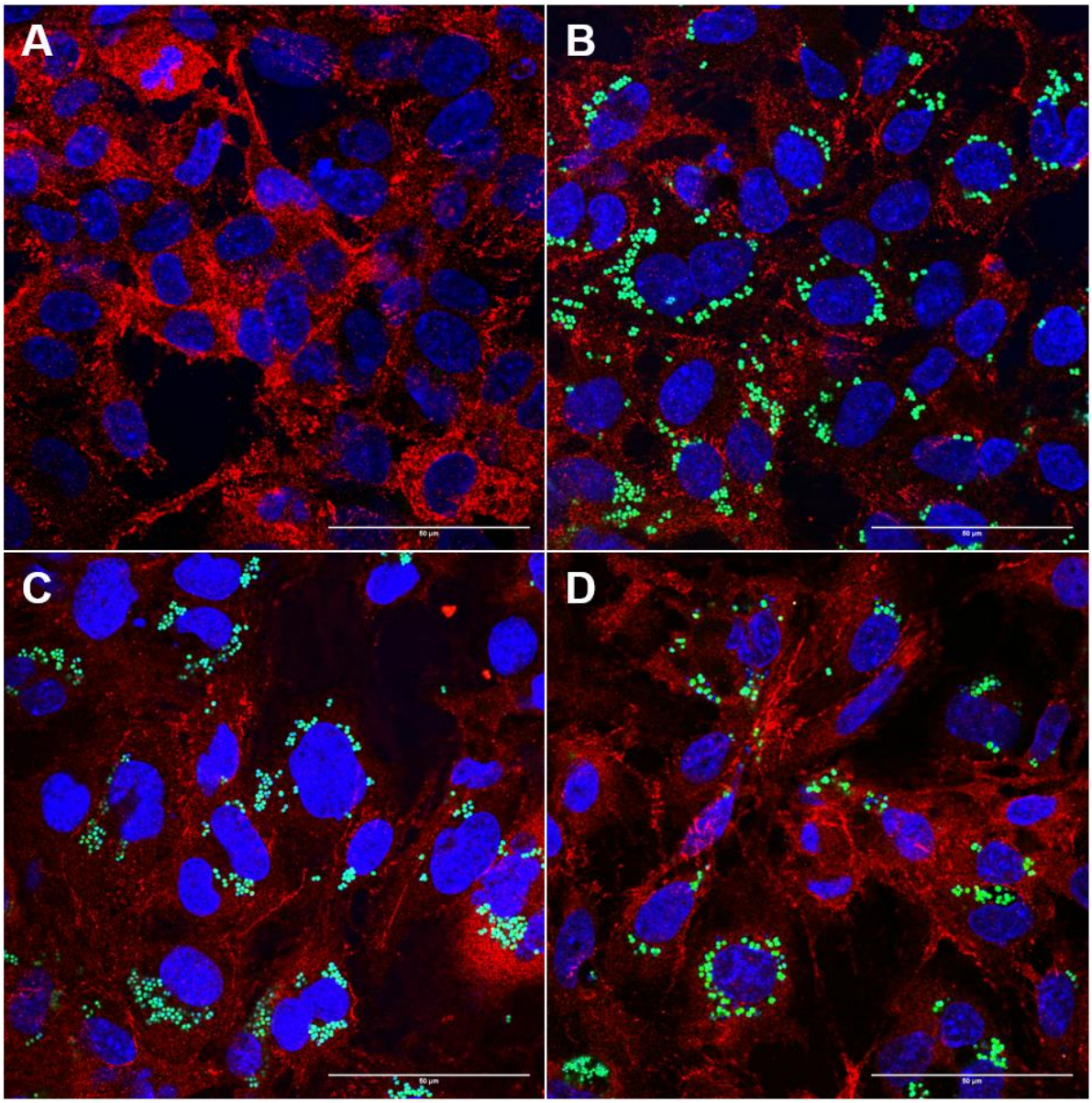

S-Fig. 2 ***EOMA proof to be resistant against intracellular S. aureus infection:***
*EOMA were infected with S. aureus JE2 MOI for 30 min. Cell culture medium was removed and Lysostaphin-containing medium was added for lysis of extracellular bacteria. Infection were carried on for 2 h (**B**), 4 (**C**) and 24 h (**D**). A Cuninfected control (**A**) was issued to determine potential TJP degradation*

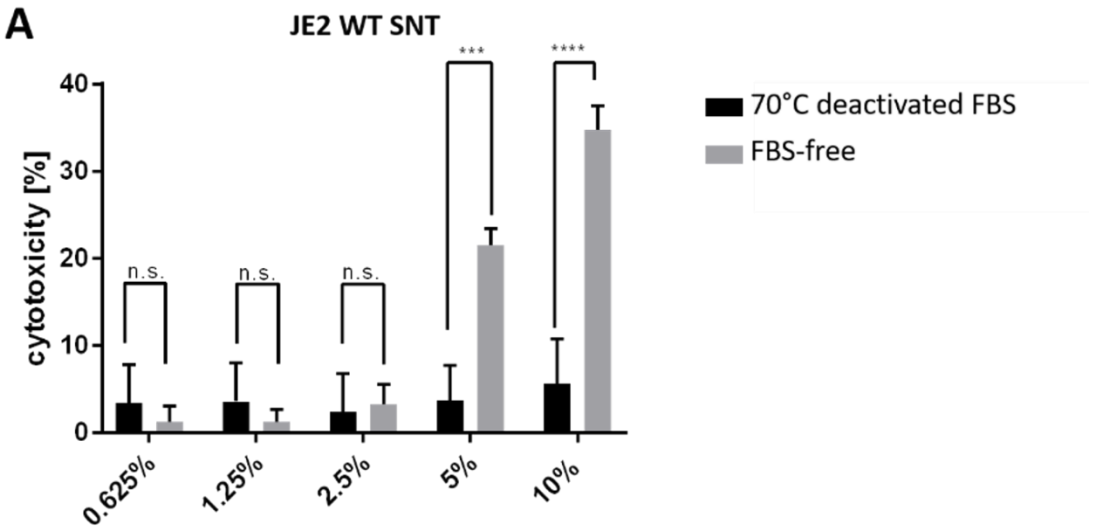

S-Fig. 3 ***FBS is essential for S. aureus PSM inhibition*** *HuLEC-5a were either cultured in medium without FBS or containing 10% FBS heat inactivated at 70°C. Cells were then treated with varying concentrations of S. aureus JE2 supernatant and cell cytotoxicity was assessed via LDH-Assay. Experiment performed by Marcel Rühling.*

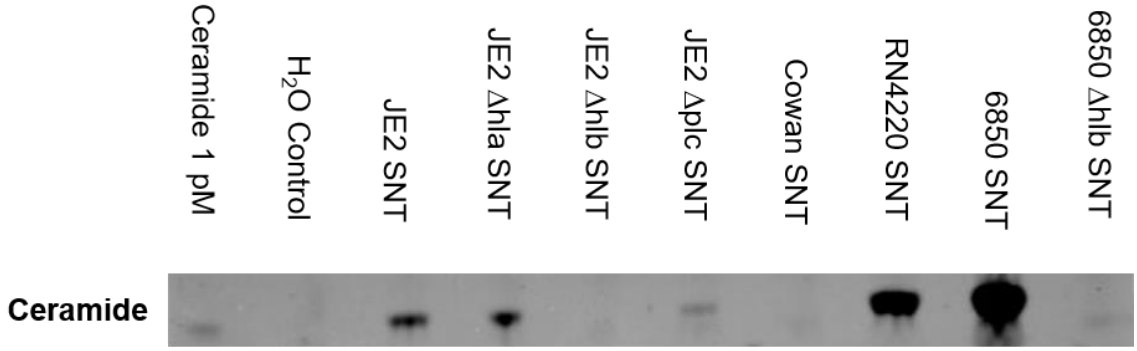

S-Fig. 4 ***S. aureus exhibits strong sphingomyelinase activity***
Supernatant of S. aureus overnight cultures were sterile filtered and tested for sphingomyelinase activity. Therefore 100 µl of each supernatant was tested as described previously. S. aureus proofs to exhibit a strain and toxin specific conversion of sphingomyelin to ceramide under tested conditions.

S-Fig. 5 *S. aureus SpA is able to bind antibodies of different origin.*
EOMA were infected with S. aureus JE2 for 30 min at MOI10. Further cells (MOI10) and cell culture media (SNT) were harvested, centrifuged and proteins separated as previous described via SDS-PAGE and Western Blot. Samples were incubated with an insignificant antibody. Samples containing bacteria were able to bind antibodies via protein A. Hence for experiments conducted with S. aureus its needs to be taken into consideration, that antibodies may indicate false-positive signals due to protein A binding if not treated accordingly.

Appendix

Glossary

ADAM10	A Disintegrin and metalloproteinase domain-containing protein 10
agr	Accessory gene regulator
AJ	Adherence junctions
AMR	Antimicrobial resistance
APS	Ammonium persulfate
ASM	Acid sphingomyelinase
BCA	Bicinchoninic acid assay
BHI	Brain Heart Infusion
bSM	Bacterial neutral sphingomyelinase
Ca^{2+}	Calcium
Casp8	Cysteinyl-aspartate specific protease 8
CA/HA-MRSA	Community/Hospital-acquired MRSA
CerS	Ceramide synthase
CF	Cystic fibrosis
CFU	Colony forming units
$CHCl_3$	Chloroform
Cna	Collagen binding protein
CRISPR	Clustered Regularly Interspaced Short Palindromic Repeats
CRP	Ceramide-rich plattforms
CWA	Cell wall-anchored
DARC	Duffy antigen receptor for chemokines
DMEM	Dulbecco's Modified Eagle's Medium
dNTPs	Desoxyribonucleotides
EC	Endothelial cells
ECL	enhanced chemiluminiscence
ECM	Extracellular matrix
EDTA	Ethylenediamineteaacetic acid
ERM	Erythromycin
EtOH	Ethanol
FnBPs	Fibronectin binding protein
FDA–	US Food and Drug Administration
FIASMA	Functional inhibitors of ASM
GFP	Green fluorescent protein

GJ	Gap junctions
GSL–	Glycosphingolipids
HBP	Heparin-binding protein
ICAM-1	Intercellular adhesion molecule 1
IL-1	Interleukin 1
JAM	Junction Adhesion molecules
kDa	Kilodalton
LAMP1	Lysosomal-associated membrane protein 1
L/S-ASM	Lysosomal/secretory ASM
LYS	Lysate
MDA5	Melanoma differentiation-associated protein 5
MeOH	Methanol
MOI	Multiplicity of Infection
MSCRAMM	Microbial Surface Component Recognizing Adhesive Matrix Molecule
MRSA	Methicillin-Resistant *Staphylococcus aureus*
MW	Molecular weight
NaCl	Natrium chloride
NPD	Niemann-Pick Disease
NTML	Nebraska transposon mutant library
OD	Optical density
OPG	Osteoprotegerin
PCR	Polymerase Chain Reaction
PFA	Paraformaldehyde
PFT	Pore-forming toxin
PMT	Photomultiplier
PVL	Panton-Valentine leucocidin
PVDF	Polyvinylidene fluoride
RIG-I	Retinoic acid inducible gene I
RIPA	Radioimmunoprecipitation Assay
RPMI	Roswell Park Memorial Institute
S1P	Sphingosine-1-phosphate
SARS-Cov-2	Severe Acute Respiratory Syndrome – Coronavirus - 2
SDS-PAGE	Sodium dodecyl sulfate polyacrylamide gel electrophoresis
SM	Sphingomyelin
SNARE	Soluble NSF Attachment Proteins Receptor
SNT	Supernatant

SpA	Staphylococcal immunoglobulin binding protein A
TAE	TRIS-Acetat-EDTA
TBS(-T)	TRIS buffer saline (-Tween20)
TEMED	Tetramethylethylenediamine
TEER	Transendothelial electrical resistance
TJ	Tight junctions
TLC	Thin Layer Chromatography
TLR	Toll like receptor
TNFα	Tumor-necrosis factor α
TNFR1	Tumor-necrosis factor receptor 1
TRAIL	TNR-related apoptosis inducing ligand
TSA	Tryptic Soy Agar
TSB	TRIS buffered saline
VCAM-1	Vascular cell adhesion molecule 1
VE-Cadherin	Vascular endothelial cadherin
VISA/VRSA	Vancomycin intermediate/resistant *Staphylococcus aureus*
vWF	von Willebrandt factor
ZO	Zonula Occludens

Affidavit

I hereby declare that my thesis entitled: „The Role of Acid Sphingomyelinase in *Staphylococcus aureus* Infection" is the result of my own work. I did not receive any help or support from commercial consultants. All sources and / or materials applied are listed and specified in the thesis.

Furthermore I verify that the thesis has not been submitted as part of another examination process neither in identical nor in similar form.

Besides I declare that if I do not hold the copyright for figures and paragraphs, I obtained it from the rights holder and that paragraphs and figures have been marked according to law or for figures taken from the internet the hyperlink has been added accordingly.

Würzburg, 2022 Signature

Eidesstattliche Erklärung

Hiermit erkläre ich an Eides statt, die Dissertation: „Die Rolle der sauren Sphingomyelinase bei *S. aureus* Infektionen", eigenständig, d. h. insbesondere selbständig und ohne Hilfe eines kommerziellen Promotionsberaters, angefertigt und keine anderen, als die von mir angegebenen Quellen und Hilfsmittel verwendet zu haben.

Ich erkläre außerdem, dass die Dissertation weder in gleicher noch in ähnlicher Form bereits in einem anderen Prüfungsverfahren vorgelegen hat.

Weiterhin erkläre ich, dass bei allen Abbildungen und Texten bei denen die Verwertungsrechte (Copyright) nicht bei mir liegen, diese von den Rechtsinhabern eingeholt wurden und die Textstellen bzw. Abbildungen entsprechend den rechtlichen Vorgaben gekennzeichnet sind sowie bei Abbbildungen, die dem Internet entnommen wurden, der entsprechende Hypertextlink angegeben wurde.

Würzburg, 2022 Unterschrift

Contributions of colleagues

All experiments for induction of ASM knock-down in various cells were performed by Kerstin Paprotka.

Transfection of cells for visualization of mCherry ASM constructs were performed by Kerstin Paprotka, microscopy was performed by Jan Schlegel and Marcel Rühling.

Cell cytotoxicity measurements regarding FBS presence in cell culture medium was performed by Marcel Rühling.

Danksagungen

Zum Schluss dieser Arbeit möchte mich ich noch bei allen Personen bedanken, dich mir auf diesem Weg geholfen und zur Seite gestanden haben.

Als erstes möchte ich mich bei meinem Betreuer und Doktorvater Dr. Martin Fraunholz bedanken für das Vertrauen und die angenehme Zusammenarbeit. Durch ihn habe ich die Chance erhalten an diesem spannenden Projekt zu arbeiten und durch seine fachliche und persönliche Betreuung hat er wesentlich zum Erfolg des Projekts und meiner Ausbildung zum Nachwuchswissenschaftler beigetragen.

Mein Dank möchte ich ebenso an Prof. Dr. Thomas Rudel und Prof. Dr. Sibylle Schneider-Schaulies richten, die als Teil meines Prüfungskomitees durch Rat und Unterstützung mir dabei geholfen haben, dieses Projekt erfolgreich zu beenden.

Weiterhin möchte ich den Mitgliedern der *S. aureus* Forschungsgruppe – Jessica Horn, Kathrin Stelzner, Michaela Groma, Adriana Moldovan, und Kerstin Paprotka – für die tolle und erfolgreiche Zusammenarbeit bedanken. Ihr habt mich wunderbar aufgenommen und mit euren Tipps sowie Unterhaltungen für ein wunderbares Arbeitsklima gesorgt.

Ebenfalls als neustes Mitglied der *S. aureus* Forschungsgruppe möchte ich Marcel Rühling danken. Ich bin erfreut darüber, dass ich ihn bei der Vollendung seiner Master Thesis behilflich sein konnte und durch sein fleißiges Zutun hat er essentiellen Einfluss auf dieses Projekt gehabt.

Zusätzlich möchte ich mich bei Dr. Tobias C. Kunz, Dr. Maximilian Klepsch, Dr. Suvagata Roy Chowdhury und M.Sc Tristan Beste bedanken für eine wundervolle Zeit am Lehrstuhl für Mikrobiologie. Nicht nur als Kollegen, sondern auch als Freunde mit denen ich erlebnisreiche Stunden verbringen durfte.

Dem kompletten Lehrstuhl für Mikrobiologie gehört ebenso mein Dank, die mich zu jedem Zeitpunkt in meiner Arbeit unterstützt haben.

Auch möchte ich allen Mitgliedern und des SphingoFOR 2123 danken für ihre Zusammenarbeit und dem ständigen Austausch über das übergeordnete Forschungsthema unserer Arbeitsgruppen in Würzburg, Essen und Potsdam.

Meinen größten Dank möchte ich an meine Frau, Familie und Freunde richten, ohne deren Unterstützung ich heute nicht an diesem Punkt wäre.

Hervorzuheben ist meine Frau Kim Krones, die mich in schweren Situationen stets unterstützt hat und mich darin bestätigt meine Träume zu erfüllen. Ich bin dankbar sie als Lebensgefährten bei mir zu wissen und als Mutter meines ersten Sohns Levi zu haben. Deine Familie hat mich von Beginn an in ihre Mitte aufgenommen und ich freue mich sie zu meiner Familie zählen zu dürfen.

Meine Eltern Karin Roth und Hans-Peter Krones, die es mir ermöglicht haben in einem unbeschwerten Umfeld aufzuwachsen und maßgeblich dazu beigetragen haben, dass ich eine Hochschule besuchen durfte. Vielen Dank dass ihr immer in mich vertraut habt und mich in meinen Vorhaben unterstützt habt. Ich hoffe, dass ich meinem Kind ein ebenso guter Elternteil und Vorbild sein kann. Auch möchte ich mich bei meiner Schwester Leonie Krones bedanken. Auch wenn wir uns nicht so oft sehen, du bist meine Lieblingsschwester und ich freue mich wieder auf unsere Stadionbesuche.

Natürlich möchte ich auch meiner gesamten Familie danken, seien es Omas, Opas, Onkels, Tanten, Cousinen oder Cousins. Ihr seid die beste Familie, die man sich wünschen kann und ich freue mich euch bei mir zu haben.

Zum Schluss möchte ich all meinen Freunden danken, für alle wunderbaren Momente zusammen. An Marco David, Timo David und Duy Anh Nguyen sowie eure Partner, danke dass ihr auch meine Freunde in der Ferne geblieben seid und wir eine großartige Zeit bis jetzt hatten. An alle meine Fußballer der SG Randersacker, die mir hier ein herzliches Willkommen in Würzburg beschert haben und tolle Momente gebracht haben.